Steel Sheet Piling

Design Manual

Steel Sheet Piling Sections

Profile		Section Index	Distri Rolled	Driving Distance per Pile	Weight Per Foot	Weight Per Square Foot of Wall	Web Thickness	Section Modulus Per Pile	Section Modulus Per Foot of Wall	Area Per Pile	Moment of Inertia Per Pile	Moment of Inertia Per Foot of Wall
				In.	Lbs.	Lbs.	In.	In.³	In.³	In.²	In.⁴	In.⁴
	Interlock with Each Other	PSX 32	H.	16½	44.0	32.0	$29/64$	3.3	2.4	12.94	5.1	3.7
		PS 32*	H.S.	15	40.0	32.0	½	2.4	1.9	11.77	3.6	2.9
		PS 28	H.S.	15	35.0	28.0	⅜	2.4	1.9	10.30	3.5	2.8
	Interlock with Each Other	PSA 28*	H.	16	37.3	28.0	½	3.3	2.5	10.98	6.0	4.5
		PSA 23	H.S.	16	30.7	23.0	⅜	3.2	2.4	8.99	5.5	4.1
		PDA 27	H.S.	16	36.0	27.0	⅜	14.3	10.7	10.59	53.0	39.8
		PMA 22	H.S.	19⅝	36.0	22.0	⅜	8.8	5.4	10.59	22.4	13.7
	Interlock with Each Other and with PSA 23 or PSA 28	PZ 38	H.	18	57.0	38.0	⅜	70.2	46.8	16.77	421.2	280.8
		PZ 32	H.	21	56.0	32.0	⅜	67.0	38.3	16.47	385.7	220.4
		PZ 27	H.	18	40.5	27.0	⅜	45.3	30.2	11.91	276.3	184.2
		PZ 22	H.	22	30.3	22.0	⅜	34.8	9.0	11.9	167	91.1

*Sections PS32 and PSA28 are infrequently rolled and we do not advise their use in a design unless an adequate tonnage can be ordered at one time to assure a minimum rolling.

Complete data regarding these sections will be found in a separate publication entitled "USS Steel Sheet Piling?

H-Homestead, Pa. (Pittsburgh District)
S-South Chicago (Chicago District)

Suggested Allowable Design Stresses-Sheet Piling

Steel Brand or Grade	Minimum Yield Point, psi	Allowable Design Stress, psi*
USS-EX-TEN 55 (ASTM A572 GR 55)	55,000	35,000
USS EX-TEN 50 (ASTM A572 GR 50)	50,000	32,000
USS MARINER STEEL	50,000	32,000
USS EX-TEN 45 (ASTM A572 GR 45)	45,000	29,000
Regular Carbon Grade (ASTM A 328)	38,500	25,000

*Based on 65% of minimum yield point. Some increase for temporary Overstresses generally permissible.

USS Steel Sheet Piling

Design Manual

Notice

"The information, including technical and engineering data, figures, tables, designs, drawings, details, suggested procedures, and suggested specifications, presented in this publication are for general information only. While every effort has been made to insure its accuracy, this information should not be used or relied upon for any specific application without independent competent professional examination and verification of its accuracy, suitability and applicability. Anyone making use of the material does so at his own risk and assumes any and all liability resulting from such use. UNITED STATES STEEL CORPORATION DISCLAIMS ANY AND ALL EXPRESS OR IMPLIED WARRANTIES OF MERCHANTABILITY FITNESS FOR ANY GENERAL OR PARTICULAR PURPOSE OR FREEDOM FROM INFRINGEMENT OF ANY PATENT, TRADEMARK, OR COPYRIGHT IN REGARD TO INFORMATION OR PRODUCTS CONTAINED OR REFERRED TO HEREIN. Nothing herein contained shall be construed as granting a license, express or implied, under any patents."

Notice by U.S. DOT

This document is disseminated under the sponsorship of the Department of Transportation in the interest of information exchange. The United States Government assumes no liability for its contents or use thereof. The contents of this report reflect the views of the USS, who is responsible for the accuracy of the data presented herein. The contents do not necessarily reflect the official views or policy of the Department of Transportation. This report does not constitute a standard, specification, or regulation.

The United States Government does not endorse products or manufacturers. Trade or manufacturers' names appear herein only because they are considered essential to the object of this document.

TABLE OF CONTENTS

FOREWORD

This manual is directed to the practicing engineer concerned with safe, economical designs of steel sheet pile retaining structures. The content is directed basically toward the designer's two primary objectives: overall stability of the structural system and the integrity of its various components.

Emphasis is placed on step-by-step procedures for estimating the external forces on the structure, evaluating the overall stability, and sizing the sheet piling and other structural elements. Graphs and tables are included to aid the designer in arriving at quick solutions.

Three basic types of sheet pile structures are considered: (3) cantilevered and anchored retaining walls, (2) braced cofferdams and (3) cellular cofferdams. Consideration is also given to the design of anchorage systems for walls and bracing systems for cofferdams.

The design procedures included in this manual are in common use today by most engineers involved in the design of sheet pile retaining structures. These methods have consistently provided successful retaining structures that have performed well in service. However, in using these procedures, one should not be lulled into a false sense of security about the accuracy of the computed results. This is especially true with regard to lateral earth pressures on retaining structures. The simplifying assumptions inherent in any of these procedures and their dependence on the strength properties of the soil provide only approximations to reality.

It is assumed throughout that the reader has a fundamental knowledge of soil mechanics and a working knowledge of structural steel design. It is further assumed that the subsurface conditions and soil properties at the site of the proposed construction have been satisfactorily established and the designer has-chosen the type of sheet pile structure best suited to the site.

LATERAL PRESSURES ON SHEET PILE WALLS

EARTH PRESSURE THEORIES

Earth pressure is the force per unit area exerted by the soil on the sheet pile structure. The magnitude of the earth pressure depends upon the physical properties of the soil, the interaction at the soil-structure interface and the magnitude and character of the deformations in the soil-structure system. Earth pressure is also influenced by the time-dependent nature of soil strength, which varies due to creep effects and chemical changes in the soil.

Earth pressure against a sheet pile structure is not a unique function for each soil, but rather a function of the soil-structure system. Accordingly, movements of the structure are a primary factor in developing earth pressures. The problem, therefore, is highly indeterminate.

Two stages of stress in the soil are of particular interest in the design of sheet pile structures, namely the active and-passive states. When a vertical plane, such as a flexible retaining wall, deflects under the action of lateral earth pressure, each element of soil adjacent to the wall expands laterally, mobilizing shear resistance in the soil and causing a corresponding reduction in the lateral earth pressure. One might say that the soil tends to hold itself up by its boot straps; that is, by its inherent shear strength. The lowest state of lateral stress, which is produced when the full strength of the soil is activated (a state of shear failure exists), is called the active state. The active state accompanies outward movement of the wall. On the other hand, if the vertical plane moves toward the soil, such as the lower embedded portion of a sheet pile wall, lateral pressure will increase as the shearing resistance of the soil is mobilized. When the full strength of the soil is mobilized, the passive state of stress exists. Passive stress tends to resist wall movements and failure.

There are two well-known classical earth pressure theories; the Rankine Theory and the Coulomb Theory. Each furnishes expressions for active and passive pressures for a soil mass at the state of failure.

Rankine Theory - The Rankine Theory is based on the assumption that the wall introduces no changes in the shearing stresses at the surface of contact between the wall and the soil. It is also assumed that the ground surface is a straight line (horizontal or sloping surface) and that a plane failure surface develops.

When the Rankine state of failure has been reached, active and passive failure zones will develop as shown in Figure 1.

where ϕ = angle of internal friction of soil (degrees)
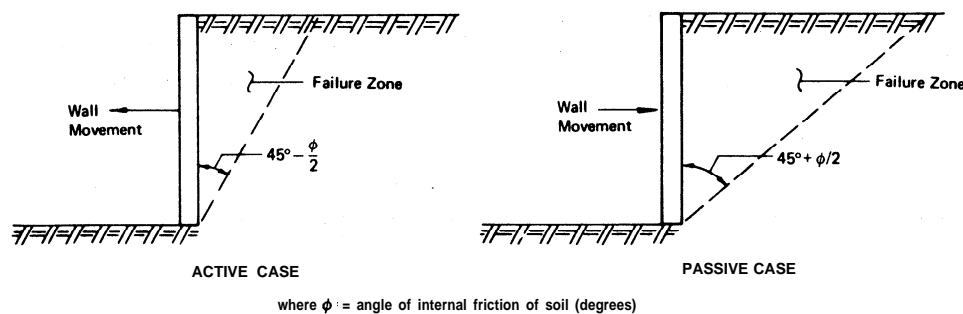
Fig. 1 - Rankine failure zones

The active and passive earth pressures for these states are expressed by the following equations:

$$p_a = \gamma Z K_a - 2c \sqrt{K_a}$$

$$p_\rho = \gamma K Z_\rho + 2c \sqrt{K_\rho}$$

where p_a and p_ρ = unit active and passive earth pressure, respectively, at a depth Z below the ground surface

γZ = vertical pressure at a depth Z due to the weight of soil above, using submerged weight for the soil below ground water level

c = unit cohesive strength of soil

K_a and K_ρ = coefficients of active and passive earth pressures, respectively

The coefficients K_a and K_p, according to the Rankine Theory, are functions of the ϕ--angle of the soil and the slope of the backfill, β. They are given by the expressions

$$K_a = \cos\beta \frac{\cos\beta - \sqrt{\cos^2\beta - \cos^2\phi}}{\cos\beta + \sqrt{\cos^2\beta - \cos^2\phi}}$$

$$K_\rho = \cos\beta \frac{\cos\beta + \sqrt{\cos^2\beta - \cos^2\phi}}{\cos\beta - \sqrt{\cos^2\beta - \cos^2\phi}}$$

Note that for the case of a level backfill, these equations reduce to

$$K_a = \frac{1 - \sin\phi}{1 + \sin\phi} = \tan^2(45 - \phi/2)$$

$$K_\rho = \frac{1 + \sin\phi}{1 - \sin\phi} = \tan^2(45 + \phi/2)$$

The triangular pressure distributions for a level backfill are shown in Figure 2. For various slope conditions, refer to *Mechanics of Soils* by A. Jumikis.[16]

Fig. 2 - Rankine earth pressure (after Teng[1])

(c)
Cohesive Soil - Active Pressure

(d)
Cohesive Soil - Passive Pressure

Fig. 2 - (Continued)

Coulomb Theory - An inherent assumption of the Rankine Theory is that the presence of the wall does not affect the shearing stresses at the surface of wall contact. However, since the friction between the retaining w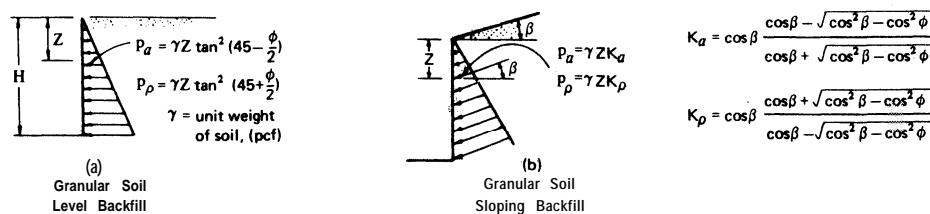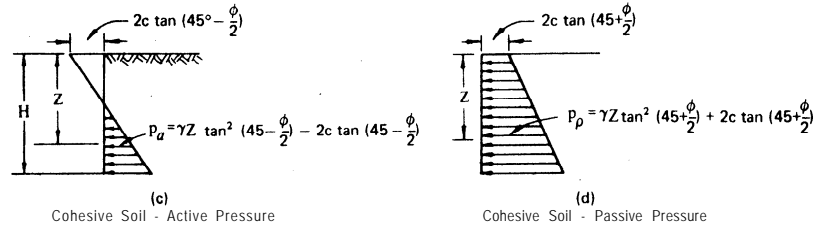all and the soil has a significant effect on the vertical shear stresses in the soil, the lateral stresses on the wall are actually different than those assumed by the Rankine Theory. Most of this error can be avoided by using the Coulomb Theory, which considers the changes in tangential stress along the contact surface due to wall friction.

As the wall yields, the failure wedge tends to move downward for the active case. For the passive case, where the wall is forced against the soil, the wedge slides upward along the failure plane. These differential movements involve vertical displacements between the wall and backfill and create tangential stresses on the back of the wall due to soil friction and adhesion. The resulting force on the wall is, therefore, inclined at an angle to the normal to the wall. This angle is known as the angle of wall friction, δ. For the active case, when the active wedge slides downward relative to the wall, δ is taken as positive. For the passive case, when the passive wedge slides upward relative to the wall, δ is taken as negative. If the angle of wall friction is known, the following analytical expressions for K_a and K_p in the horizontal direction for a vertical wall are:

$$K_a = \frac{\cos^2\phi}{\cos\delta \left[1 + \sqrt{\dfrac{\sin(\phi+\delta)\,\sin(\phi-\beta)}{\cos\delta\,\cos\beta}}\right]^2}$$

$$K_p = \frac{\cos^2\phi}{\cos\delta \left[1 - \sqrt{\dfrac{\sin(\phi+\delta)\,\sin(\phi+\beta)}{\cos\delta\,\cos\beta}}\right]^2}$$

where ϕ = angle of internal friction of soil
δ = angle of wall friction
β = angle of the backfill with respect to horizontal

Figure 3(a) is included for ease in obtaining K_a and K_p.

As in the Rankine Theory, the Coulomb Theory also assumes a plane surface of failure. However, the position of the failure plane is a function of both the ϕ-angle of the soil and the angle of wall friction, δ. The position of the failure plane for the active and passive cases for a level backfill is given by:

$$\alpha_a = 90° - \phi - \arctan\left[\frac{-\tan\phi + \sqrt{\tan\phi(\tan\phi+\cot\phi)\,(1+\tan\delta\cdot\cot\phi)}}{1 + \tan\delta\,(\tan\phi + \cot\phi)}\right]$$

$$\alpha_p = 90° + \phi - \arctan\left[\frac{\tan\phi + \sqrt{\tan\phi(\tan\phi+\cot\phi)\,(1+\tan\delta\cdot\cot\phi)}}{1 + \tan\delta\,(\tan\phi + \cot\phi)}\right]$$
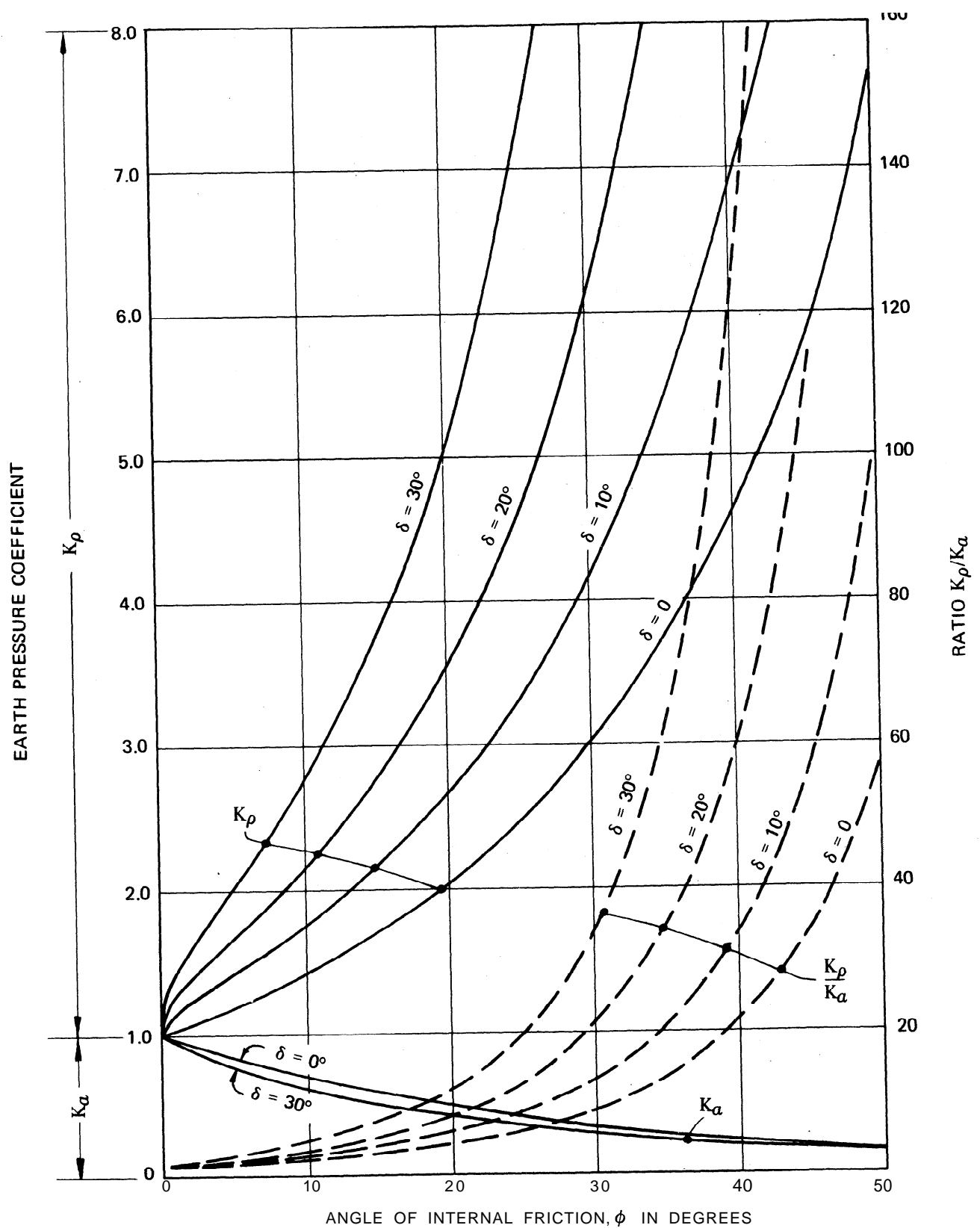
Fig. 3(a) - Coulomb earth pressure coefficient vs. ϕ-angle for level backfill and dredge line

where α_a and α_p = angle between the failure plane and the vertical for the active and passive cases, respectively

Figure 3(b) shows the Coulomb active and passive failure wedges together with the Corresponding pressure distributions.
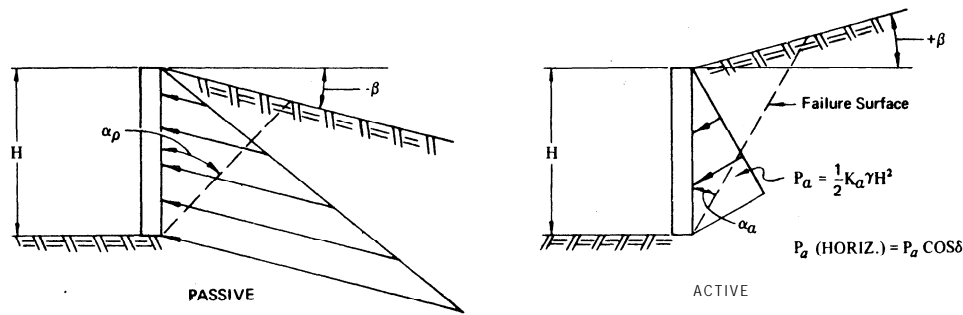
Fig. 3 (b) - **Coulomb earth pressure**

For a smooth wall (zero wall friction) with level backfill or if $\delta = \beta$ for a sloping backfill, the Rankine and Coulomb Theories give identical results.

Log-Spiral Theory - The Coulomb Theory of earth pressure assumes that the surface of sliding or failure is a plane. This assumption deviates somewhat from reality. For the active case the error introduced is small. However, for the passive case the error can be large and is always on the unsafe side. If the angle of wall friction, δ, is low the failure surface is almost plane. However, if δ is high, the passive failure plane deviates considerably from Coulomb's assumption, which predicts unrealistically high passive pressures. Large angles of wall friction that cause a downward tangential shearing force will increase the vertical pressures in the soil close to the wall, thus causing a curved failure surface as shown in Figure 4(a). The soil fails on this curved surface of least resistance and not on the Coulomb plane, which would require a greater lateral driving force. Figure 4(b) shows the reduction in the passive earth pressure coefficient, K_p, for increasing values of wall friction for the actual curved surface of failure.

(a)
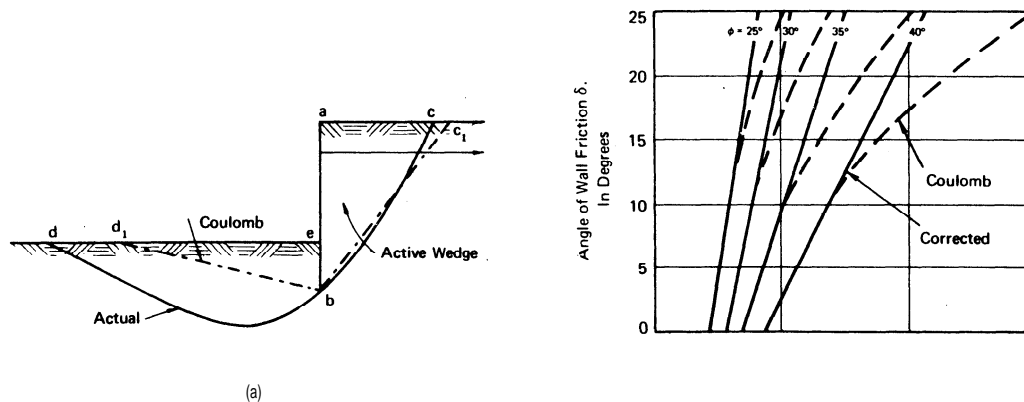
Fig. 4 - Comparison of Coulomb and log-spiral failure surface (after Terzahgi[22])

The method of computing earth pressures for a log-spiral failure surface is summarized in *Soil Mechanics in Engineering Practice* by Terzaghi and Peck. Table 1 lists values of passive lateral earth pressure coefficients for a curved surface of failure and level backfill for various relative values of the angle of internal friction, ϕ, and the angle of wall friction, δ. The charts in Figure 5(a) give the active and passive coefficients for a log-spiral failure surface for the case of wall friction and sloping backfill.

$\phi =$	10°	2.5°	15°	7.5°	20°	25°	30°	35°	40°
$\delta = -\phi$	1.65	1.89	2.19	2.55	3.01	4.29	6.42	10.20	17.50
$\delta = -\phi/2$	1.56	1.76	1.98	2.25	2.59	3.46	4.78	6.88	10.38
$\delta = \pm 0$	1.42	1.55	1.70	1.85	2.04	2.46	3.00	3.70	4.60
$\delta = +\phi$	0.73	0.68	0.64	0.61	0.58	0.55	0.53	0.53	0.52

Table 1. Values of Passive Lateral-earth-pressure Coefficients K_p (Curved Surfaces of Failure)

(after Caquot and Kerise1[21])

REDUCTION FACTOR (R) OF K_p FOR VARIOUS RATIOS OF $-\delta/\phi$

ϕ \ δ/ϕ	-0.7	-0.6	-0.5	-0.4	-0.3	-0.2	-0.1	-0.0
10	.978	.962	.946	.929	.912	.898	.881	.864
15	.961	.934	.907	.881	.854	.830	.803	.775
20	.939	.901	.862	.824	.787	.752	.716	.678
25	.912	.860	.808	.759	.711	.666	.620	.574
30	.878	.811	.746	.686	.627	.574	.520	.467
35	.836	.752	.674	.603	.536	.475	.417	.362
40	.783	.682	.592	.512	.439	.375	.316	.262
45	.718	.600	.500	.414	.339	.276	.221	.174

COEFFICIENT OF PASSIVE PRESSURE, K_p

FAILURE SURFACE

$90° - \phi$

LOGARITHMIC SPIRAL

$\sigma_p = K_p \gamma H$

PASSIVE PRESSURE

$P_p = K_p \gamma H^2/2; \quad P_H = P_p \cos \delta; \quad P_v = P_p \sin \delta$

NOTE: CURVES SHOWN ARE FOR $\delta/\phi = -1.0$

EXAMPLE: $\phi = 25°$; $\beta/\phi = -.2$
$\delta/\phi = -.3$
$K_p = R(K \text{ FOR } \delta/\phi = -.1)$
$R = .711$
$(K_p \text{ FOR } \delta/\phi = -1.0) = 3.62$
$K_p = .711 \times 3.62 = 2.50$

COEFFICIENT OF ACTIVE PRESSURE, K_a

FAILURE SURFACE

$90° - \phi$

LOGARITHMIC SPIRAL

$\sigma_a = K_a \gamma H$

ACTIVE PRESSURE
$P_a = K_a \gamma H^2/2$
$P_H = P_a \cos \delta$
$P_v = P_a \sin \delta$

ANGLE OF INTERNAL FRICTION ϕ, DEGREES

$\beta/\phi = +1$ $\beta/\phi = +.8$

$\beta/\phi = +.6$
$\beta/\phi = +.4$
$\beta/\phi = +.2$
$\beta/\phi = 0$
$\beta/\phi = -.2$
$\beta/\phi = -.4$
$\beta/\phi = -.6$
$\beta/\phi = -.8$
$\beta/\phi = -.9$
$\beta/\phi = -1$

PASSIVE ZONE

ACTIVE ZONE

$\delta = \phi$
$\delta = 0$ } $\beta/\phi = +1$

$\delta = \phi$
$\delta = 0$ } $\beta/\phi = +.8$

$\delta = \phi$
$\delta = 0$ } $\beta/\phi = +.6$

$\delta = \phi$
$\delta = 0$ } $\beta/\phi = +.4$

$\delta = \phi$
$\delta = 0$ } $\beta/\phi = 0$

$\delta = \phi$
$\delta = 0$ } $\beta/\phi = -.4$
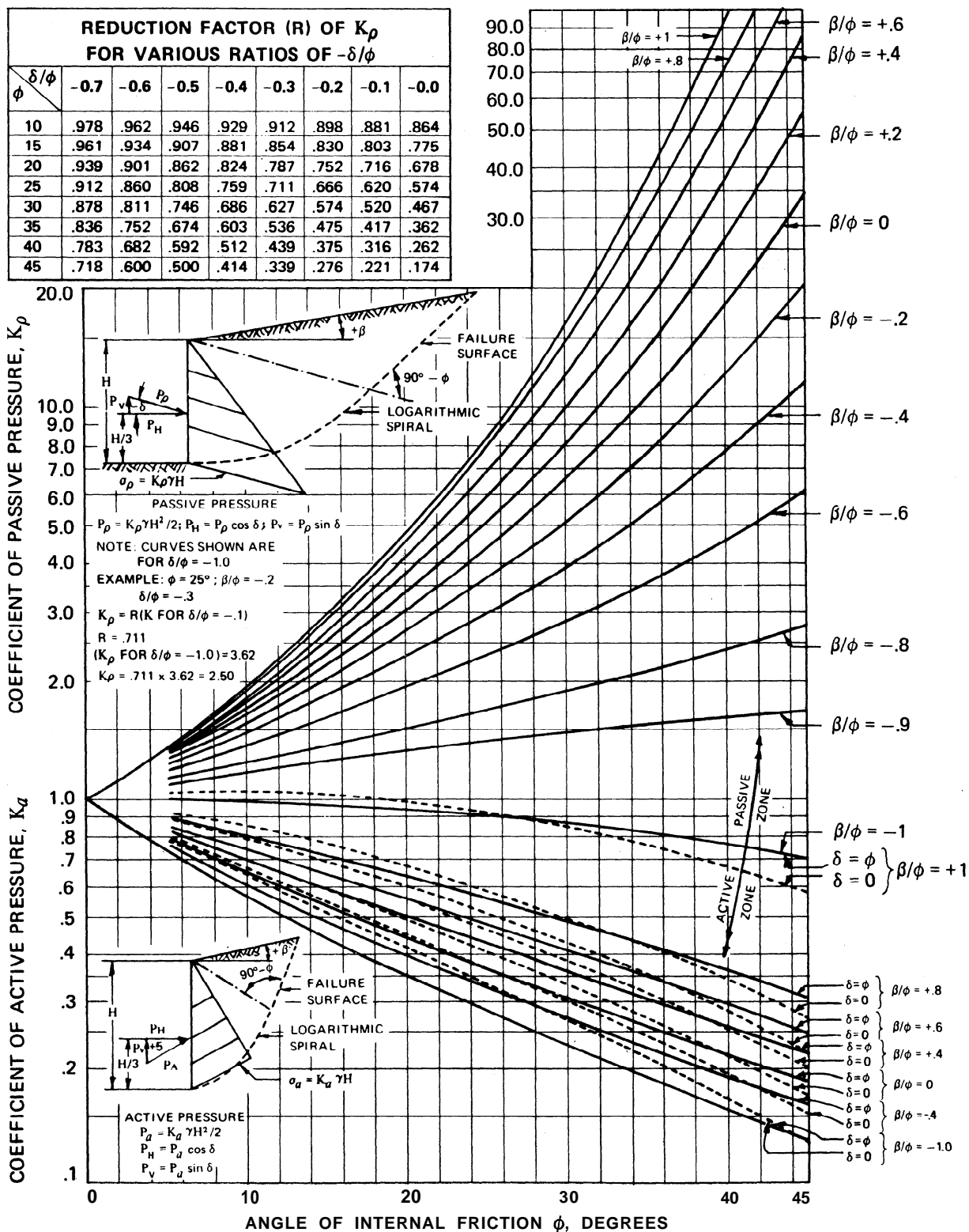
$\delta = \phi$
$\delta = 0$ } $\beta/\phi = -1.0$

Fig. 5(a) - Active and passive coefficients with wall friction (sloping backfill) (after Caquot and Kerisel[21])
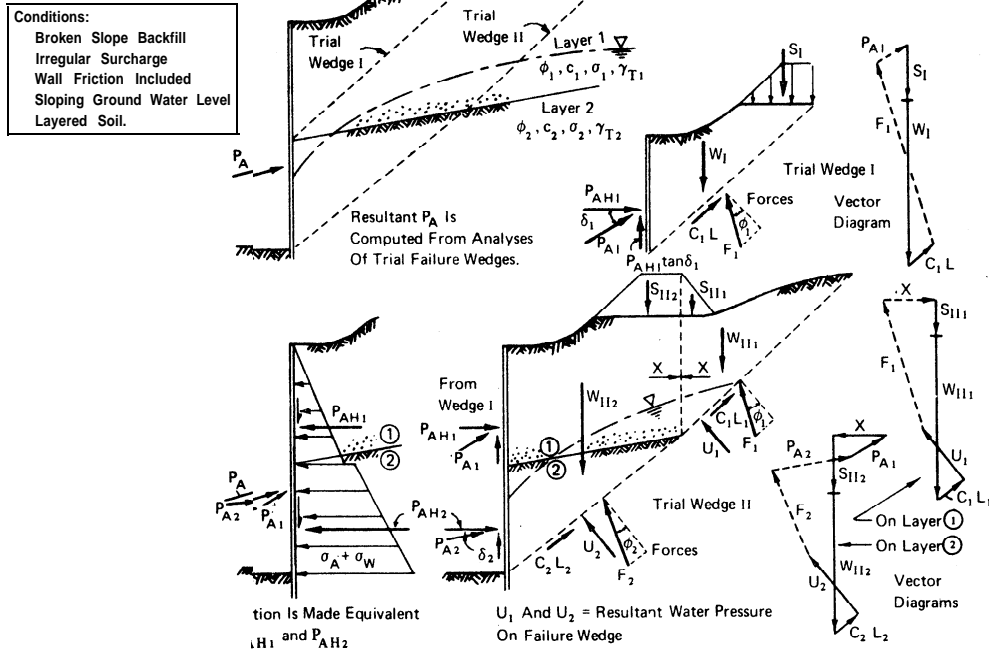
Fig. 5(b) - Generalized determination of active pressures (after Navdock[11])
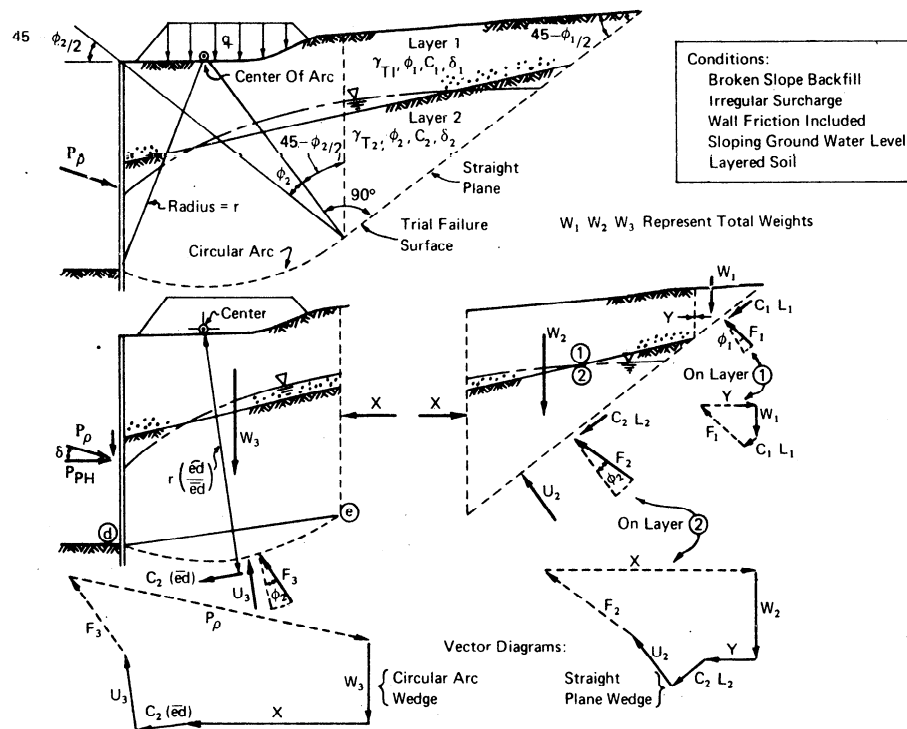
Fig. 5(c) - Generalized determination of passive pressures (after Navdock[11])

In summary for the determination of lateral earth pressures on sheet pile walls:

1. Active pressures should be computed using the Coulomb Theory or the logarithmic spiral method as shown in Figure 5(a).

2. Passive pressures should be computed using the Coulomb Theory with an appropriate safety factor or the logarithmic spiral method as shown in Figure 5(a).

3. For 'complicated cross sections involving irregular and stratified backfills, the reader should consult such texts as *Fundamentals of Soil Mechanics* by Taylor and *Soil Mechanics in Engineering Practice* by Terzaghi and Peck. A graphical analysis for complicated cross sections is shown on Figures 5(b) and 5(c).

Soil Properties - Independent of the theory used to compute earth pressure on retaining structures, the results can be no more accurate than the soil properties used in the calculations. Because of the wide variations of subsurface conditions at various sites, the soil constants should be determined on the basis of an exploratory boring program and laboratory tests of representative samples. Only then can a safe and economical design be assured. However, for the purpose of preliminary design it is often necessary to presume appropriate soil properties. The following tables and graphs are included for this purpose merely as a guide.

Table 2 shows an approximate relationship between the relative density, standard penetration resistance, angle of internal friction, and unit weight of granular soils.

Compactness	Very Loose	Loose	Medium	Dense	Very Dense
Relative density D_d	0	15%	35%	65%	85% 100%
Standard penetration resistance, N = no. of blows per foot	0	4	10	30	50
ϕ (degrees) *		28	30	36	41
Unit weight, pcf moist	<100	95-125	110-130	110-140	>130
submerged	< 60	55-65	60-70	65-85	> 75

*highly dependent on gradation

Table 2 - Granular soil (after Teng[1])

Table 3 shows an approximate relationship between the unconfined compressive strength, standard penetration resistance and the unit weight of cohesive soils.

Consistency	Very Soft	Soft	Medium	Stiff	Very Stiff	Hard
q_u = unconfined compression strength, tons per square ft	0	0.25	0.50	1.00	2.00	4.00
Standard penetration resistance, N = no. of blows per ft	0	2	4	8	16	32
Unit weight, pcf (saturated)		100-120	110-130		120-140	130+
Identification characteristics	Exudes from between fingers when squeezed in hand	Molded by light finger pressure	Molded by strong finger pressure	Indented by thumb	Indented by thumb nail	Difficult to indent by thumb nail

Table 3 - Cohesive soil (after Teng[1])

Figure 6 shows the approximate relationship between the angle of internal friction and the dry unit weight for various relative densities and types of granular soils. The porosity, n, and the void ratio, e, are also shown for coarse grained soils that have a specific gravity, G, equal to 2.68.
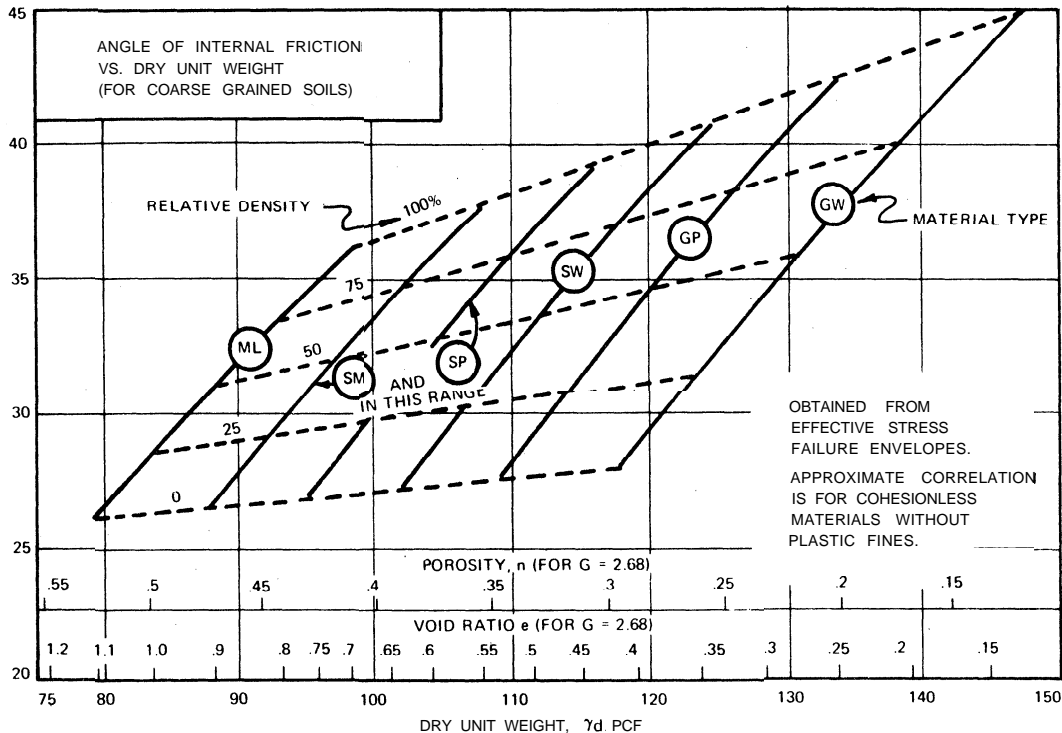

Fig. 6 - Granular soils (after Navdocks[11])

Table 4 shows friction angles for various soils against steel sheet piles.

Steel sheet piles against the following soils:	tanδ	δ (degree)
Clean gravel, gravel-sand mixtures, well-graded rock fill with spalls	0.40	22
Clean sand, silty sand-gravel mixture, single size hard rock fill	0.30	17
Silty sand, gravel or sand mixed with silt or clay	0.25	14
Fine sandy silt, non-plastic silt	0.20	11

Table 4 - Wall friction (after Navdocks[11])

As mentioned previously, earth pressure is time-dependent in nature. This is particularly true in clay and clayey soils where the values of cohesion, c, and internal friction, ϕ, tend to change with time. Sheet pile structures in clayey soils should be designed for both the period immediately after construction and long term conditions. Limited information indicates that due to creep effects the long term value of c approaches zero and that of ϕ somewhere between 20 and 30 degrees. The long term case thus approaches that for sheet piling in granular soils.

13

SURCHARGE LOADS

The function of a sheet pile structure is often to retain various surface loadings as well as the soil behind it. These surface loads, or surcharge, also exert lateral pressures on the wall which contribute to the active pressure tending to move the wall outward. Typical surcharge loadings are railroads, highways, buildings, ore piles, cranes, etc.

The loading cases of particular interest in the determination of lateral soil pressures are:

1. Uniform Surcharge
2. Point Loads
3. Line Loads Parallel to the Wall
4. Strip Loads Parallel to the Wall

For the case of a uniform surcharge loading, the conventional theories of earth pressure can be effectively utilized. On the other hand, for point, line and strip loads the theory of elasticity (Boussinesq Analysis) modified by experiment provides the most accurate solutions. These solutions are summarized in *Foundation Design* by Wayne C. Teng[1] and "Anchored Bulkheads" by Karl Terzaghi.[22]

Uniform Surcharge - When a uniformly distributed surcharge is applied at the surface, the vertical pressures at all depths in the soil are increased equally. Without the surcharge the vertical pressure at any depth h would be γh, where γ is the unit weight of the soil. When a surcharge of intensity q (force/area) is added, the vertical pressures at depth h become $\gamma h + q$.

The lateral pressure, σ_H, due to the uniform surcharge q, is equal to Kq, as shown in Figure 7 below.

q lb/ft²
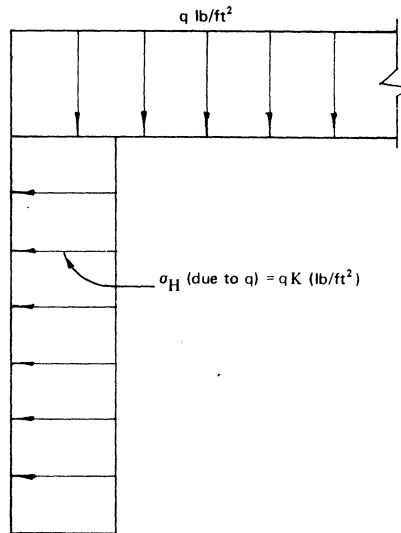
σ_H (due to q) = q K (lb/ft²)

Fig. 7 - Lateral pressure due to uniform surcharge

The K value is either the active coefficient K_a or the passive coefficient K_p depending upon whether the wall tends to move away from or toward the surcharge area. The uniform lateral pressure due to the surcharge is then added to the lateral dead weight earth pressures as described in previous sections.

For the case of a uniform surcharge loading, lateral movement of the plane on which the horizontal stresses are being computed is taken into account by considering that the entire "active wedge" of soil is in a state of impending shear failure. On the other hand, computations of lateral stresses due to surcharge applied on a limited area (point, line and strip loads) is complicated by the lack of a rational approach to the distribution of shear stresses in the soil adjacent a yielding vertical plane. Therefore, semi-empirical methods of analysis have been developed based upon elastic theory and experiments on rigid unyielding walls. The lateral pressures computed by these methods are conservative for sheet pile walls since, as the wall deflects, soil shear resistance is mobilized and the lateral pressure on the wall in reduced.

Point Loads - The lateral pressure distribution on a vertical line closest to a point load may be calculated as shown in Figure 8(a).

$$\sigma_H = 0.28 \frac{Q_p}{H^2} \cdot \frac{n^2}{(0.16 + n^2)^3} \quad \text{(for } m \leq 0.4\text{)}$$

$$P_H = 0.78 \frac{Q_p}{H} \quad \text{(see Fig. 11)}$$

$$\sigma_H = 1.77 \frac{Q_p}{H^2} \cdot \frac{m^2 n^2}{(m^2 + n^2)^3} \quad \text{(for } m > 0.4\text{)}$$

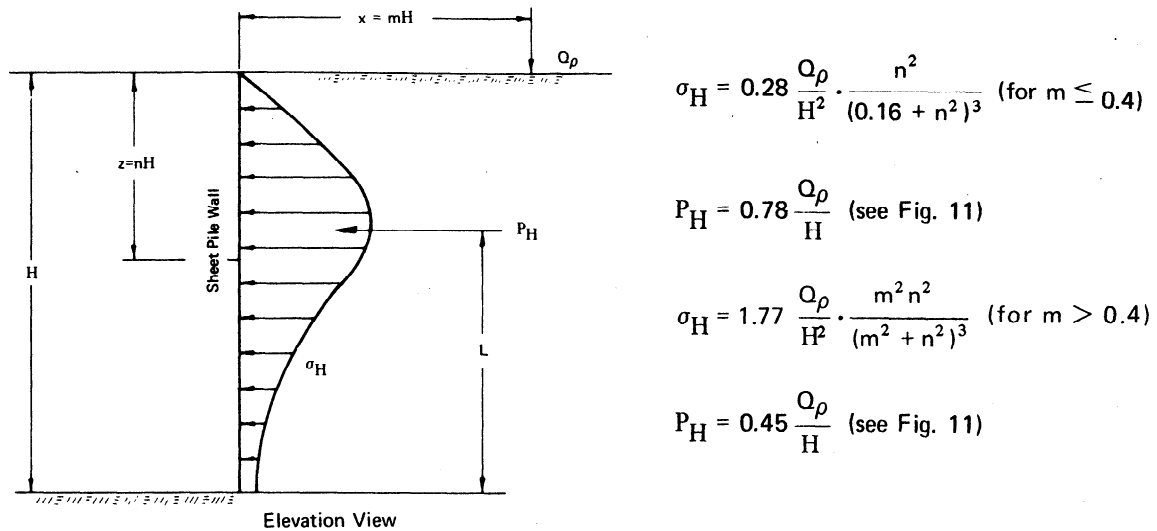$$P_H = 0.45 \frac{Q_p}{H} \quad \text{(see Fig. 11)}$$

Fig. 8(a) - Lateral pressure due to point load (after Terzaghi[22])

Away from the line closest to the point load the lateral stress decreases as shown in the plan view of Figure 8(b).
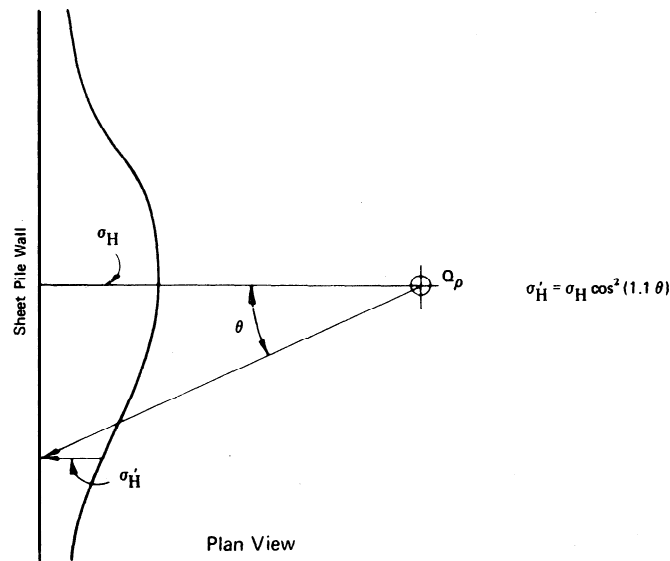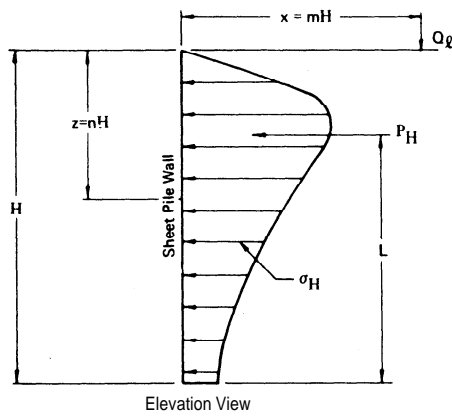

$$\sigma'_H = \sigma_H \cos^2(1.1\,\theta)$$

Fig. 8(b) - Lateral pressure due to point load (Boussinesq equation modified by experiment) **(after Terzaghi[22])**

Line Loads - A continuous wall footing of narrow width or similar load parallel to a retaining structure may be taken as a line load. For this case the lateral pressure increases from zero at the ground surface to a maximum value at a given depth and gradually diminishes at greater depths. The lateral pressure distribution on a vertical plane parallel to a line load may be calculated as shown in Figure 9.

$$\sigma_H = 0.20 \frac{Q\ell}{H} \cdot \frac{n}{(0.16 + n^2)^2} \quad \text{(for } m \leq 0.4\text{)}$$

$$P_H = 0.55\, Q\ell, \text{ resultant force}$$

$$\sigma_H = 1.28 \frac{Q\ell}{H} \cdot \frac{m^2 n}{(m^2 + n^2)^2} \quad \text{(for } m > 0.4\text{)}$$

$$P_H = \frac{0.64\, Q\ell}{(m^2 + 1)} \text{ resultant force}$$

Fig. 9 - Lateral pressure due to line load (Boussinesq equation modified by experiment) (after Terzaghi[22])

Strip Loads - Highways and railroads are examples of strip loads. When they are parallel to a sheet pile wall, the lateral pressure distribution on the wall may be calculated as shown in Figure 10.
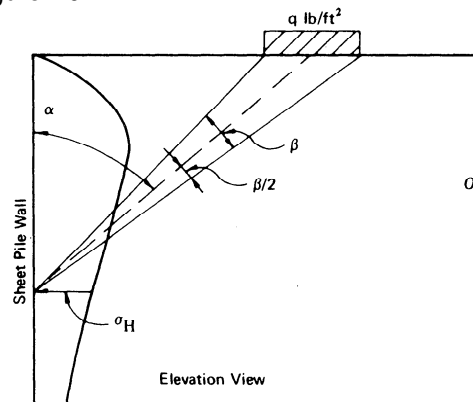
$$\sigma_H = \frac{2q}{\pi} [\beta - \sin\beta \cos 2\,\alpha\,]$$

Fig. 10 - Lateral pressure due to strip load (Boussinesq equation modified by experiment) (after Teng[1])

Based on the relationships given above, Figure 11 shows plots of the lateral pressure distributions under point and line loads and gives the positions of the resultant force for various values of the parameter m.
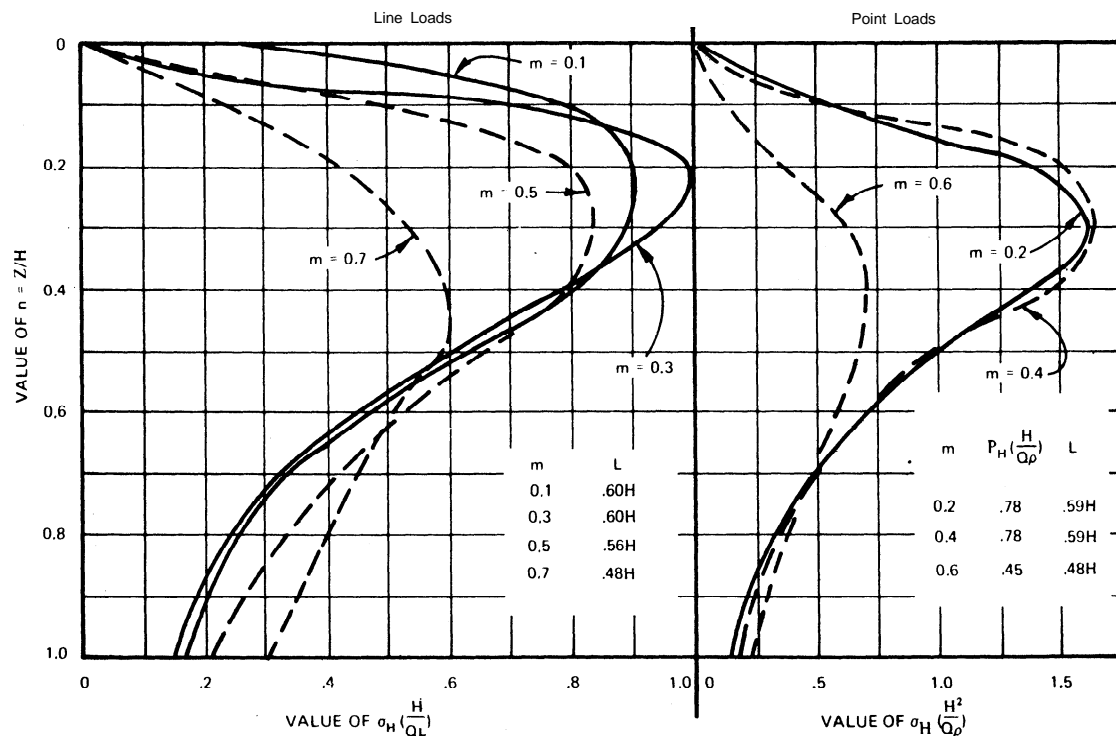

Fig. 11 - Horizontal pressures due to point and line loads (after Navdocks[11])

EFFECTS OF UNBALANCED HYDROSTATIC AND SEEPAGE FORCES

Sheet pile structures built today in connection with waterfront facilities are subjected to maximum earth pressure when the tide or river level is at its lowest stage. A receding tide, receding high water, or heavy rainstorm may cause a higher water level behind a sheet pile wall than in front of it, depending on the type of backfill used. If the backfill is fine or silty sand, the height of water behind the sheet pile wall may be several feet. If the soil behind the wall is silt or clay, full hydrostatic pressure in back of the wall should be assumed up to the highest position of the previous water level.

The difference in water level on either side of the wall introduces (1) additional pressure on the back of the wall due to hydrostatic load and (2) reduction in the unit weight of the soil in front of the piling (thus, a reduction of passive resistance). The distribution of the unbalanced water pressure on the two faces of the structure corresponding to a hydraulic head, H_U, can be determined by means of the flow net method as illustrated in Figure 12(a). If a sheet. pile structure is driven in granular soil with fairly uniform permeability, the unbalanced water pressure may be approximated by the trapezoid in Figure 12(b). If the permeability of the soil varies greatly in the vertical direction, a flow net should be used to determine the unbalanced pressure.
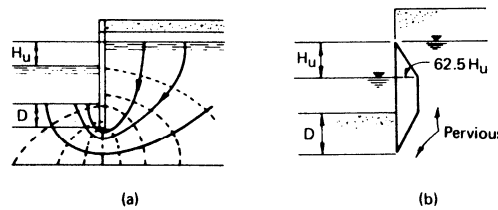

Fig. 12 - Hydrostatic and seepage pressures (after Terzaghi[22])

The upward seepage pressure exerted by the rising ground water in front of the outer face of a sheet pile wall reduces the submerged unit weight in front of the wall by approximately the amount:

$$\triangle \gamma' = 20\, \frac{H_u}{D}$$

where $\triangle \gamma'$ = reduction in submerged unit weight of soil, pcf.
Hence, the effective unit weight to be used in the computation of passive pressure is

$$\gamma' - \triangle \gamma' = \gamma' - 20\, \frac{H_u}{D}$$

where H_u =   unbalanced water head, feet
           D =   as shown in Figure 12

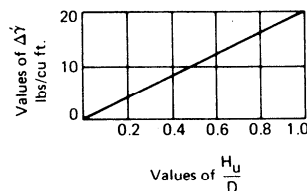The relationship between $\triangle \gamma'$ and H_U/D is given in Figure 13.

Fig. 13 - Average reduction of effective unit weight of passive wedge due to seepage pressure exerted by the upward flow of water (after Terzaghi[22])

The effect of downward seepage in the soil behind the piling is very small and may be neglected.

It must be anticipated that some seepage will occur through interlocks, although the amount is difficult to predict. As an approximation, the seepage should be assumed to equal at least 0.025 gallons per minute per square foot of wall per foot of net head across the wall for installations in moderately to highly permeable soils.

OTHER LATERAL LOADS

In addition to the lateral pressures described previously, sheet pile structures may be subjected to some of the lateral loads described below.

Ice Thrust - Lateral thrusts can be caused by the volume expansion of ice in fine-grained soils (very fine sand, silt and clay). The possibility of lateral thrust from ice or frozen ground should be eliminated by placing free-draining coarse granular soil above the frost line behind a sheet pile wall. Steel sheet piling also offers the advantage that it can yield laterally to relieve any thrust load due to ice.

Wave Forces - There are many theories concerning wave pressure against a vertical surface. In general, wave pressure is a function of wave height, length, velocity and many other factors. The reader is directed to the following references for a detailed explanation of methods of analysis. *Design and Construction of Ports and Marine Structures* by Alonzo DeF. Quinn, *Substructure Analysis and Design* by Paul Anderson, *Pile Foundations* by Robert D. Chellis and *Shore Protection, Planning and Design,* TR No. 4 Dept. of the Army, Corps of Engineers.

Ship impact - Sheet pile dock and waterfront structures may often be subjected to the direct impact of a moving ship. Fender systems should be used in this case to spread out the reaction and reduce the impact to a minimum. Allowance for the effect of a ships' impact is sometimes made by the inclusion of an arbitrary horizontal force such as 50 to 100 tons. The reader is directed to the above mentioned references for further discussion.

Mooring Pull - Sheet pile dock and water front structures generally provide mooring posts for anchoring and docking ships. The magnitude of the mooring pull in the direction of the ship may be taken as the winch capacity used on the ship. When the spacing of the mooring posts is known, an evaluation of moor post pull on the structure can be made.

Earthquake Forces - During an earthquake the vibration of the ground may temporarily increase the lateral pressure against a retaining structure. This increase is a result of a number of factors including inertia force, direction, horizontal acceleration and period. For the design of retaining walls of moderate height, the lateral pressure for design may be increased by about 10 per cent. In the case of high retaining structures, the trial wedge method of analysis should be used. The trial sliding wedge is assumed to be acted upon by a horizontal force in additional to all other forces. Some engineers assume that the horizontal force is equal to 18 to 33 percent of the weight of the sliding wedge. The designer, of course, should consider the location of the structure relative to previous earthquake history.

DESIGN OF SHEET PILE RETAINING WALLS

GENERAL CONSIDERATIONS

The design of sheet pile retaining walls requires several successive operations: (a) evaluation of the forces and lateral pressures that act on the wall, (b) determination of the required depth of piling penetration, (c) computation of the maximum bending moments in the piling, (d) computation of the stresses in the wall and selection of the appropriate piling section and (e) the design of the waling and anchorage system. Before these operations can be initiated, however, certain preliminary information must be obtained. In particular, the controlling dimensions must be set. These include the elevation of the top of the wall, the elevation of the ground surface in front of the wall (commonly called the dredge line), the maximum water level, the mean tide level or normal pool elevation and the low water level. A topographical survey of the area is also helpful.

Earth pressure theories have developed to the point where it is possible to obtain reliable estimates of the forces on sheet pile wails exerted by homogeneous layers of soil with known physical constants. The uncertainties involved in the design of sheet pile structures no longer result from an inadequate knowledge of the fundamentals involved. They are caused by the fact that the structure of natural soil deposits is usually quite complex, whereas the theories of bulkhead design inevitably presuppose homogeneous materials. Because of these conditions, it is essential that a subsurface investigation be performed with exploratory borings and laboratory tests of representative samples. On this basis, a soil profile can be drawn and the engineering properties of the different soil strata can be accurately determined. These properties should reflect the field conditions under which the wall is expected to operate. Only after these preliminary steps are taken should the final design be undertaken.

There are two basic types of steel sheet pile walls: cantilevered walls and anchored walls. The design of each type for various subsurface conditions will be discussed in the following sections.

CANTILEVER WALLS

In the case of a cantilevered wall, sheet piling is driven to. a sufficient depth into the ground to become fixed as a vertical cantilever in resisting the lateral active earth pressure. This type of wall is suitable for moderate height. Walls designed as cantilevers usually undergo large lateral deflections and are readily affected by scour and erosion in front of the wall. Since the lateral support for a cantilevered wall comes from passive pressure exerted on the embedded portion, penetration depths can be quite high, resulting is excessive stresses and severe yield. Therefore, cantilevered walls using steel sheet piling are restricted to a maximum height of approximately 15 feet.

Earth pressure against a cantilevered wall is illustrated in Figure 14. When the lateral active pressure (P) is applied to the top of the wall, the piling rotates about the pivot point, b, mobilizing passive pressure above and below the pivot point. The term (p_p-p_a) is the net passive pressure, p_P, minus the active pressure, p_a. (Since both are exerting pressure upon the wall.)
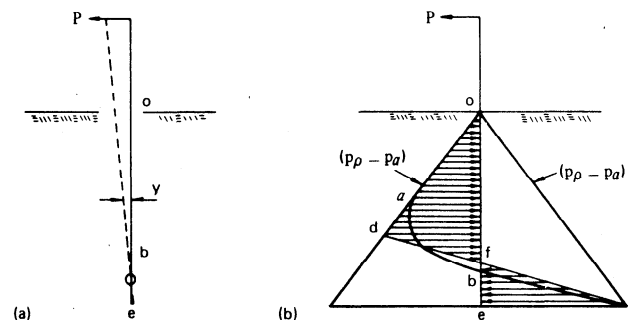

Fig. 14 - Earth pressure on cantilever sheet piling (after Teng[1])

At point b the piling does not move and would be subjected to equal and opposite at-rest earth pressures with a net pressure equal to zero. The resulting earth pressure is represented by the diagram oabc. For the purpose of design, the curve abc is replaced by a straight line dc. The point d is located so as to make the sheet piling in a state of static equilibrium. Although the assumed pressure distribution is in error, it is sufficient for design purposes.

The distribution of earth pressure is different for sheet piling in granular soils and sheet piling in cohesive soils. Also, the pressure distribution in clays in likely to change with time. Therefore, the design procedures for steel sheet piling in both types of soils are discussed separately.

Cantilever Sheet Piling in Granular Soils - A cantilevered sheet pile wall may be designed in accordance with the principles and assumptions just discussed or by an approximate method based on further simplifying assumptions shown in Figure 15.
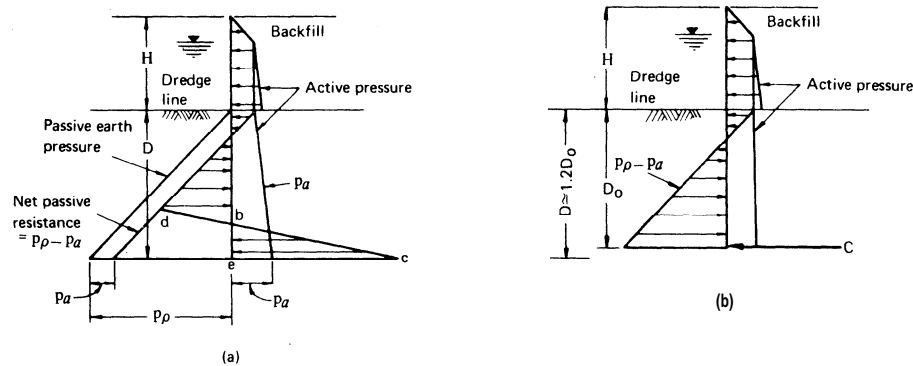

Fig. 15 - Design of cantilever sheet piling in granular soils: (a) conventional method; (b) simplified method. (after Teng[1])

For cases of two or more layers of soil, the earth pressure distributions would be somewhat different due to the different soil properties; however, the design concept is exactly the same. Lateral pressures should be calculated using the curved failure surface (log spiral) method as shown in Figure 5 (a).

Conventional Method - The conventional design procedure for granular soils is as follows:

1. Assume a trial depth of penetration, D. This may be estimated from the following approximate correlation.

Standard Penetration Resistance, N Blows/Foot	Relative Density of Soil, D_d	Depth of Penetration*
0-4	Very loose	2.0 H
5-10	Loose	1.5 H
11-30	Medium dense	1.25 H
31-50	Dense	1.0 H
+50	Very dense	0.75 H

*H = height of piling above dredge line.

2. Determine the active and passive lateral pressures using appropriate coefficients of lateral earth pressure. If the Coulomb method is used, it should be used conservatively for the passive case. The resulting earth pressure diagram for a homogeneous granular soil is shown in Figure 16 where the active and passive pressures are overlain to pictorially describe the resulting soil reactions.
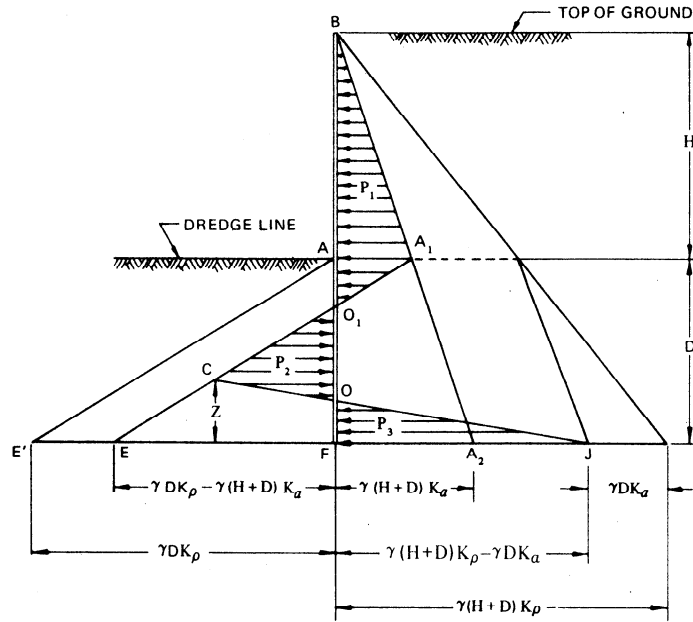
20

Fig. 16 - Resultant earth-pressure diagram

3. Satisfy the requirements of static equilibrium: the sum of the forces in the horizontal direction must be zero and the sum of the moments about any point must be zero. The sum of the horizontal forces may be written in terms of pressure areas:

$$\triangle(E\overrightarrow{A_1 A_2}) - \triangle(F\overleftarrow{B}A_2) - \triangle(E\overleftarrow{C}J) = 0$$

Solve the above equation for the distance, Z. For a uniform granular soil,

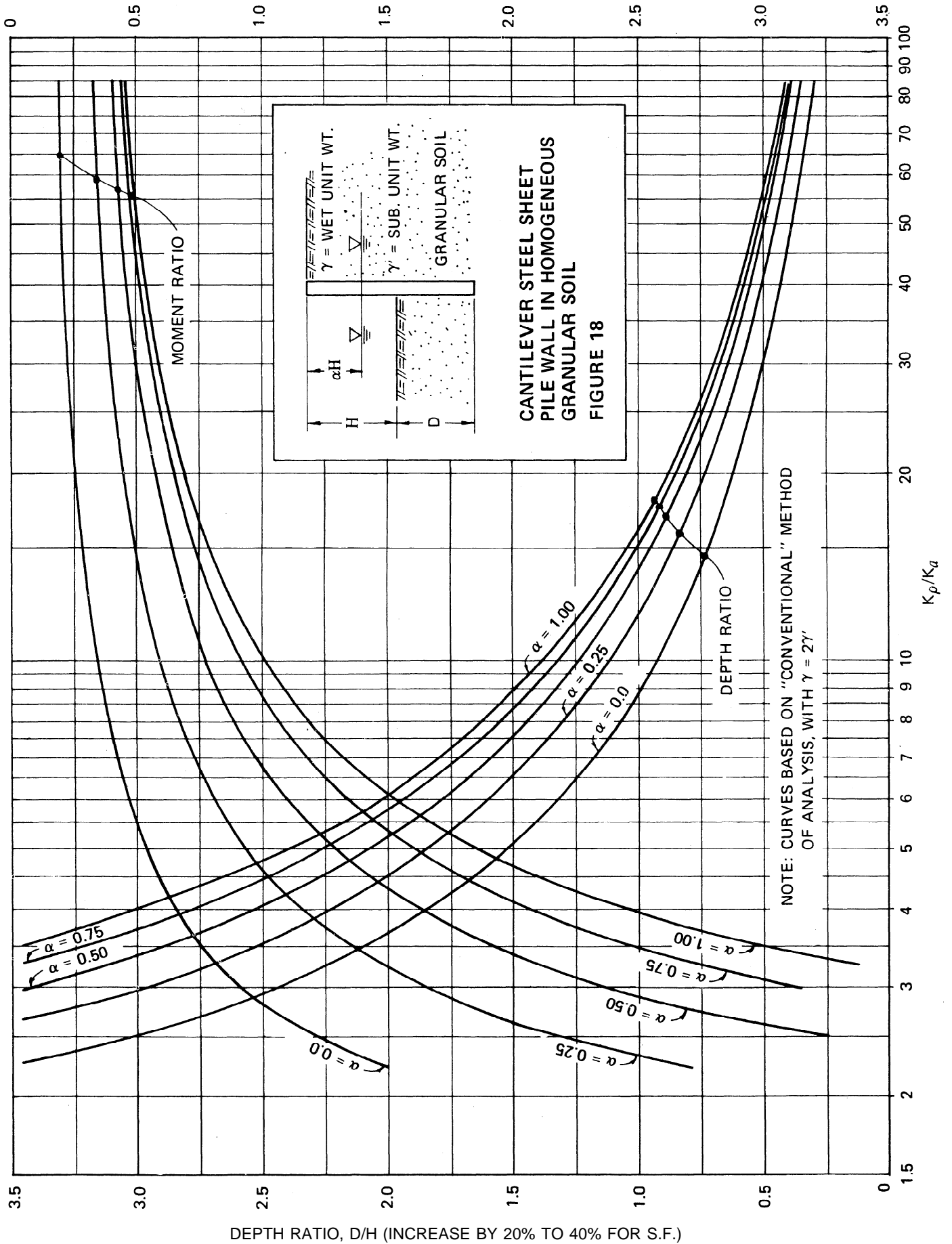$$Z = \frac{K_\rho D^2 - K_a (H+D)^2}{(K_\rho - K_a)(H + 2D)}$$

Take moments about the point F and check to determine if the sum of the moments is equal to zero, as it must be. Readjust the depth of penetration, D, and repeat until convergence is reached; i.e., the sum of the moments about F is zero.

4. Add 20 to 40 percent to the calculated depth of penetration. This will give a safety factor of approximately 1.5 to 2.0. An alternate and more desirable method is the use of a reduced value of the passive earth pressure coefficient for design. The maximum allowable earth pressure should be limited to 50 to 75 percent to the ultimate passive resistance.

5. Compute the maximum bending moment, which occurs at the point-of zero shear, prior to increasing the depth by 20 to 40 percent.

A rough estimate of the lateral displacement may be obtained by considering the wall to be rigidly held at an embedment of ½D and subjected to a triangular load distribution approximating the actual applied active loading. The displacement at any distance y from the top of the pile is then given by the following expression:

$$\triangle_\ell = \frac{Pt}{60EI\ell^2} \cdot (y^5 - 5\ell^4 y + 4\ell^5)$$

21

MOMENT RATIO PER FT. WIDTH, $M_{max}/\gamma' K_a H^3$

CANTILEVER STEEL SHEET
PILE WALL IN HOMOGENEOUS
GRANULAR SOIL
FIGURE 18

γ = WET UNIT WT.

γ' = SUB. UNIT WT.

GRANULAR SOIL

MOMENT RATIO

DEPTH RATIO

α = 1.00

α = 0.25

α = 0.0

α = 0.75

α = 0.50

α = 0.0

α = 1.00

α = 0.75

α = 0.50

α = 0.25

K_p/K_a

NOTE: CURVES BASED ON "CONVENTIONAL" METHOD
OF ANALYSIS, WITH $\gamma = 2\gamma'$

DEPTH RATIO, D/H (INCREASE BY 20% TO 40% FOR S.F.)

where $\triangle_\ell$ = displacement in inches

P_t = total applied load over length in pounds

ℓ = H + ½ D in inches

in which   H = exposed length of sheeting in inches

and   D = penetration of sheeting in surface stratum, plus one-half of penetration in any lower, more dense, coarse grained stratum. Neglect any penetration in rock (inches).

Simplified Method - A simplified method of design isillustrated in Figure 15(b). The passive resistances are simplified by assuming a right triangular pressure on the left side of the piling and by substitution of a concentrated force C for the net passive resistance on the right side of the piling. This method results in some error but saves greatly in the computations. The distance, Do, must satisfy both the requirements of equilibrium. The calculated value of D_o should be increased by 20 to 40 percent to get the total design depth of penetration.

Figure 18 gives a useful method to design cantilever sheet piling in homogeneous granular soil, analyzed by the conventional method. This chart allows the designer to obtain directly the depth ratio, D/H, and the maximum moment ratio, $M_{max}/\gamma'K_aH^3$ as a function of the ratio of passive to active pressure coefficients, K_p/K_a, for various positions of water level. It is, therefore, independent of the method of obtaining K_p or K_a. The chart was developed for a wet unit weight, γ, equal to twice the submerged unit weight, γ'. To use Figure 18, one may determine ϕ and γ from Table 2, δ from Table 4 and K_P/K_a and K_a from Figure 3 (a). A design example is given at the end of problem No. 1 (pages 86-90).

Cantilever Sheet Piling in Cohesive Soils - Two cases of cantilevered walls in cohesive soils are of interest: (1) sheet pile walls entirely in clay and (2) walls driven in clay and backfilled with sand. Different lateral earth pressures develop for each case.

Wall Entirely in Cohesive Soil - Design of sheet piling in cohesive soils is complicated by the fact that the strength of clay changes with time and, accordingly, the lateral earth pressures also change with time. The depth of penetration and the size of piling must satisfy the pressure conditions that exist immediately after installation and the long-term conditions after the strength of the clay has changed. Immediately after the sheet piling is installed, earth pressure may be calculated on the assumption that undrained strength of the clay prevails. That is, it is assumed that the clay derives all its strength from cohesion and no strength from internal friction. The analysis is usually carried out in terms of total stress using a cohesion value, c, equal to one-half the unconfined compressive strength, q_u. The method is usually referred to as a "$\phi = 0$" analysis.

Figure 19 illustrates the initial pressure conditions for sheet piling embedded in cohesive soil for its entire depth.
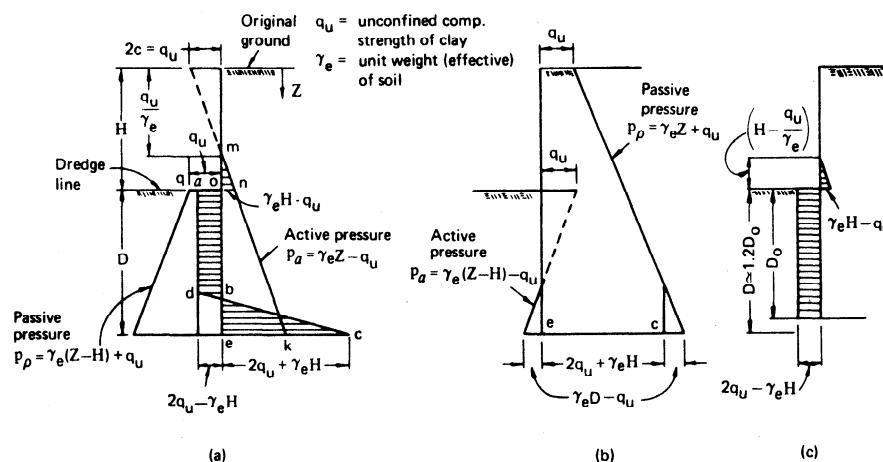

Fig. 19 - Initial earth pressure for design of cantilever sheet piling entirely on cohesive soil (after Teng[1])

23

Since $K_a = K_p = 1$ when $\phi = 0$, the passive earth pressure on the left side of the piling is given by:

$$p_\rho = \gamma_e (Z - H) + q_u$$

and the active pressure on the right side of the piling is given by:

$$p_a = \gamma_e Z - q_u$$

where Z = depth below the original ground surface, ft.
q_u = 2c = unconfined compressive strength, lbs-per sq. ft.
γ_e = effective unit soil weight (moist unit weight above the water level and submerged unit weight below the water level), lbs-per cubic ft.

The negative earth pressure or tension zone, as shown by the dotted line, is ignored because the soil may develop tension cracks in the upper portion. Since the slopes of the active and passive pressure lines are equal ($K_a = K_p$), the net resistance on the left side of the wall is constant below the dredge line and is given by:

$$p_\rho - p_a = 2q_u - \gamma_e H$$

Note that, theoretically, there will be no net pressure and the wall will fail $\gamma_e H$ is greater than $2q_u$. The height, $H_c = 2q_u/\gamma_e$, is often called the critical wall height.

For the lower portion, where the piling moves to the right, the net resistance is given by:

$$p_\rho - p_a = 2q_u + \gamma_e H$$

which is illustrated in Figure 19 (b). The resulting net pressure distribution on the wall is as shown in Figure 19 (a), and the method of solution is the same as that presented for the design of cantilevered sheet pile walls in granular soils. The point d and the depth of penetration D are chosen so as to satisfy the conditions of static equilibrium; i.e., the sum of the horizontal forces equal to zero-and the sum of the moments about any point equal to zero.

Similar to the simplified method for granular soils, the design may be made using the pressure diagram shown in Figure 19 (c); i.e., by assuming the passive pressure on the right side of the piling is replaced by the concentrated reaction, C. The depth, Do, should be increased by 20 to 40 percent to obtain the total design depth of penetration using this method.

Wall in Cohesive Soil Below Dredge Line - Granular Backfill Above Dredgeline - The above methods may also be extended to the case where sheet piling is driven in clay and backfilled with granular soil as shown in Figure 20. The only difference is the active pressure above the dredge line is equal to $K_a \gamma_e Z$ for a granular backfill. The simplified method is shown in Figure 20 (b). The methods of design are exactly the same as discussed previously.
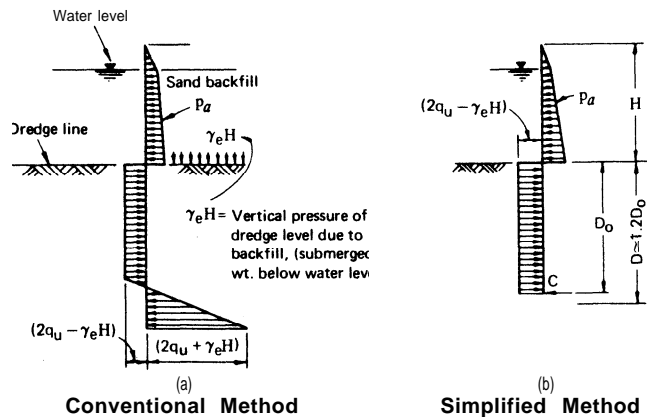
Fig. 20 - Initial earth pressure for design of cantilever sheet piling:
in cohesive soil backfilled with granular soil (after Teng[1])

The long-term condition for sheet piling in clays must also be considered, as mentioned previously, due to time dependent changes in ϕ and c. The analysis should be carried out using effective stress parameters c' and ϕ' obtained from consolidated-drained tests, or from consolidated-undrained tests in which pore pressure measurements are made. Limited experimental data indicates that the long-term value of c is quite small, and that for design purposes c may be conservatively taken as zero. The final value of ϕ is usually between 20 and 30 degrees. The lateral pressures in the clay over a long period of time approach those for a granular soil. Therefore, the long-term condition is analyzed as described in the preceding section for granular soils.

Figure 22, page 26 provides design curves for cantilever sheet piling in cohesive soil with granular soil backfill based upon the simplified method of analysis. This chart allows the designer to obtain directly the depth ratio, D/H, and the maximum moment ratio, $M_{max}/\gamma'K_aH^3$ as a function of the net passive resistance, $2q_u$ - γ_eH, divided by the expression $\gamma'K_a$. The chart is, therefore, independent of the method of obtaining K_a and was developed for a wet unit weight, γ_s, equal to twice the submerged unit weight, γ'. To use Figure 22, the values for q_u and γ_e may be obtained from Table 3. For the sand backfill, δ may be found in Table 4 and K_a from Figure 3(a). A design example is given at the end of Problem No. 2 (pages 91-94).

ANCHORED WALLS

General - Anchored sheet pile walls derive their support by two means: passive pressure on the front of the embedded portion of the wall and anchor tie rods near the top of the piling. This method is suitable for heights up to about 35 feet, depending on the soil conditions. For higher walls the use of high-strength steel piling, reinforced sheet piling, relieving platforms or additional tiers of tie rods may be necessary. The overall stability of anchored sheet pile walls and the stresses in the members depends on the interaction of a number of factors, such as the relative stiffness of the piling, the depth of piling penetration, the relative compressibility and strength of the soil, the amount of anchor yield, etc. In general, the greater the depth of penetration the lower the resultant flexural stresses.

Figure 21 shows the general relationship between depth of penetration, lateral pressure distribution and elastic line or deflection shape.
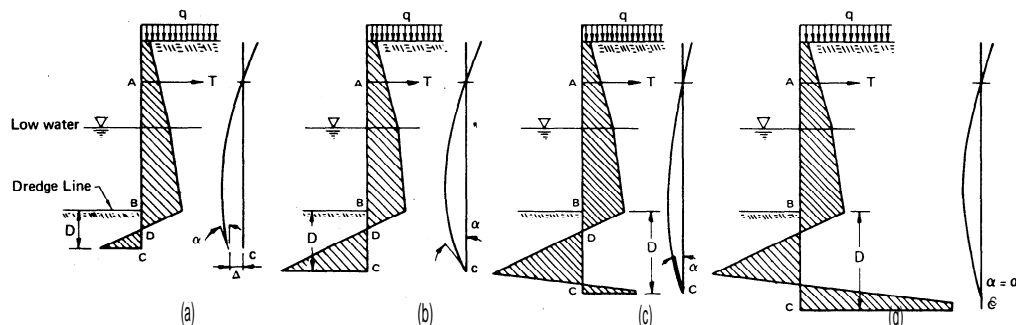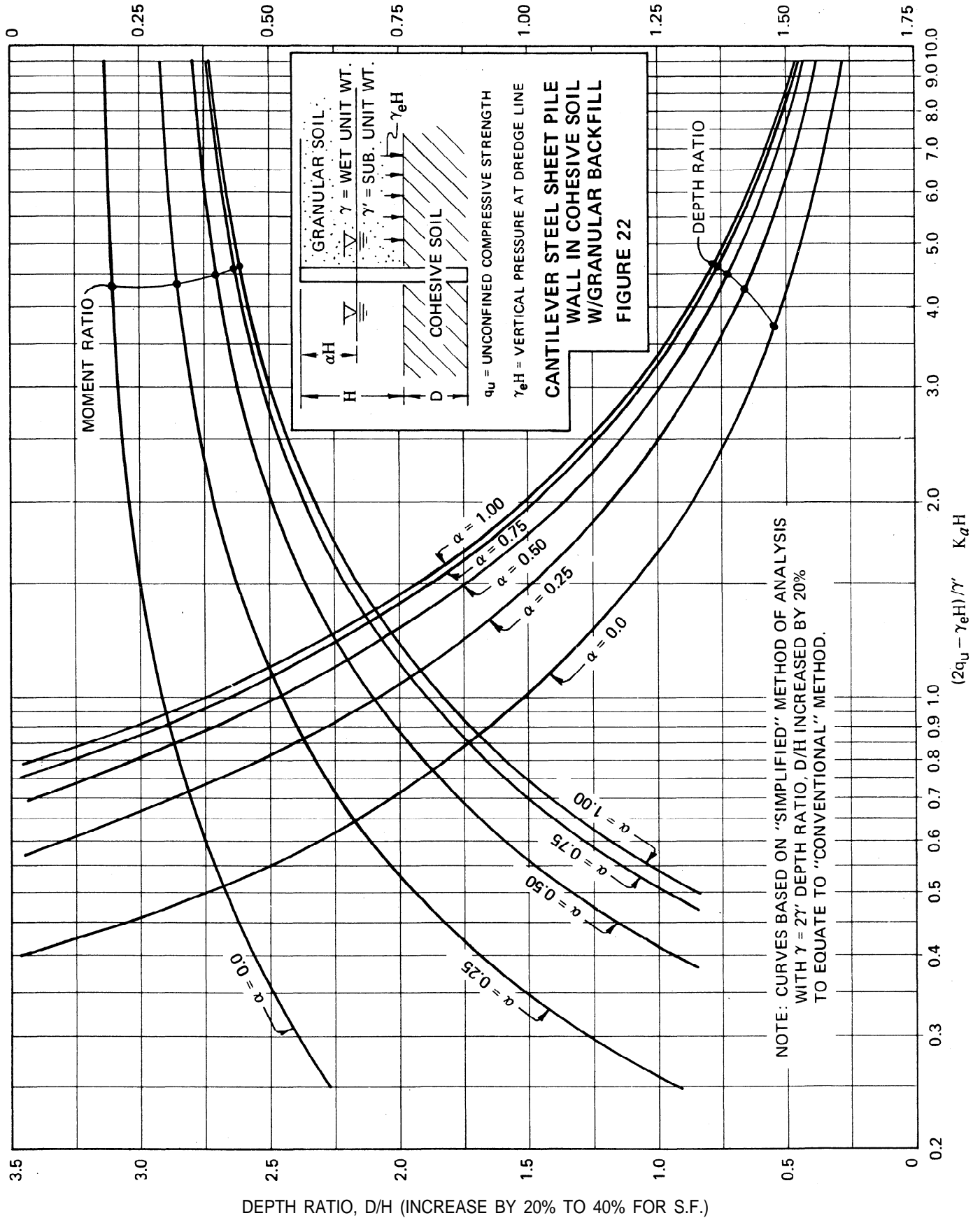

Fig. 21 - Affect of depth of penetration on pressure distribution and deflected shape

MOMENT RATIO PER FT. WIDTH,$M_{max}/\gamma' K_a H^3$

MOMENT RATIO

q_u = UNCONFINED COMPRESSIVE STRENGTH

$\gamma_e H$ = VERTICAL PRESSURE AT DREDGE LINE

GRANULAR SOIL :
γ = WET UNIT WT.
γ' = SUB. UNIT WT.

COHESIVE SOIL

CANTILEVER STEEL SHEET PILE
WALL IN COHESIVE SOIL
W/GRANULAR BACKFILL

FIGURE 22

DEPTH RATIO

$\alpha = 1.00$
$\alpha = 0.75$
$\alpha = 0.50$
$\alpha = 0.25$
$\alpha = 0.0$

$\alpha = 1.00$
$\alpha = 0.75$
$\alpha = 0.50$
$\alpha = 0.25$
$\alpha = 0.0$

$(2q_u - \gamma_e H)/\gamma'$ $K_a H$

NOTE: CURVES BASED ON "SIMPLIFIED" METHOD OF ANALYSIS
WITH $\gamma = 2\gamma'$ DEPTH RATIO, D/H INCREASED BY 20%
TO EQUATE TO "CONVENTIONAL" METHOD.

DEPTH RATIO, D/H (INCREASE BY 20% TO 40% FOR S.F.)

Case (a) is commonly called the free earth support method. The passive pressures in front of the wall are insufficient to prevent lateral deflection and rotations at point C. Cases (b), (c) and (d) show the effect of increasing the depth of penetration. In cases (b) and (c) the passive pressure has increased enough to prevent lateral deflection at C; however, rotation still occurs. In case (d) passive pressures have sufficiently developed on both sides of the wall to prevent both lateral deflection and rotation at C. This case is commonly called the fixed earth support method because point C is essentially fixed. Cases (a) and (d) represent the two extremes in design.

Some different methods in current usage for the design of anchored sheet pile walls are grouped and discussed in the following order:

> Free Earth Support Method
> Rowe's Moment Reduction Method
> Fixed Earth Support Method (Equivalent Beam)
> Graphical Methods
> Danish Rules

Free Earth Support Method - This method is based on the assumption that the soil into which the lower end of the piling is driven is incapable of producing effective restraint from passive pressure to the extent necessary to induce negative bending moments. The piling is driven just deep enough to assure stability, assuming that the maximum possible passive resistance is fully mobilized. The sheet piling is assumed to be inflexible and that no pivot point exists below the dredge line i.e., no passive resistance develops on the backside of the piling. Earth pressures may be computed by the Coulomb or log-spiral method. With these assumptions the design becomes a problem in simple statics. Procedures for the design of anchored sheet piling in granular and cohesive soil are discussed separately below.

Design in Granular Soil - Figure 23 shows the resulting pressure distributions for an anchored sheet pile wall in granular and cohesive soil. The following design procedure as suggested in Teng[1], may be used:
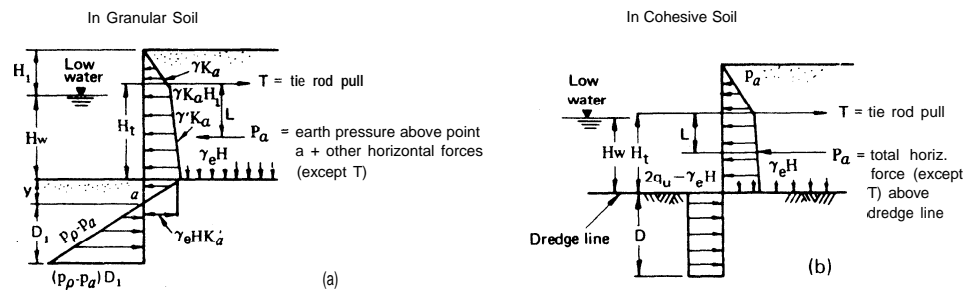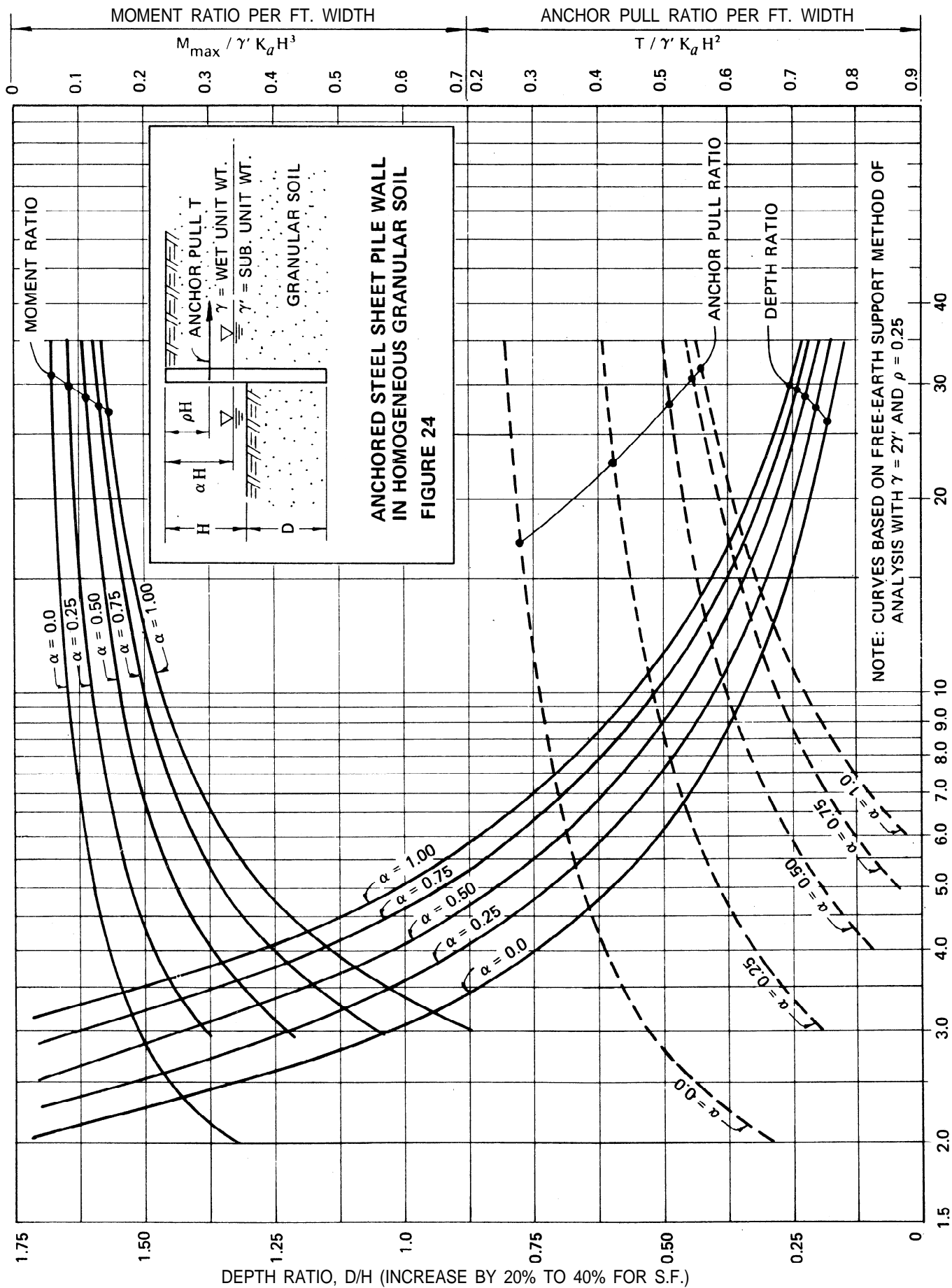

Fig. 23 - Design or anchored sheet piling by free-earth method (after Teng[1])

1. Compute the active and passive lateral pressures using appropriate coefficients of lateral earth pressure. If the Coulomb method is used, it should be used conservatively for the passive case.

Note: Figure 23 (a) shows the general case for an anchored wall in granular soil backfilled with granular material having different soil properties. Therefore, Ye refers to the equivalent soil unit weight, either wet to submerged, for the particular soil layer in question. Also, K_a' refers to the active pressure coefficient for the natural in-place granular soil.

2. Calculate the weight of overburden and surcharge load at the dredge level, $\gamma_e H$.

3. Locate the point of zero pressure given by

$$y = \gamma_e H K_a' / (p_\rho - p_a)$$

ANCHORED STEEL SHEET PILE WALL
IN HOMOGENEOUS GRANULAR SOIL
FIGURE 24

MOMENT RATIO PER FT. WIDTH

$M_{max} / \gamma' K_a H^3$

ANCHOR PULL RATIO PER FT. WIDTH

$T / \gamma' K_a H^2$

MOMENT RATIO

ANCHOR PULL T

γ = WET UNIT WT.
γ' = SUB. UNIT WT.

GRANULAR SOIL

ANCHOR PULL RATIO

DEPTH RATIO

NOTE: CURVES BASED ON FREE-EARTH SUPPORT METHOD OF
ANALYSIS WITH $\gamma = 2\gamma'$ AND $\rho = 0.25$

α = 0.0
α = 0.25
α = 0.50
α = 0.75
α = 1.00

α = 1.00
α = 0.75
α = 0.50
α = 0.25
α = 0.0

α = 1.0
α = 0.75
α = 0.50
α = 0.25
α = 0.0

DEPTH RATIO, D/H (INCREASE BY 20% TO 40% FOR S.F.)

28

4. Calculate P_a, the resultant force of the earth pressure above a, and its distance, L below the tie rod level.

5. To satisfy equilibrium, the wall must be deep enough so that the moment due to the net passive pressure will balance the moment due to the resultant active force P_a. Sum moments about the tie rod level.

$$\Sigma \ M_T = (L)(P_a) - \tfrac{1}{2}(p_\rho - p_a)D_1{}^2 \ (H_t + y + \tfrac{2}{3} D_1) = 0$$

Solve for D_1. Since the equation is cubic in D_1, a trial and error method would be appropriate.

6. Compute the tie rod tension given by

$$T = P_a - \tfrac{1}{2}(p_\rho - p_a)D_1{}^2$$

7. The maximum bending moment occurs at the point of zero shear in the wall, below the tie rod level.

8. Select the appropriate sheet pile section (Note: Use of Rowe's moment reduction theory can be utilized. This theory is discussed in a subsequent section.)

9. Add 20 to 40 per cent to D_1, to provide a margin of safety, or divide P_p by a factor of safety of 1.5 to 2.0 in steps 1, 3 and 4.

Design charts have also been developed for anchored walls in homogeneous granular soil for the free earth support method as shown in Figure 24.

These curves give the depth ratio, D/H, the maximum moment ratio, $M_{max}/\gamma' K_a H^3$, and the tie rod ratio, $T/\gamma' K_a H^2$, as a function of the ratio of the passive to active earth pressure coefficients, K_ρ/K_a. The curves are independent of the method of obtaining K_ρ or K_a. The curves in Figure 24 were developed for a wet unit soil weight, γ, equal to twice the submerged unit weight, γ', and a depth of anchor equal to 0.25H as shown. Resulting moments and tie rod tension are force per unit length of wall. To use Figure 24, one may determine ϕ and γ from Table 2, δ from Table 4, and K_ρ/K_a from Figure 3 (a). A design example is given at the end of Problem No. 1 (pages 95-100).

Design in Cohesive Soils - Figure 25 shows the resulting pressure distribution and application of the free earth support method for an anchored sheet pile wall in cohesive soil. The following design procedure may be used:

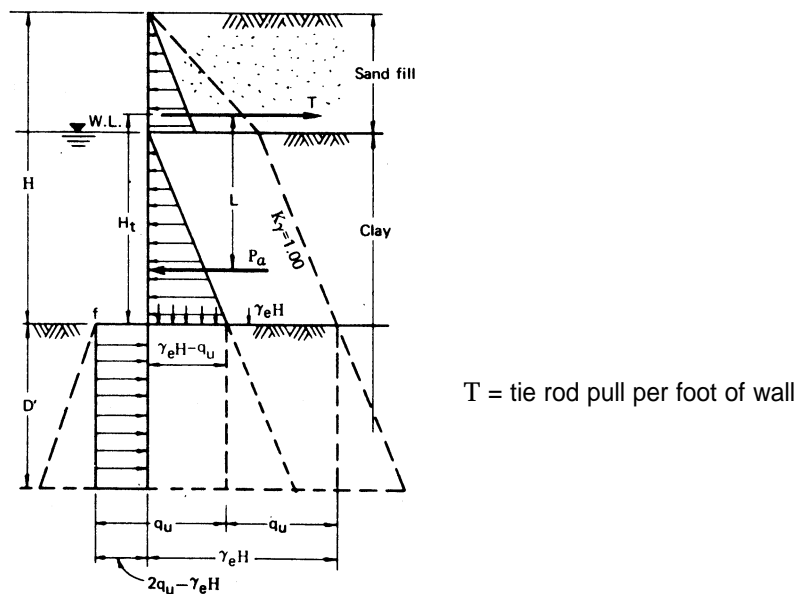T = tie rod pull per foot of wall

Fig. 25 - The free-earth-support method of anchored-bulkhead design in clay with granular backfill

1. Determine the immediate and long-term strength of the soil by undrained tests ($\phi \cong 0$) and drained tests ($c \cong 0$), respectively. Check stability to see that the design height is less than the critical height, $H < 2q_u/\gamma_e$, in order that a net passive pressure will result.
2. Calculate P_a, the resultant force due to active earth pressure (and surcharge, if any) above the dredge line.
3. To satisfy equilibrium sum moments about the tie rod level:

$$\Sigma\ M_T = (L)(P_a) - (4c - \gamma_e H)D'(H_t + \tfrac{1}{2}D') = 0$$

Solve for D'.
4. Compute the tie rod tension given by

$$T = P_a - (4c - \gamma_e H)D'$$

5. Determine the maximum bending moment at the point of zero shear.
6. Select the appropriate pile section. (Note: Use of Rowe's moment reduction theory can be utilized. This theory is discussed in a subsequent section.)
7. Add 20 to 40 per cent of D' or use 50 to 75 per cent of the full cohesion in steps 1 and 2.

Figure 26 presents design curves for anchored steel sheet pile walls in cohesive soil with granular backfill. These curves give the depth ratio, D/H, the maximum moment ratio, $M_{max}/\gamma'K_a H^3$, and the anchor pull ratio, $T/\gamma'K_a H^2$, as a function of the "net passive pressure coefficient," $(2q_u - \gamma_e H)/\gamma'K_a H$. The term $2q_u - \gamma_e H$ is the net passive pressure on the left side of the wall below the dredge line where $\gamma_e H$ is the vertical pressure at the dredge line. The term $\gamma'K_a H$ will normally vary from about 300 to 500, therefore practical values of $(2q_u - \gamma_e H)/\gamma'K_a H$ can be quite small for low strength soils. For this reason the curves have been extended to include this lower range. The curves in Figure 26 were developed for a wet unit soil weight, γ, equal to twice the submerged unit weight, γ', and for a depth of anchor rod below the top of the wall equal to 0.25H. To use Figure 26, the values for q_u and γ_e may be obtained from Table 3. For the sand backfill, 6 may be found on Table 4 and K_a from Figure 3 (a). A design example is given at the end of Problem No. 2 (pages 101-103).

Rowe's Moment Reduction Theory

Steel sheet piling is quite flexible causing earth pressures to redistribute or differ from the classical hydrostatic distribution. In particular it has been observed that the bending moment in sheet piling generally decreases with increasing flexibility of the piling. This is due to the interdependence between the type of deflection or yield of the buried portion of the sheet piling and the corresponding distribution of passive earth pressure. With increasing flexibility, the yield of the buried part assumes the character of a rotation about the lower edge of the bulkhead causing the center of the passive pressure to move closer to the dredge line. This in turn decreases the maximum bending moment. As a consequence, if a reduction in the maximum bending moment calculated by the free earth support method is neglected, an uneconomical and wasteful design will result. However, if the moment reduction is considered, a lower section modulus will be required introducing the possibility of using a lighter piling section.

Rowe [24, 25, 26, 27] has established a definite relationship between the degree of flexibility of an anchored bulkhead, expressed as a coefficient $\rho = (H + D)^4/EI$, and the reduction of the actual bending moment, M, as compared to the free earth support value, M_{max}. Figure 27 shows the relationship between the ratio M/M_{max} and p for both medium dense and very dense granular soils. For a given wall of height, H, analyzed by the free earth support method, the designer can develop "structural curves" for various piling sections and each grade of steel. Any section falling below the moment reduction curve for the appropriate relative soil density would be inadequate. A design example is given at the end of Problem No. 1 (pages 95-100) illustrating the use of Rowe's Moment Reduction Theory.
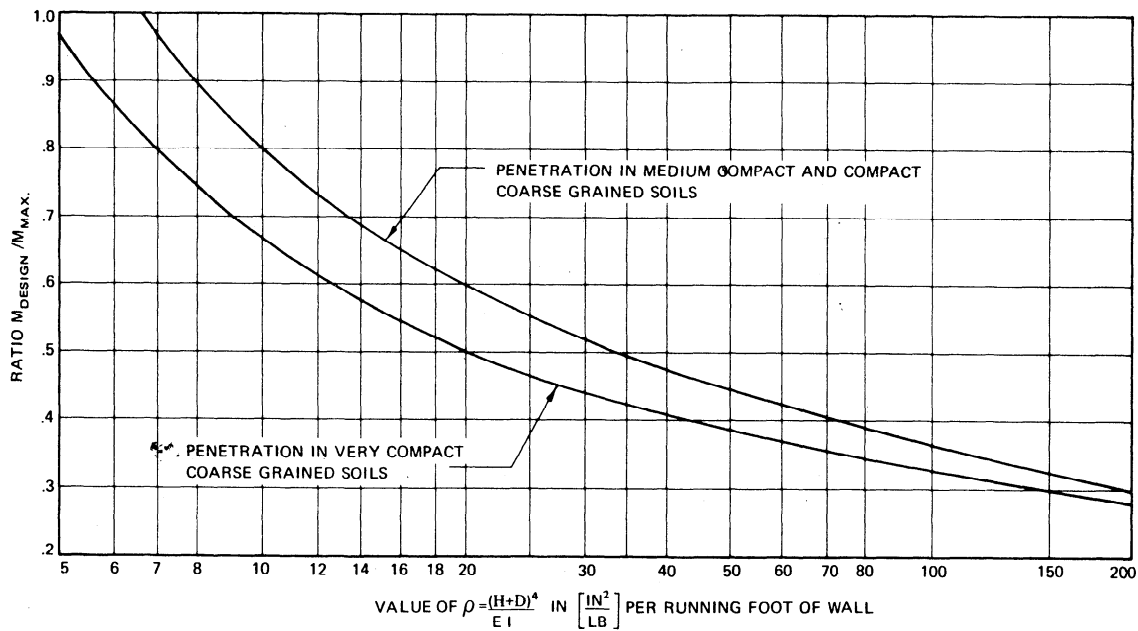
MOMENT RATIO PER FT. WIDTH

$$M_{max} / \gamma' K_a H^3$$

ANCHOR PULL RATIO PER FT. WIDTH

$$T / \gamma' K_a H^2$$

MOMENT RATIO

NOTE: CURVES BASED ON FREE-EARTH SUPPORT METHOD
OF ANALYSIS WITH $\gamma = 2\gamma'$ AND $\rho = 0.25$

$\alpha = 0.0$

$\alpha = 0.25$

$\alpha = 0.50$

$\alpha = 0.75$

$\alpha = 1.0$

q_u = UNCONFINED COMPRESSIVE
STRENGTH

$\gamma_e H$ = VERTICAL PRESSURE
AT DREDGE LINE

$\alpha = 0.75$

ANCHOR PULL RATIO

GRANULAR SOIL
ANCHOR PULL T

γ = WET UNIT WT.
γ'= SUB. UNIT WT.

$\gamma_e H$

COHESIVE SOIL

ANCHORED STEEL SHEET PILE WALL IN
COHESIVE SOIL W/GRANULAR BACKFILL

FIGURE 26

ρH

αH

H

D

DEPTH RATIO

$\alpha = 1.0$

$\alpha = 0.50$

$\alpha = 0.25$

$\alpha = 0$

$\alpha = 0.0$

$\alpha = 0.25$

$\alpha = 0.50$

$\alpha = 0.75$

$\alpha = 1.0$

DEPTH RATIO, D/H (INCREASE BY 20% TO 40% FOR S.F.)

Fig. 27 - Rowe's moment reduction curves (after Navdocks[1i])

Rowe has also extended the moment reduction theory to cohesive soils by introducing the stability number concept. The stability number is the ratio of the cohesion below the dredge line to $\gamma_e H$ at the dredge line and is a measure of the net passive resistance. To account for adhesion, Rowe has proposed the definition:

$$S = \frac{c}{\gamma_e H} \sqrt{1 + \frac{c_a}{c}} = 1.25 \frac{c}{\gamma_e H} \qquad \text{(for design purposes)}$$

Figure 28 shows the relationship established between the stability number as defined above and the ratio of the design moment, M, to the maximum moment, M_{max}, calculated by the Free earth support method for various height to total length ratios, α.

Flexibility number $\rho = \dfrac{(H+D)^4}{EI}$ Stability number $S = \dfrac{1.25c}{\gamma_e (H+D)}$

H = f t

E = psi

I = in.^{4}/ft of piling

c = cohesion, psf

$\gamma_e \doteq$ pcf

H = ft
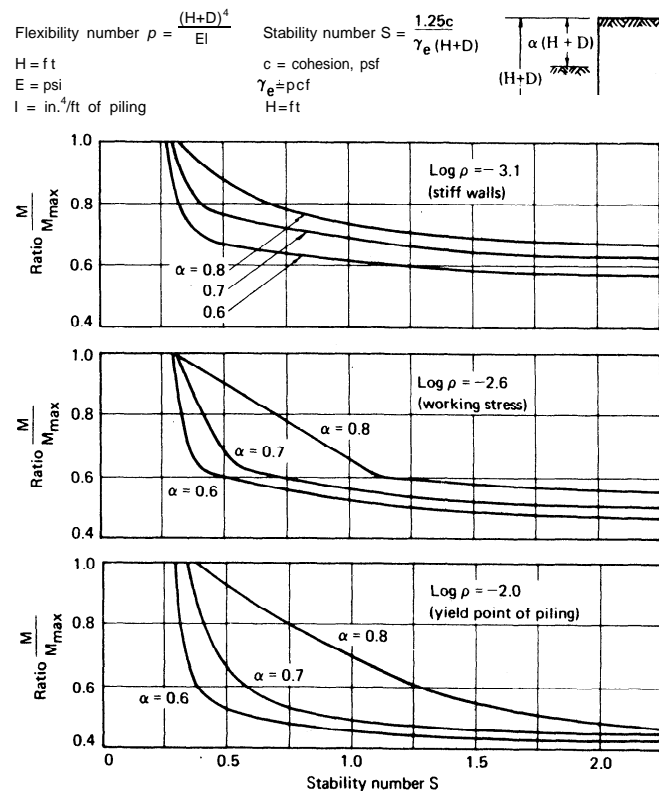
Fig. 28 - Moment reduction for cohesive soils (after Teng[1])

32

Curves for three wall flexibility numbers are given. The designer, knowing the stability number, S, and the depth to height ratio, α, can determine the moment reduction and, therefore, size the piling for a particular flexibility p. Values of p between those given can be interpolated. The stability number concept will be expanded in a later section.

Fixed Earth Support Method (Equivalent Beam Method) -- This method is based on the assumption that the wall deflections, $\triangle$, are such that the elastic line of the wall will take the shape indicated on Figure 29.

Fig. 29 - Fixed earth support method

The deflected shape reverses its curvature at the point of contraflexure, c, and becomes vertical at point t. Consequently, the wall acts like a partially built-in beam subjected to bending moments.

To produce this deflected shape, the wall must be driven deep enough so that the soil beneath the dredge line provides the required restraint on the bulkhead deformations. The elastic line method of assuming a depth of penetration and calculating the resulting deflected shape to see that it agrees with the assumption is very time consuming and very seldom used in practice. Blum (see Tschebotarioff[3]) has developed a much simpler procedure known as the equivalent beam method, utilizing a theoretical relationship between the angle of internal friction, ϕ, and the distance, x, to a point of contraflexure. Figure 30 illustrates the method, which is limited in its use to granular soils.

Fig. 30 - Equivalent beam method (after Teng[1])

The equivalent beam method assumes a hinge at the point of contraflexure, since the bending moment there is zero. The part above the hinge can then be treated as a separate, freely supported beam with an overhanging end as shown in Figure 30 (d). The reactions R and T and the bending moments can then be determined from statics and simple beam theory. The lower portion, below the point of contraflexure, can also be analyzed as a separate, freely supported beam on two supports, R and C. Based on these assumptions, the sheet piling in granular soils may be designed by the following steps:

1. Compute the active and passive lateral pressures using the appropriate earth pressure coefficients.

2. Determine the distance, y, from:
$$y = \frac{\gamma_e H K_a'}{p_\rho' - p_a'}$$

where $\gamma_e H$ = weight of backfill and surcharge load above the dredge line, using buoyant weight for soil below the water level

K_a' = coefficient of active earth pressure for the soil below the dredge line

3. Locate the point of contraflexure by the chart shown in Figure 30 (e).
4. Determine the reaction R at the point of contraflexure. R is the horizontal reaction at point b obtained by treating the piling above b as a simple beam supported at b and at the tie rod level as shown in Figure 30 (d).
5. Treat the lower portion of the piling, eb, as a simple beam and determine the dimension eb by equating the moment about the base e to zero.
6. The depth of penetration, D, is equal to the sum of the dimensions eb and x. To provide a margin of safety, either add 20 to 40 per cent to the calculated depth of penetration, D, or use a reduced value of K_ρ' by dividing it by a safety factor of 1.5 to 2.0.
7. Determine the maximum bending moment at the point of zero shear and size the piling.

Generally the point of contraflexure and the point of zero pressure are very close and for design purposes the value of x may be taken equal to y. For this case, the depth of penetration may be expressed by the following equation:

$$D = y + \sqrt{\frac{6R}{p_\rho' - p_a'}}$$

where
Y = distance from the dredge line to the point of zero pressure

R = horizontal reaction at o, obtained by assuming the piling is simply supported at point o and at the tie rod level

p_ρ', p_a' = passive and active earth pressures in the soil below the dredge line

A design example is given illustrating the Equivalent Beam Method (Problem No. 3, pages 104 - 106).

Tschebotarioff[3] has proposed the use of an even more simplified equivalent beam procedure, as shown in Figure 31.
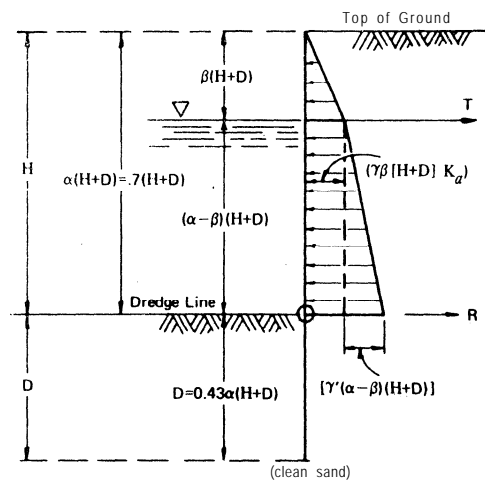
Fig. 31 - Simplified equivalent beam method (after Tschebotarioff[3])

By this method, a hinge is assumed at the dredge line and the depth of penetration is set at $0.43\alpha(H+D)$. To determine bending moments, the bulkhead above the dredge line is treated as a statically determinate beam on two supports, T and R, with an overhanging end. The reader is directed to Soil *Mechanics, Foundations and Earth Structures,* by G. P. Tschebotarioff for a more detailed discussion.

Graphical Methods - Graphical methods can sometimes be advantageously used to design sheet pile retaining walls especially for cases of complex or irregular loading. The lateral pressure distribution is first determined by the methods previously outlined. The maximum bending moment and the anchor pull are then determined by application of the graphical methods. The wall and the corresponding pressure diagram is divided into a number of equal panels or sections as shown in Figure 32. The resultant earth pressure on each panel is replaced by an equivalent concentrated force acting through the center of the section and drawn to a convenient scale. The method for the design of anchored and cantilevered walls differs slightly and will be discussed separately below.

Cantilevered Wall - Once the wall has been divided and the equivalent forces determined, a vector diagram or string polygon is constructed (Figure 32) as follows. On a horizontal base line, commencing at the right, the successive force vectors for each panel from the point of zero pressure to the bottom of the wall are laid off end to end i.e., the passive equivalent forces. The theoretical depth of the sheet piling is unknown; therefore, arbitrary depth must be chosen. A pole 0 is then selected at a distance from the base line equal to

$$\frac{\text{selected scale of the moments}}{\text{scale of the equivalent forces x scale of lengths}}$$

The moment scale is selected so as to give a convenient size of drawing. The successive equivalent active force vectors above the point of zero pressure are laid off end to end on a horizontal line originating at the pole 0 and extending to the right. From pole 0 lines are drawn to the ends of all the passive load vectors and from the right hand edge of the passive load line to the ends of all the active load vectors. This procedure is relatively simple and is illustrated in Figure 32.

The moment diagram is then drawn as follows. Starting at the top of the piling at point 0', the line 0'-1' in the moment diagram is drawn parallel to line A-l of the vector diagram, intersecting the first or top load line of action at point 1'; from point 1' line 1'-2' is then drawn parallel to line A-2 of the vector diagram intersecting the second load line of action at 2'. The process is continued through all sections including both active and passive lines.

62.1	
186.2	
310.4	
434.6	
558.8	
683.0	
809.2	
461.0	

434.7 PSF

y = 2.14

$K_p - K_a$

204.4
613.3
1022.2
1431.1
1840.
2248.9
2657.8
3066.7

SOIL PROPERTIES

γ = 115 PCF
γ' = 65 PCF
ϕ = 35°
K_a = 0.27
K_p = 6.29

SCALES

DISTANCE: 1″ = 8 FT.

MOMENT: 1″ = 32,000 FT·LB

FORCES: 1″ = 4,000 LB

POLE DISTANCE: $\frac{32,000}{8 \times 4000} = 1$ IN.

Fig. 32

P_a = 3505.3 K/FT.

$P_p = \frac{1}{2}(K_p - K_a)\gamma' d_o^2$

$P_p = \frac{1}{2}(6.29)(65)(7.1)^2$

P_p = 10.305 K/FT.

$R_c = P_p - P_a$ = 6,800 K/FT.

$\Delta = \frac{0.45(6800)}{2903}$ = 1.05 FT.

$D = y + D_o + \Delta$

$D = 2.14 + 7.1 + 1.05$

D = 10.3 FT.

M_{max} = 30,240 FT·LB

D_o = 7.1′

5′ 4′ 3′2′ 1′

P_a

Fig. 32 - (Continued)

35
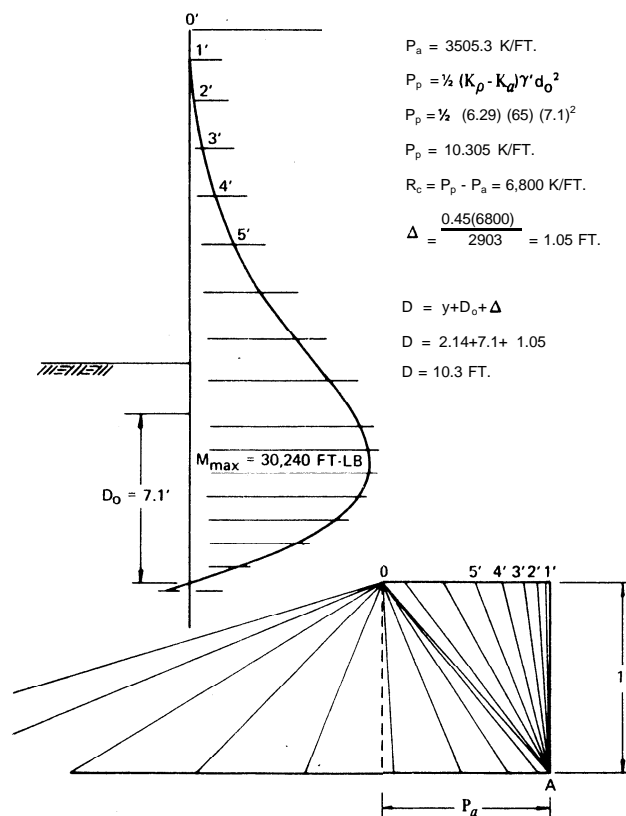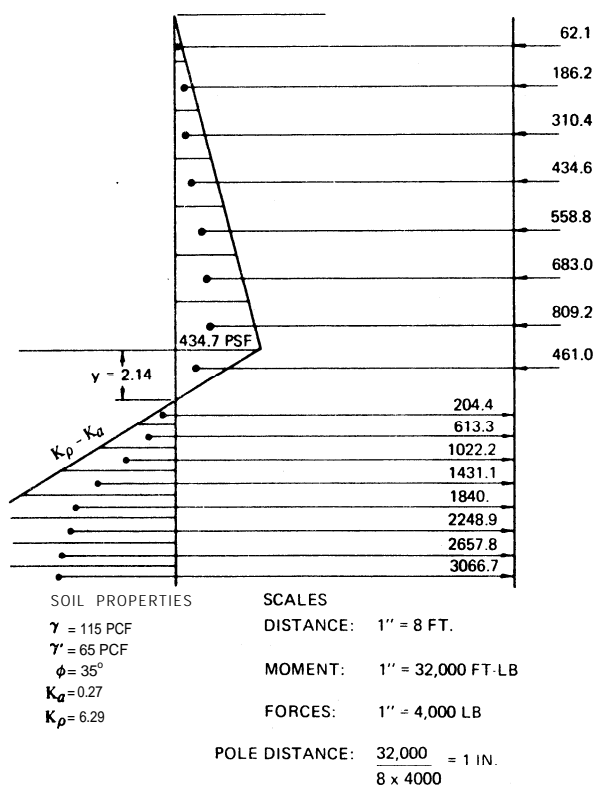
The theoretical penetration, D_o, to the point of rotation or zero deflection, c, is determined by the intersection of the line of moments with the tangent at the top of the wall. If the tangent does not intersect, more passive pressure is needed and the assumed depth must be increased. Below this point the wall deflects in the opposite direction causing passive pressure to develop on the right hand side. The additional driving depth required to develop the passive pressure to balance forces may be approximated by

$$\triangle = \frac{0.45R_c}{q_c}$$

where
$\triangle$ = the additional required driving depth
R_c = the reaction at c due to the passive pressure below c
q_c = the passive pressure (on the left) at c i.e., $(K_\rho - K_a)\gamma_e D_o$

The reaction R_c is found from the vector diagram and is equal to P_ρ - P_a where

$$P_\rho = \frac{q_c D_o}{2}$$

Therefore, the total depth required below the dredge line is

$$D = y + D_o + \triangle$$

where y is the distance from the dredge line to the point of zero pressure. The elastic line of the wall assuming fixity at point c can be found by the same method using the moment diagram as a lateral pressure diagram. In this way, the deflection at the top of the wall can be checked for tolerance.

Anchored Walls -- The vector diagram or string polygon may also be used to design anchored walls by use of the simplified equivalent beam method. The vector diagram is drawn as shown in Figure 33. On a horizontal line commencing at the right, the successive loads for the sections from the bottom to the top of the equivalent beam are laid off end to end. The pole distance is selected as for cantilevered walls. The moment diagram is constructed exactly as in the cantilevered case starting at the bottom of the equivalent beam. The line drawn for the top section of the moment diagram is projected back to intersect the line of action of the anchor pull at A'. From A' a straight line is then drawn to the starting point 0'. This straight line is the base line of the moment diagram and its inclination depends on the position of 0 in the vector diagram. The line A-O in the vector diagram is drawn through 0 parallel to A'-0' and gives the magnitude of the anchor tension and the equivalent reaction at the point of zero pressure. The maximum bending moment is found by scaling the maximum horizontal distance from A'-0' to the curve in the moment diagram. The total depth of penetration is obtained from the equation

$$D = y + \sqrt{\frac{6R}{\gamma_e(K_\rho' - K_a')}}$$

where
R = the equivalent reaction at the base found from the vector diagram
Y = the distance from the dredge line to the point of zero pressure
Y_e = effective unit soil weight below the dredge line

To provide a margin of safety, D is usually increased by about 20 per cent.

Surcharge
q = 700 Lbs. per Sq. Ft.

Scale: Length—Feet
Scale: Length—Inches

533 Lbs.
666 Lbs.

Anchor Tension = 8,450 Lbs. per Ft. of Width

799 Lbs.
932 Lbs.
566 Lbs. per Sq. Ft.
1,065 Lbs.

1,426 Lbs.
1,518 Lbs.

1,610 Lbs.

1,702 Lbs.

1,794 Lbs.

1,886 Lbs.

968 Lbs. per Sq. Ft.
1,422 Lbs.
408 Lbs.

LOADING DIAGRAM

$H = 22'0''$
$H_w = 12'0''$
$\alpha H = 10'0''$
690 Lbs. per Sq. Ft.
3.79'
D = 18.6'

R = 7,311 Lbs. per Ft. of Width

Slope = $(p_p - p_a)$ = 255 Lbs. per Sq. Ft.

0   250   500   1,000   Scale: Pressures—Lbs. per Sq. Ft.
0   500   1,000   2,000   Scale: Lateral Loads—Lbs. per Ft. of Width

490,000   Max. Bending Moment
Inch-Lbs.

MOMENT DIAGRAM

0   250,000   500,000   1,000,000
Scale: Bending Moment
Inch-Lbs. per Ft. of Width

VECTOR DIAGRAM

Pole Distance (in inches)
$\dfrac{\text{Scale of Moments (in.-lb. per in.)}}{\text{Scale of Lateral Loads (lbs. per in.)}}$
X Scale of Length (in. per in.)

Pole Distance

533
408
666 799 932 1,065 1,426 1,518 1,610 A 1,702 1,794 1,886 1,422
14 13 12 11 10 9 8 7 6 5 4 3 2 1
Anchor Tension = 8,450 Lbs.
Equivalent Reaction at Toe
R = 7,311 Lbs.

0   1,000 2,000   4,000   6,000   8,000   10,000
Scale: Lateral Loads—Lbs. per Ft. of Width

Fig. 33 - Graphical determination of bending moment and anchor load on steel sheet piling wall

Danish Rules - The Danish Rules, published by the Danish Society of Civil Engineers, are based on studies of a number of existing sheet pile structures and are purely empirical. They apply to single anchored sheet pile walls in cohesionless material and represent the least conservative approach to design. Although the Danish Rules have been subject to considerable criticism, especially with respect to the assumed pressure distribution, they have formed the design basis for many very economical sheet pile structures in use today.

Figure 34 shows the assumed pressure distribution on a sheet pile wall. The wall is assumed to be simply supported at points A and B, where B is located at the center of the passive resistance. The active earth pressure distribution is obtained by Coulomb's Theory (with no wall friction) and modified by a parabola to decrease the lateral pressure in the middle region of AB by an amount q, and increase the pressure by 1.5q at A. The quantity q may be considered a reduction factor due to the arching effect of the soil, thereby causing concentration near the top and bottom of the wall.
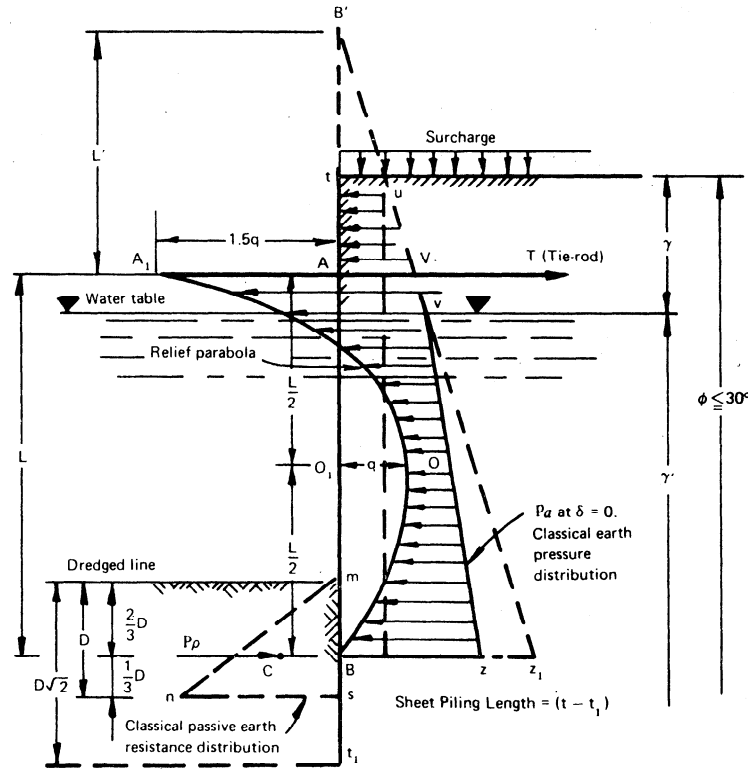
Fig. 34 - Danish method of sheet pile wall design

The magnitude of q, the parabolic stress relief ordinate, is expressed by

$$q = k \frac{10L' + 4L}{10L' + 5L} P_m$$

where L' = height of soil above point A, including the equivalent height of surcharge converted in terms of γ of the backfill

L = length AB.

P_m = the equivalent uniformly distributed pressure on the wall between the simple supports A and B that will give the same bending moment, M_l, as the trapezoidal Coulomb active pressure distribution AVZB, i.e., $p_m = 8M_L/L^2$

and $k = \dfrac{1}{1 + \dfrac{0.01}{\sin\bar{\phi}} \sqrt{\dfrac{(1 + n)Ea}{L\sigma_{all}}}}$

where $\bar{\phi}$ = average angle of internal friction between points A and B

n = ratio of the negative bending moment at the anchor level to the maximum positive bending moment of the span, L, below the tie rod

E = modulus of elasticity of steel = 29×10^6 psi

a = distance between extreme fibers of sheet piling

σ_{all} = allowable steel bending stress in sheet piling

The value of k varies from about 0.80 to 0.90 for steel and may be assumed equal to 0.9 for design purposes.

The bending moments and anchor pull can be determined from the pressure distribution established between A and B. The following approximate relationships may be used, The tension, T, in the tie rod at point A is

$$T = A_L + A_o + \frac{M_o}{L} - \frac{1}{12}qL$$

where　　A_L = reaction at A corresponding, to the earth pressure diagram AVZB.

A_o = resultant of the pressure above the tie rod

M_o = cantilever moment at A due to the pressure above the tie rod

The soil reaction at B is　　　$B = B_L - \frac{M_o}{L} - \frac{1}{3}qL$

where　　B = reaction at B corresponding to the earth pressure diagram AVZB

The maximum positive bending moment to be used for design of the sheet piling is

$$M = M_L - \frac{M_o}{2} - \frac{17}{192}qL^2$$

where　　M_L = the maximum bending moment corresponding to the earth pressure diagram AVZB

The required depth, D, is determined by the condition that the total passive earth pressure, calculated according to Coulomb's Theory (with $\delta = \frac{1}{2}\phi$), should equal the reaction B. This necessitates a trial and error approach. The driving depth should be increased to $D\sqrt{2}$ to provide a margin of safety of approximately 2.

High Sheet Pile Walls (Two Anchor System) - When the height between the dredgeline and the anchor is greater than about 35 feet, it may prove economical to utilize a second tie rod at a lower level. This will reduce both the moment in the wall and the required depth of penetration. Figure 35 shows two arrangements for a sheet pile wall having two tie rods. Method (a) is preferred because the different tie rod lengths and separate anchors used in method (b) tend to cause different horizontal deflections at the two wales.
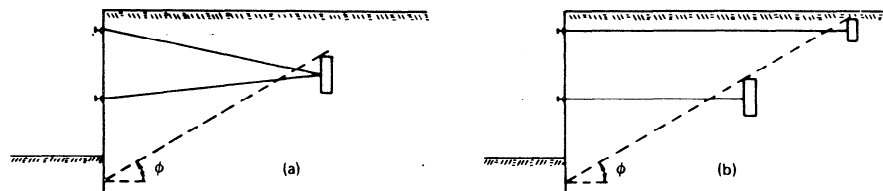
Fig. 35 - Typical anchorage for two tie rods

The principles of design for multiple tie rods are the same as for walls having one tie rod. A convenient method to investigate alternate designs for two ties is as follows:

1.　Referring to Figure 36, calculate the deflection, $\triangle_2$, of a single tie wall at the proposed level of the second tie. Then the tension, T_2, in the lower tie is simply that force applied at the lower tie rod level that is necessary to produce an equal, but opposite deflection $\triangle_2$ in the single tie wall. The wall can be treated as a simple span between the upper tie rod and the resultant, R_P, of the passive resistance, as shown in Figure 36
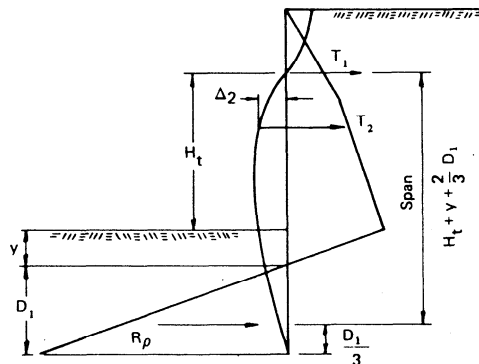
Fig. 36 - Analysis with two tie rods

If backfilling is commenced before the installation of the lower tie rod, an initial deflection, δ', will occur in the wall. Consequently, the calculated force in the lower tie rod will be reduced by the ratio $(\delta_2 - \delta')/\delta_2$, since the actual deflection, δ', cannot be counteracted.

2. The reduction of tension in the top tie rod due to the introduction of the lower tie rod is equal to the reaction of the simple span mentioned above with a single point load equal to the tension in the lower tie rod. Allowance should be made for the increased tension in both tie rods if they are inclined, as in Figure 35 (a). Once T_1 and T_2 are determined, the depth of penetration can be revised by statics; however, it is wise to keep in mind that the above methods are only approximate. It is recommended that any reduction factor be omitted if a wall has two or more tiers of tie rods.

STABILITY OF SHEET PILE WALLS

The height of a sheet pile wall driven in cohesive soils is limited by the initial strength of the clay below the level of the dredge line. This is true for anchored or cantilevered walls and for either granular or cohesive backfill above the dredge line. For heights in excess of this limit, the wall will fail. Therefore, the first step in the design of sheet pile walls in cohesive soils should be the investigation of the limiting height.

Figure 37 shows a sheet pile wall driven in cohesive soil together with the lateral earth pressures below the dredge line. The net passive resistance below the dredge line is given by:

$$p_\rho - p_a = [q_u + \gamma(Z-H)] - [\gamma_e H + \gamma(Z-H) - q_u] = 2q_u - \gamma_e H$$

where
q_u = unconfined compressive strength = twice the cohesion, c.
γ_e = the effective unit weight of soil above the dredge line = moist unit weight above water level and submerged unit weight below water level
Z = depth below ground line.
H = the height of the soil above the dredge line, including the equivalent height of any uniform surcharge
γ = unit weight of soil below the dredge line

If the height of the wall, H, is such that the net passive resistance is zero, failure will occur. This will occur when $2q_u = \gamma_e H$, that is, when the ratio $2q_u/\gamma_e H = 1$. Rowe[27] has introduced the concept of the stability number, S, defined as:

$$S = \frac{q_u}{2\gamma_e H}$$
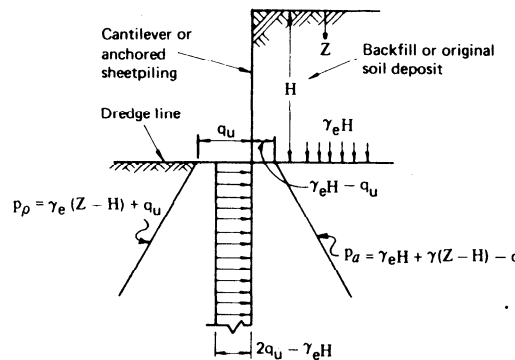
Fig. 37 - Stability of sheet piling in cohesive soils (after Teng[1])

Since adhesion, c_a, will develop between the soil and the sheet piling, the stability number may be modified as:

$$S = \frac{c}{\gamma_e H} \sqrt{1 + \frac{c_a}{c}}$$

where
C_a = the wall adhesion

Table 5 gives recommended values of adhesion for various soil strengths.

CONSISTENCY OF SOIL	COHESION, C PSF	ADHESION, C_a PSF
VERY SOFT	0 - 250	0 - 250
SOFT	250 - 500	250 - 480
MEDIUM STIFF	500 - 1000	480 - 750
STIFF	1000 - 2000	750 - 950
VERY STIFF	2000 - 4000	950 - 1300

Table 5 - Approximate values of adhesion (after Navdocks[11])

For design, it is sufficient to take the value of $\sqrt{1 + (c_a/c)}$ as 1.25 and, therefore, S = 0.31. Hence, a sheet pile wall driven into cohesive soils should have a minimum stability number of about 0.31 times an appropriate safety factor.

The conventional Swedish Circular Arc method for unretained earth slopes can also be used to check the stability of the soil adjacent to a sheet pile wall. The method can be applied to soil having both internal friction, ϕ, and cohesion, c. Figure 38 illustrates the method. The factor of safety is defined as the resisting moment divided by the driving moment. Referring to Figure 38, the resisting and driving moments are:

$$\text{Driving Moment} = \sum_{i=1}^{N} W_i \times \ell_i \text{ or } R \sum_{i=1}^{N} T_i$$

$$\text{Resisting Moment} = R \sum_{i=1}^{N} L_i c_i + R \sum_{i=1}^{N} N_i \tan\phi_i$$

where
W_i = weight of the ith slice
ℓ_i = lever arm of the ith slice about 0
L_i = length of circular arc at the base of the ith slice.
c_i = cohesion at the base of the ith slice.
N_i = normal component of the weight of the ith slice.
R = radius of the circular arc.
$\tan\phi_i$ = angle of internal friction at the base of the ith slice.
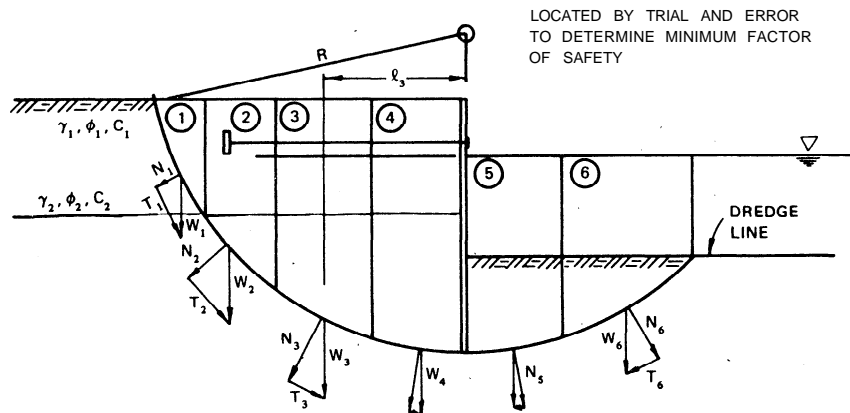
Fig, 38 - Swedish arc method of stability

This method is also applicable to stratified deposits. The soil properties for each layer should be used to calculate the weights and resistance at the base of each slice. Any water above the dredge line should be included in the weight of the slice. The reader should refer to a standard text on soil mechanics, such as *Fundamentals of Soil Mechanics* by D. Taylor[18] for a more detailed discussion;

DESIGN OF ANCHORAGE SYSTEMS FOR SHEET PILE WALLS

TIE RODS

Tie rods are frequently subjected to tensions much greater than the calculated values. The conventional methods of calculating anchor pull involve the assumption that the resulting active pressure distribution is hydrostatic, or triangular. In reality, the real distribution may be somewhat different and the corresponding anchor tension may be greater. than that computed. The anchor pull may also increase because of repeated application and removal of heavy surcharges or an unequal yield of adjacent anchorages that causes overloading. Because of these possibilities, the computed tie rod design tension should be increased by about 30 per cent for the tie rod proper, and 50 to 100 per cent at splices and connections where stress concentration can develop. The pull on a tie rod before any increase is assessed would then be

$$A_\rho = \frac{T \times d}{\cos \alpha}$$

where A_ρ = the anchor pull in pounds per tie, rod
          T = the anchor pull in pounds per foot width of wall
          d = distance between rods in feet (center to center)
          a = inclination of tie rod with the horizontal

Any soft soil below the tie rods, even at great depth, may consolidate under the weight of recent backfill, causing the ground to settle. A small settlement will cause the tie rods to sag under the weight of the soil above them. This sagging will result in an increase in tensile stress in the tie rod as it tends to pull the sheeting. In order to eliminate this condition, one of the following methods may be used:

1. Support the tie rods with light vertical piles at 20 to 30-foot intervals.
2. Encase the anchor rods in large conduits

Tie rods are usually round structural steel bars with upset threaded ends to avoid a reduction in the net area due to the threads. In order to take up slack, turnbuckles are usually provided in every tie rod.

WALES

The horizontal reaction from an anchored sheet pile wall is transferred to the tie rods by a flexural member known as a wale. It normally consists of two spaced structural steel channels placed with their webs back to back in the horizontal position. Figure 39 shows common arrangements of wales and tie rods located on both the inside and outside of a sheet pile wall. The channels are spaced with a sufficient distance* between their webs to clear the upset end of the tie rods. Pipe segments or other types of separators are used to maintain the required spacing when the channels are connected together. If wales are constructed on the inside face of the sheet piling, every section of sheet piling is bolted to the wale to transfer the reaction of the piling. While the best location for the wales is on the outside face of the wall, where the piling will bear against the wales, they are generally placed inside the wall to provide a clear outside face.
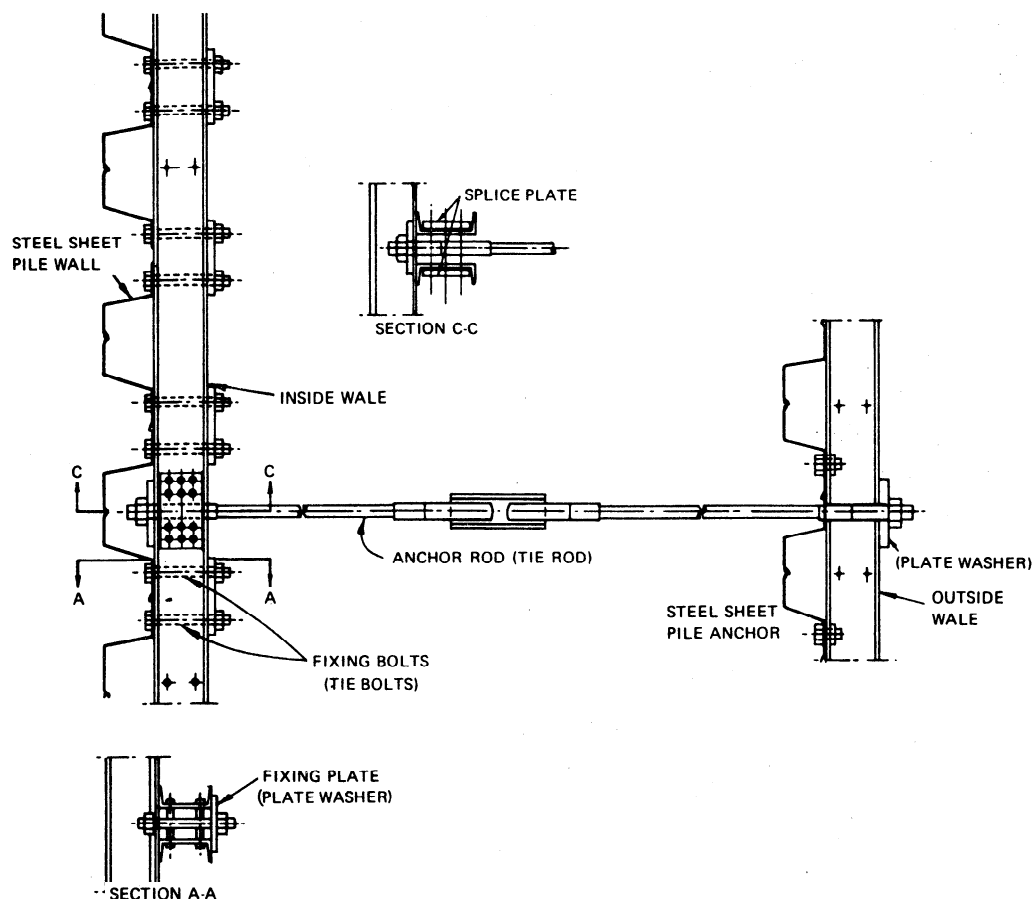
Fig. 39 - Typical wale and anchor rod details

For sizing purposes, the response of a wale may be assumed to be somewhere between that of a continuous beam on several supports (the tie rods) and a single span on simple supports. Therefore, the maximum bending moment for design will be somewhere between

$$M_{max} = (1/10)Td^2 \quad \text{(three continuous spans - simply supported)}$$

$$M_{max} = (1/8)Td^2 \quad \text{(single span - simply supported)}$$

where   T = the anchor pull in pounds per foot (before increase).
               d = distance between rods in feet (center to center)

The above expressions are only approximations. An exact analysis would have to take into account the elasticity of the tie rods, the rigidity of the wale and the residual stresses induced during bolting operations.

The required section modulus of the wale is

$$S = \frac{M_{max}}{\sigma_{all}}$$

where   S = the section modulus of the wale for both channels
          = allowable steel bending stress

Wales are connected to the sheet piling by means of fixing plates and bolts. Each bolt transmits a pull proportional to the width, ℓ, of a single sheet pile, and equal to

$$R_b = T \times \ell \times F.S.$$

where R_b = pull in pounds per bolt

         ℓ = the driving distance of a single sheet pile *(if* each section is bolted)

    F.S. = a desired safety factor to cover stresses induced during bolting (between 1.2 and 1.5)

The fixing plate (as shown in Figure 39, Section A-A) may be designed as a beam simply supported at two points (the longitudinal webs of the wale) and bearing a single load, R_b, in the center.

The wales are field bolted at joints known as fish plates or splices, as shown in Figure 39, Section C-C. It is preferable to splice both channels at the same point and place the joint at a recess in the double piling element. Splices should be designed for the transmission of the bending moment. The design of tie rods and wales is illustrated in Problem No. 4a (pages 107-110).

ANCHORS

The stability of an anchored sheet pile bulkhead depends mainly on the stability of the anchor device to which the wall is fastened. The reaction of the tie rods may be carried by any one of the types of anchorages shown in Figure 40.
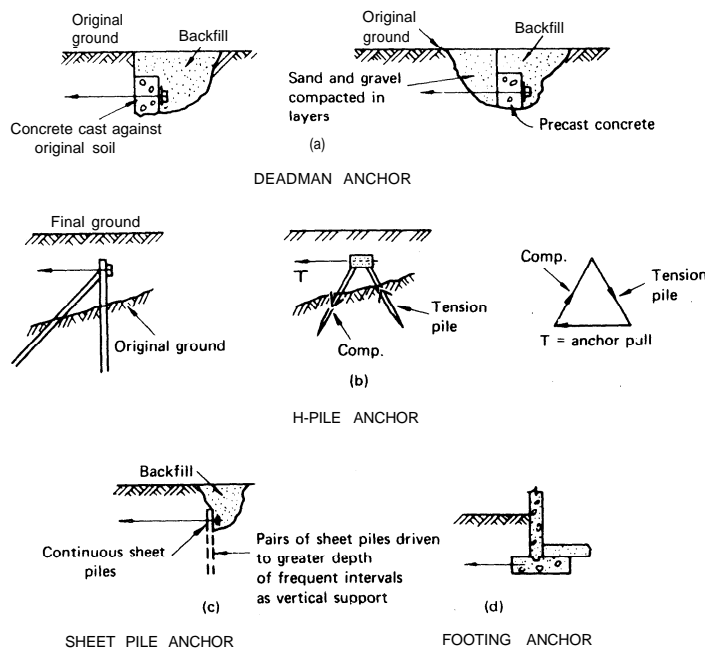
Fig. 40 - Types of anchorage systems (after Teng[1]).

Location of Anchorage - In order for an anchorage system to be effective it must be located outside the potential active failure zone developed behind a sheet pile wall. Its capacity is also impaired if it is located in unstable ground or if the active failure zone prevents the development of full passive resistance of the system. Figure 41 shows several installations that will not provide the full anchorage capacity required because of failure to recognize the above considerations.
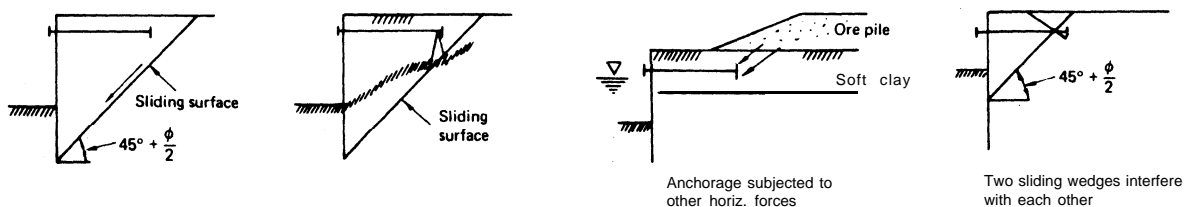
Fig. 41 - Installations having reduced anchorage capacity (after Teng[1])

44

Figure 42 shows the effect of anchorage location on the resistance developed.

Anchor left of bc provides no resistance.

Anchor right of bf provides full resistance with no transfer to wall.

Anchor between bc and bf provides partial resistance and transfers $\triangle P_\rho$ to wall.

Vector diagram for free body abde where P_a = active force on back of de at anchor block.
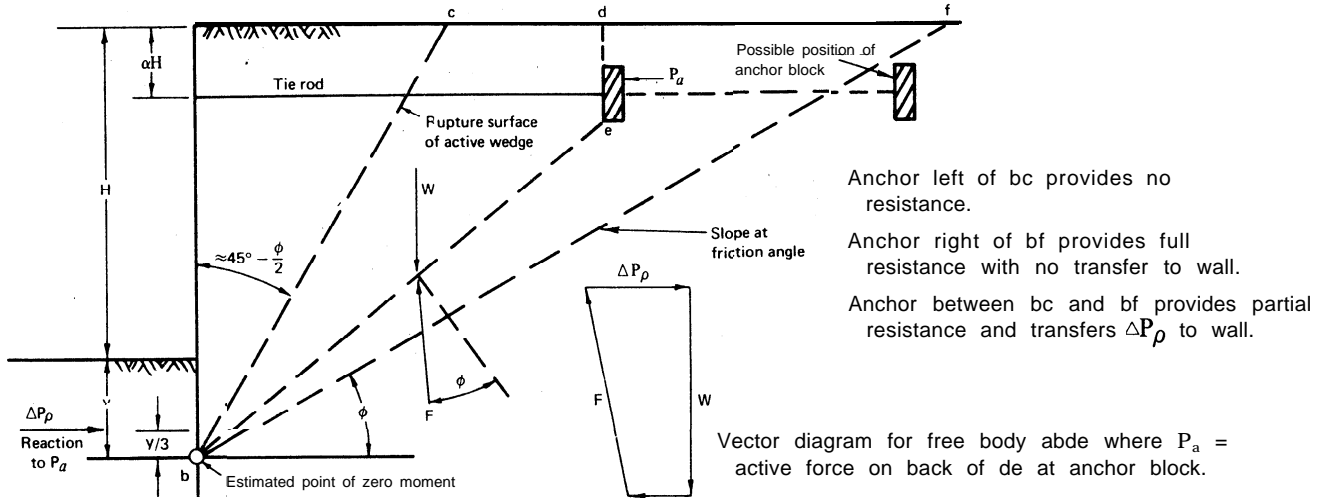
Fig. 42 - Effects of anchor location relative to the wall (after Navdocks[11], Terzaghi[13])

If the anchorage is located between bc and bf, only partial resistance is developed due to the intersection of the active and passive failure wedges. However, the theoretical reduction in anchor capacity may be analytically determined *(see Theoretical Soil Mechanics* by K. Terzaghi,[13] p. 232.)

Sheet Pile Anchor Walls - Short steel sheet piles driven in the form of a continuous wall may be used to anchor tie rods. The tie rods are connected with a waling system similar to that for the "parent" wall, and resistance is derived from passive pressure developed as the tie rod pulls against the anchor wall. To provide some stability during installation of the piling and the wales, pairs of the piling should be driven to a greater depth at frequent intervals. The anchor wall is analyzed by conventional means considering full passive pressure developed only if the active and passive failure zones do not intersect. However, if the failure wedges do intersect, the total passive resistance of the anchor wall will be reduced by the amount

$$\triangle P_\rho = (K_\rho - K_a) \frac{\gamma (h_2)^2}{2} \quad \text{(for granular soils)}$$

where h_2 = depth to the point of intersection of the failure wedges as shown in Figure 43.

Forces per linear foot of anchor wall

Anchor wall right of cc'

$P_p = (1/2) K_p \gamma h^2$

$P_a = (1/2) K_a \gamma h^2$

K_p obtained from Fig. 5a. using $-\delta/\phi = 0.5$

Anchor wall left of cc'

$P_\rho = (1/2) K_\rho \gamma h^2 - (P'_\rho - P'_a)$

$P_\rho = (1/2) K_\rho \gamma h^2 - [(1/2) K_\rho \gamma h_2{}^2 - (1/2) K_a \gamma h_2{}^2]$

$P_a = (1/2) K_a \gamma h^2$

K_a is obtained from Fig. 5a.
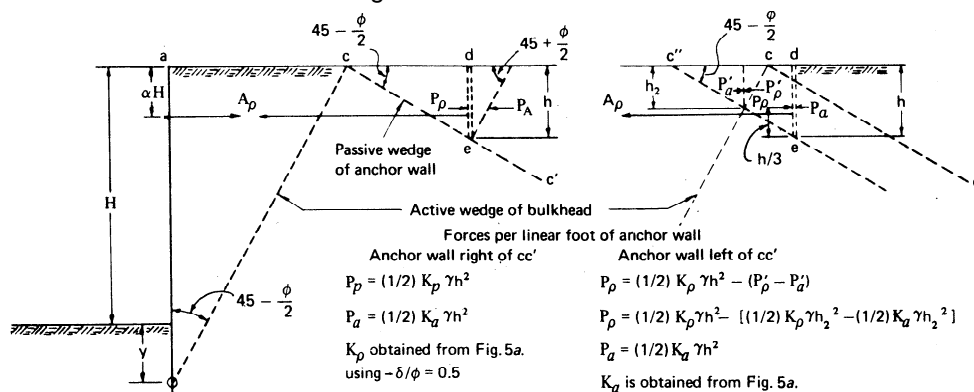
Fig. 43 - Continuous anchor wall (after Navdocks[11])

The tie rod connection to the anchorage should be ideally 'located at the point of the resultant earth pressures acting on the anchorage. Problem No. 4a (pages 107-110) illustrates the design of sheet pile anchor walls.

Deadmen Anchors - The effects of interaction of the active and passive failure surfaces, as mentioned above, also apply to the design of deadmen anchors.

Care must be exercised to see that the anchor block or deadman does not settle after construction. This is generally not a problem in undisturbed soils, however, where the anchorage must be located in unconsolidated fill, piles may be needed to support the blocks. Also, the soil within the passive wedge of the anchorage should be compacted to at least 90 per cent of maximum density unless the deadman is forced against firm natural soil.

Continuous Deadmen Near Ground Surface - A continuous deadman is shown in Figure 44.
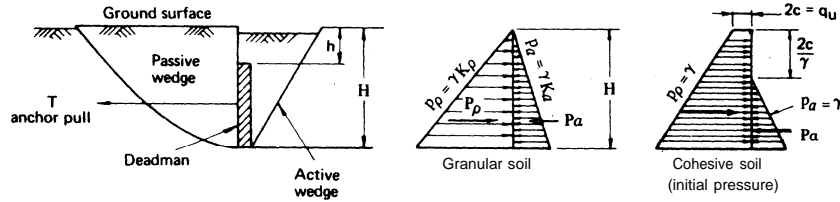
Fig. 44 - Continuous deadmen near ground surface (after Teng[1])

If $1/2 H > h$, assume deadman extends to ground surface and the ultimate capacity of the deadman is
$$T_{ult} = P_\rho - P_a$$

where T_{ult} = ultimate capacity of the deadman, pounds per linear foot

P_ρ = total passive earth pressure, pounds per linear foot

P_a = total active earth pressure, pounds per linear foot

The active and passive pressure distributions for granular and cohesive soils are also shown in Figure 44. For design in cohesive soils, both the immediate and the long-term pressure conditions should be checked to determine the critical case. A safety factor of two against failure is recommended; i.e.,
$$T \leq T_{ult}/2$$

Short Deadmen Near Ground Surface - Figure 45 shows a deadman of length, L, located near the ground surface, subjected to an anchor pull, T. Experiments have indicated that at the time of failure, due to edge effects, the heave of the ground surfaces takes place in an area as shown. The surface of sliding at both ends is curved.
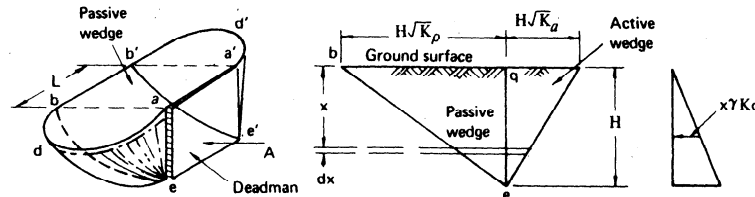
Fig. 45 - Short deadmen near ground surface (after Teng[1])

Integration of the resistance along these curved sliding surfaces results in the following expression for the ultimate capacity of short deadmen in granular soils

$$A_{ult} \leq L\ (P_\rho - P_a) + \frac{1}{3} K_0 \gamma\ (\sqrt{K_\rho} + \sqrt{K_a})\ H^3\ \tan\phi$$

where A_{ult} = ultimate capacity of the deadman, pounds

L = length of the deadman, feet

P_ρ, P_a = total passive and active pressure, pounds per lineal foot

K_0 = coefficient of earth pressure at rest. (It may be taken as 0.4 for design of deadman)

γ = unit weight of soil, pounds per cubic foot.

K_ρ, K_a = coefficients of passive and active earth pressure.

H = height of deadman, feet.

ϕ = angle of internal friction.

For cohesive soils, the second term in the above expression should be replaced by the cohesive resistance, thus
$$A_{ult} \leq L\ (P_\rho - P_a) + 2cH^2$$

where c = the cohesion of the soil, pounds per square foot.

ANCHOR SLAB DESIGN BASED ON MODEL TESTS

General Case in Granular Soils

N. K. Ovesen[50] conducted 32 different model tests in granular soil and developed a procedure for designing anchor slabs located in a zone where the anchor resistance can be fully mobilized. The proposed method considers that the earth pressure in front of the slab is calculated on the basis of a rupture surface corresponding to a translation of the slab. This method can be used to solve the general case in Figure 46 (a) for rectangular anchors of limited height and length located at any depth as shown in Figure 46 (b). Surface loads behind the anchor slab are not included in this publication since their influence is small on the anchor resistance for granular soils with an angle of internal friction equal to or greater than 30 degrees.
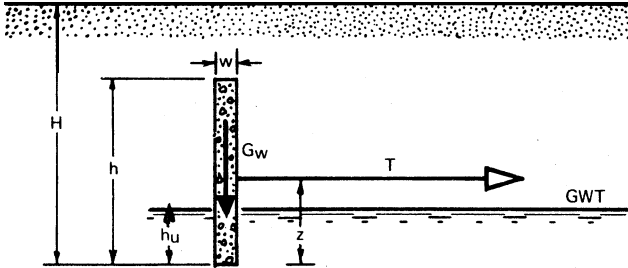
Fig. 46 (a) - Geometrical parameters for an anchor slab.
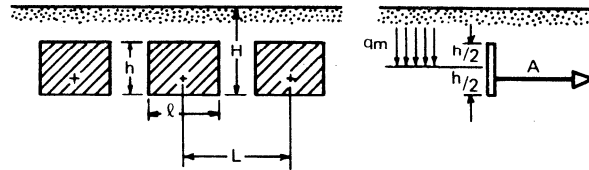
Fig. 46 (b) - Geometrical parameters for anchor slabs with limited height and length.

Where
A	=	resultant anchor force per slab, lbs.	
GWT	=	ground water table	
G_W	=	weight per foot of wall of the anchor plus the soil on top of the slab, lbs. per foot	
H	=	distance from base of slab to ground surface, ft.	
L	=	distance between centers of two consecutive slabs, ft.	
T	=	resultant anchor force, lbs. per foot	
W	=	thickness of anchor slab, ft.	
Z	=	distance from base of slab to resultant anchor force, ft.	
h_u	=	distance from base of slab to ground water table, ft.	
h	=	actual height of anchor slab, ft.	
ℓ	=	actual length of anchor slab, ft.	
qm	=	vertical effective stress in earth at midpoint of actual height of anchor slab, lbs. per square foot	
	=	unit weight of soil, lbs. per cubic foot	
	=	submerged unit weight of soil, lbs. per cubic foot.	

Ovesen suggests that a two-step procedure be used to find the ultimate resistance of the anchor per slab A_{ult} which equals $q_m h \ell R$. First the dimensionless anchor resistance factor, R_o, is determined for the "basic case". The basic case is a continuous strip, $\ell = L$, extending the full height, $h = H$, of the anchor. Next, the dimensionless anchor resistance factor, R, which is dependent upon R_o is calculated for the actual anchor dimensions under consideration. Knowing R, the ultimate resistance of the anchor slab A_{ult} can be calculated. A similar two-step procedure is used to find Z, the location of the line of action of the anchor tie-rod force. The application of Ovesen's method is described below and illustrated in Problem No. 4b (pages 111-113).

1. Determine the dimensionless anchor resistance factor, R_o, for the "basic case". For a given angle of internal friction, ϕ, and angle of wall friction, δ, calculate tan δ, and use Figure 46 (c) to obtain the earth pressure coefficient, $K\gamma$. Calculate the Rankine active earth pressure coefficient K_a, and then' solve for R_o.

$$K_a = \tan^2 (45 - \phi/2)$$
$$R_o = K\gamma - K_a$$
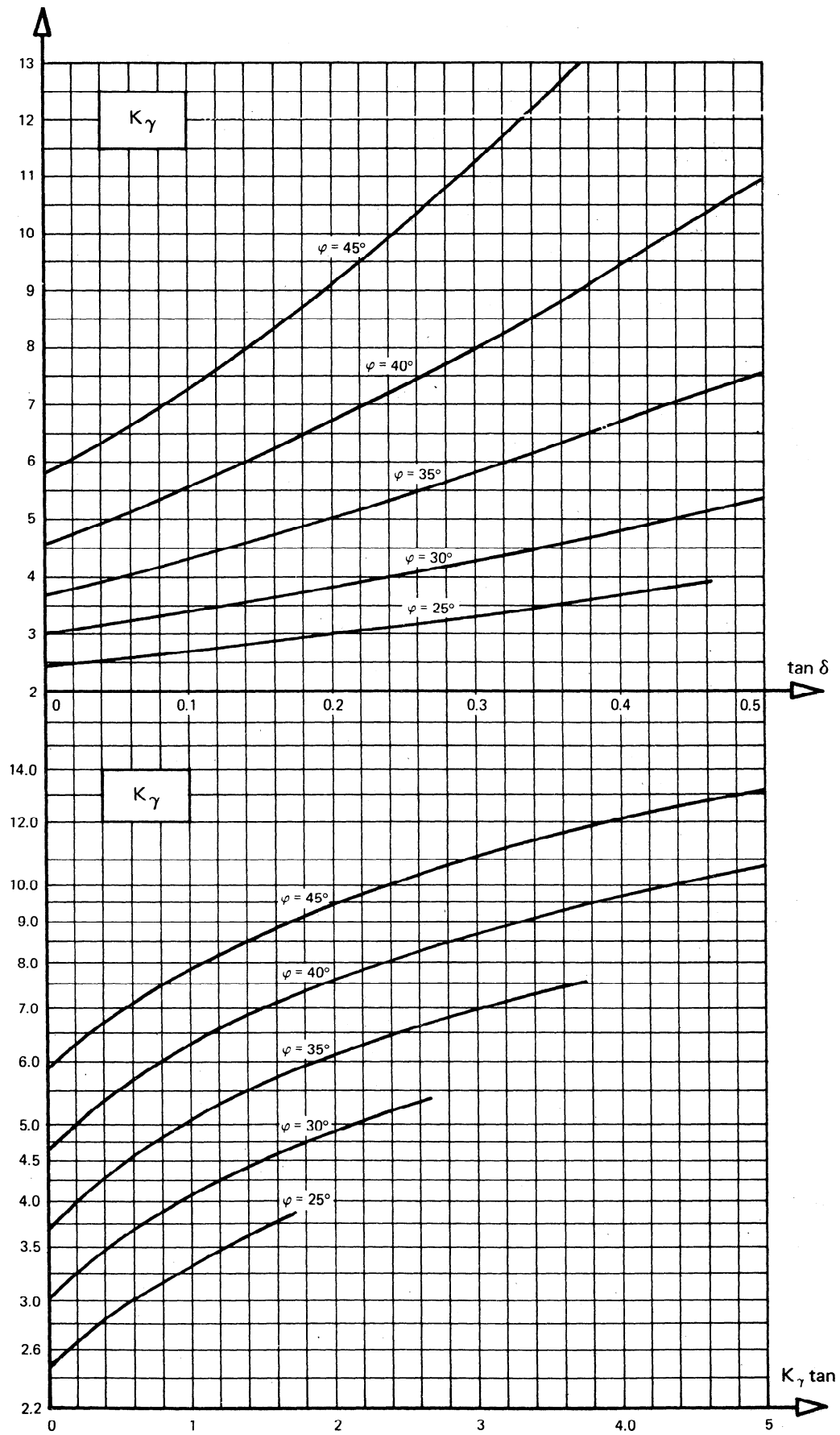
Fig. 46 (c) - Earth pressure coefficients for the normal earth pressure in front of an anchor slab.
(after Ovesen[50])

Calculate the hydrostatic earth pressure per foot of wall,

$$P_H = \frac{1}{2} \gamma H^2 - \frac{1}{2} (\gamma - \gamma') h_u^2$$

Calculate, T_o, the ultimate anchor resistance per foot of wall for the "basic case",

$$T_o = P_H R_o$$

The following method is recommended for obtaining $K\gamma$ for those cases where the tangent of the angle of wall friction, $\tan \delta$, is not known:

Calculate the normal and tangential active earth pressure per foot of wall on the back of the slab,

$$P_A = P_H K_a$$

$$F_A = -P_A \tan \phi$$

Calculate G_w, which is the weight per foot of wall of the anchor plus the soil on top of the slab, then

$$K\gamma \tan\delta = \frac{G_w - F_A}{P_H}$$

Use Figure 46 (c) to obtain $K\gamma$.

2. The dimensionless resistance factor, R, for the actual anchor slab dimensions is then calculated by the formula[51] below or by the use of Figure 46 (d), which is the below equation plotted for values of Q/L, Q/h, and h/H.

$$R/R_o = 1 + R_o^{2/3}\left(1.1E^4 + \frac{1.6B}{1+5\ell/h} + \frac{0.4\,R_o\,E^3\,B^2}{1+0.05\ell/h}\right)$$

where $E = (1 - h/H)$ and $B = 1 - (\ell/L)^2$

3. The ultimate anchor resistance per slab, A_{ult}, and the ultimate anchor resistance per foot of wall, T_{ult}, are equal to,

$$A_{ult} = q_m\, h\ell R$$

$$T_{ult} = A_{ult}/L$$

where q_m is the vertical effective stress in the earth at the midpoint of the actual height of the anchor slab, $q_m = \gamma(H - 1/2\, h)$.

4. The location of Z shown in Figure 46 (a), which is the line of action of the anchor tie-rod force, can be obtained directly from Figure 46 (e) when the ground water table is at or below the anchor slab base ($h_U = 0$).

5. Use the following method to find Z when the ground water table is above the anchor slab base ($h_u \neq 0$). Calculate M_H, the hydrostatic earth pressure moment, about the base of the anchor (Figure 46 (a)).

$$M_H = \frac{1}{6} \gamma H^3 - \frac{1}{6} (\gamma - \gamma') h_u^3$$
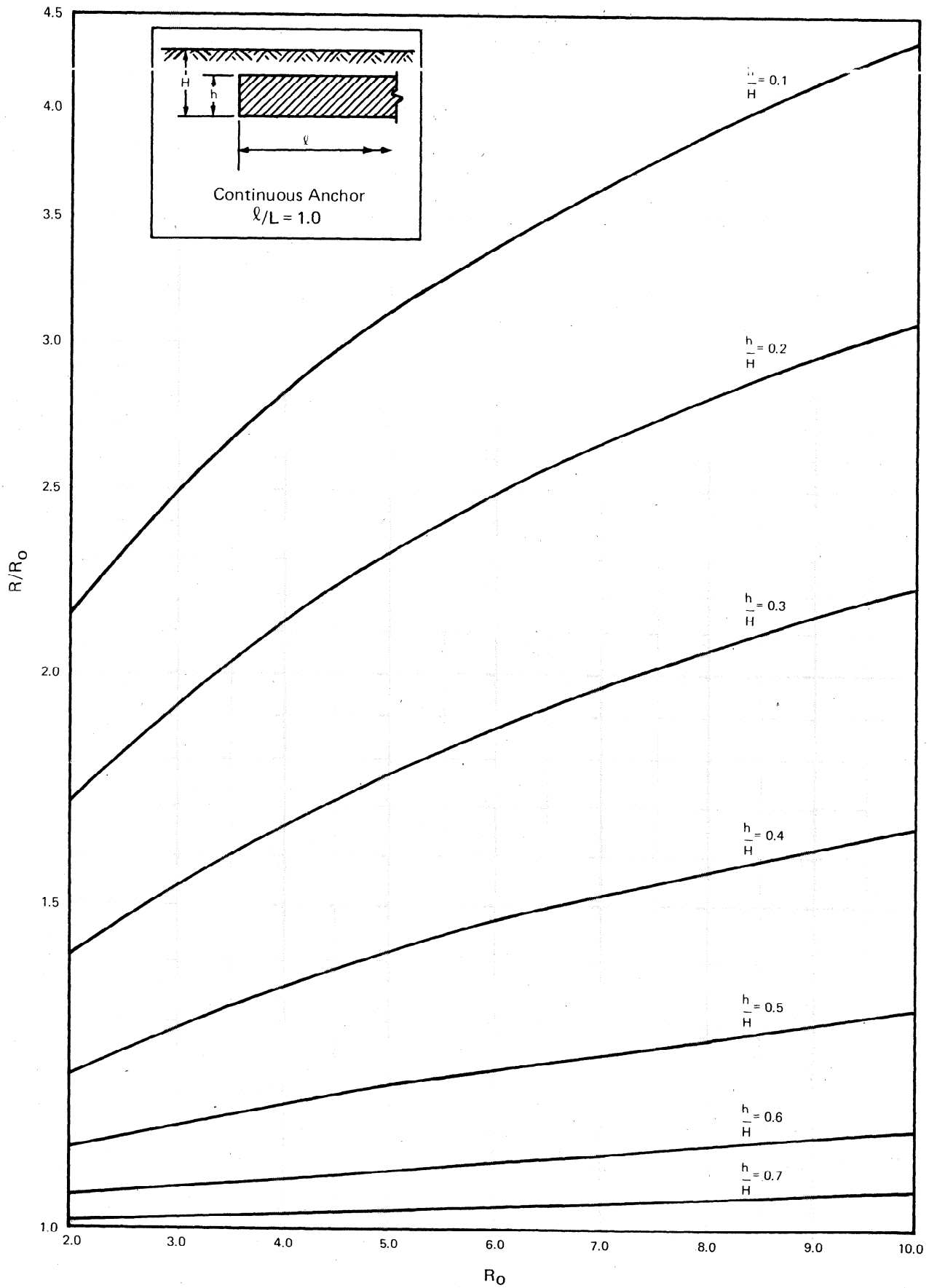
Fig. 46 (d) - Dimensionless resistance factor ratio for continuous anchor slab, $\ell/L = 1.0$
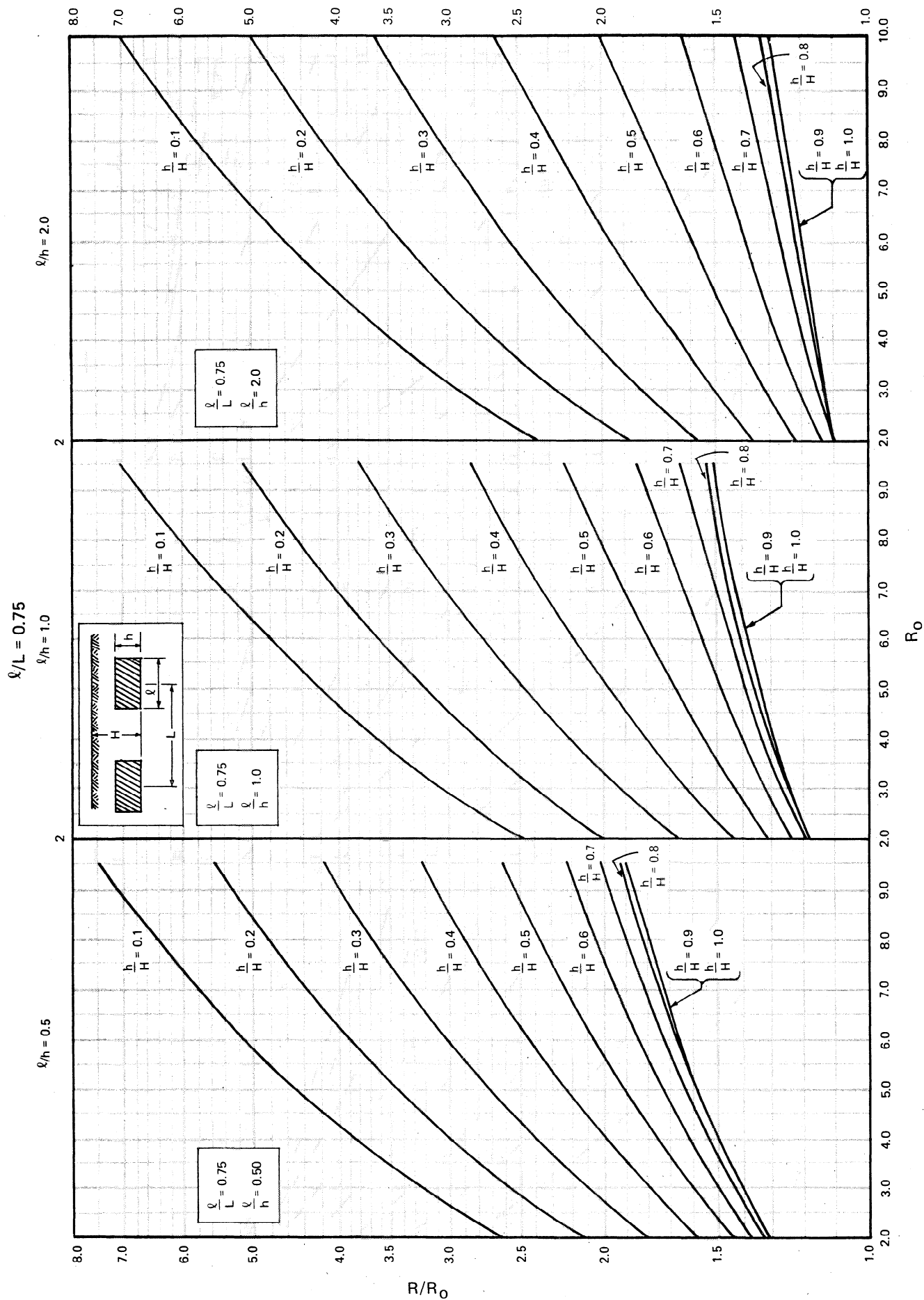
Fig. 46 (d) (Continued) — Dimensionless resistance factor ratio for anchor slab spacing $\ell/L = 0.75$

51
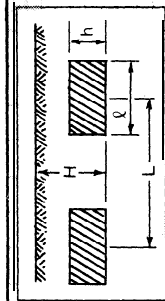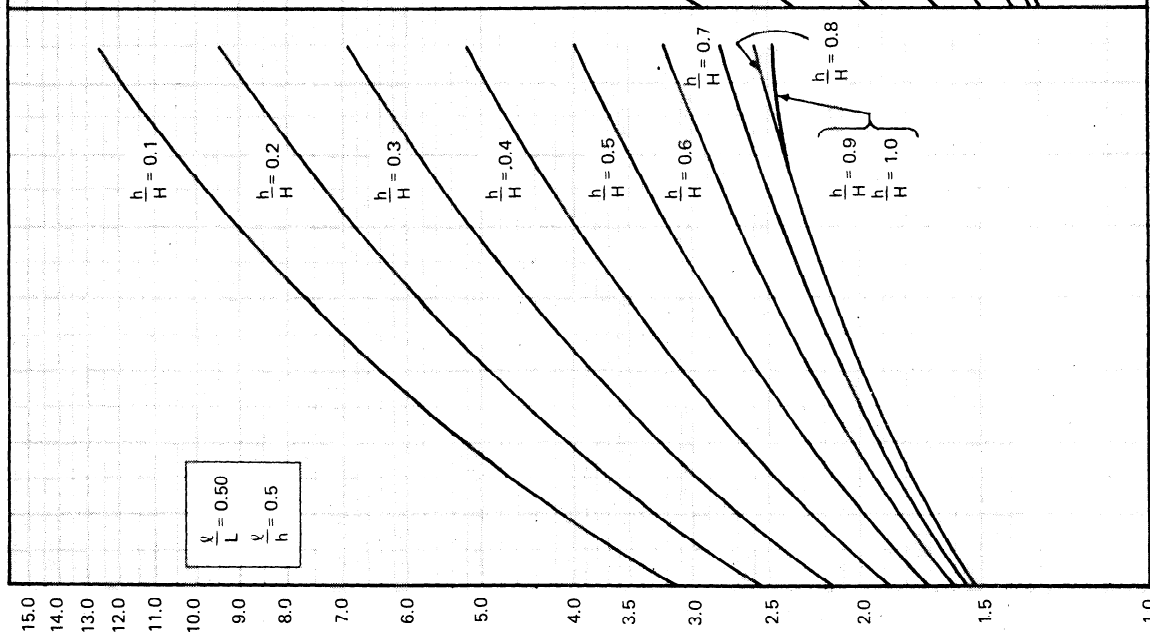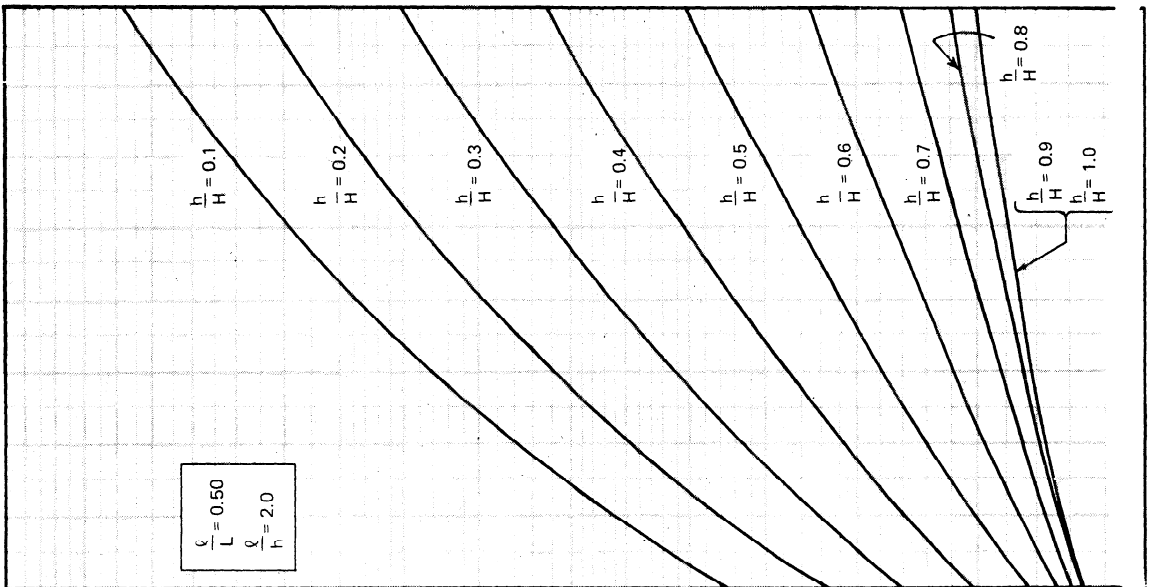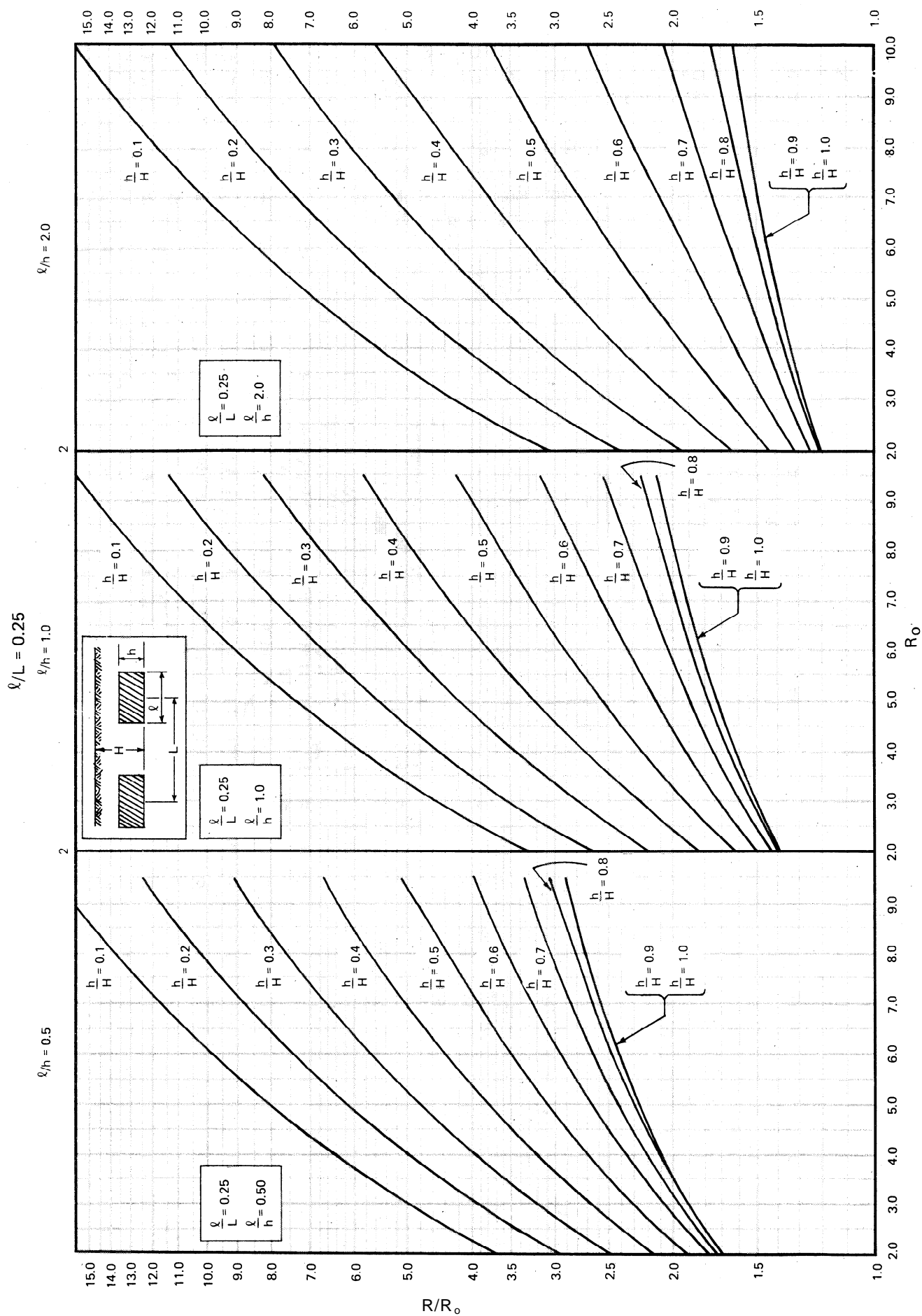
Fig. 46 (d) (Continued) — Dimensionless resistance factor ratio for anchor slab spacing ℓ/L = 0.25

calculate P_H, T_o, F_A, G_w, K_a, $K\gamma$as defined in the anchor resistance calculations previously outlined. For $K\gamma \tan \delta$ use Figure 46 (f) to obtain the dimensionless relative distance factor ζ. Then for the basic case, Z_o, the distance from the base of the anchor slab to the line of action of the anchor force is,

$$Z_o = \frac{1}{T_o}\left[3M_H K_\gamma \zeta + W(0.5G_w - F_A) - M_H K_a\right]$$

and, for the actual anchor slab dimensions, the distance, Z, from the base of the anchor to the anchor tie force is calculated using the following formula:

$$Z/H = \frac{0.5h}{H} - \left(0.5 - \frac{Z_o}{H}\right)\cdot\left(\frac{h}{H}\right)^{\left(\frac{1}{1-2Z_o/H}\right)}$$
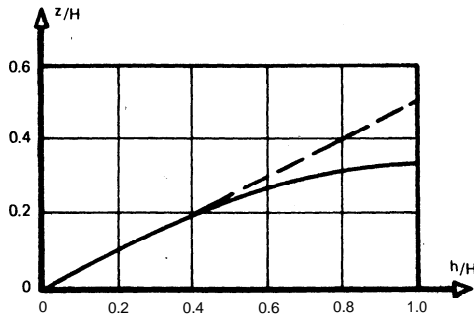
Fig. 46 (e) - Location of line of action of anchor force. (after Ovesen")
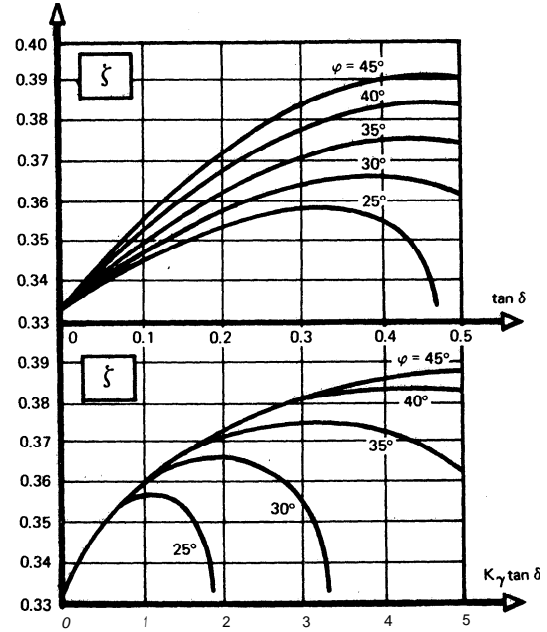
Fig. 46 (f) - Relative distance from base of slab to resultant of earth pressure in front of anchor slab. (after Ovesen")

6. An estimate of the horizontal movement, A, of the anchor slab may be obtained by solving the equation:

$$\log_{10}\left(\frac{\Delta}{H}\right) = 2.5\left(\frac{T_{act}}{T_{ult}}\right) - 2\sin\phi - 2.6$$

where

$$0.30 \le \frac{T_{act}}{T_{ult}} \le 0.90$$

$$32° \le \phi \le 41°$$

$$0.25 \le \frac{h}{H} \le 1.0$$

and either H = L in combination with:

$$0.25 \le \frac{\ell}{L} \le 1.0$$

or h = ℓ in combination with: .

$$0 \le \frac{\ell}{L} \le 1.0$$

54

Anchor Slab in Cohesive Soils

Mackenzie[52] performed model tests in plastic clay based upon the full resistance of the wedge in front of the anchor block being mobilized. The geometric parameters shown in Figure 47 (a) used in conjunction with the experimental curve shown in Figure 47 (b) give a dimensionless factor R which is dependent upon the ratio H/h. Knowing R, the ultimate capacity of the anchor slab, T_{ult}, per unit of slab width can be determined as follows:

$$T_{ult} = Rch$$

$$\text{where } R \leq 8.5$$

$$c = \text{cohesion of the soil, psf}$$

This experimental curve can be used for design purposes providing consideration is given to a proper factor of safety for a specific application.
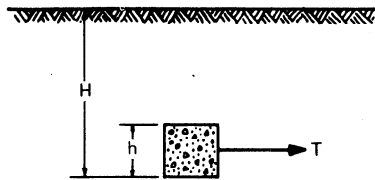
Fig. 47 (a) - Geometrical parameters for anchor slab in clay.
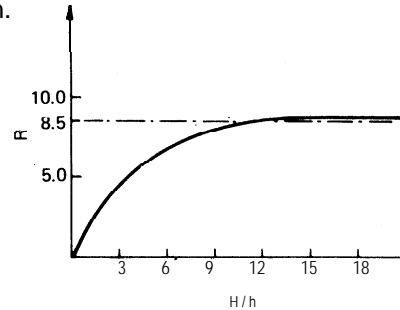
Fig. 47 (b) - Resistance of plastic clays to anchor slabs. (after Mackenzie[52])

H-Pile A-Frames - Brace piles forming A-frames can sometimes be used effectively to anchor sheet pile walls, as shown in Figure 40 (b). If only two piles form each frame, it is necessary to connect the frames with a continuous reinforced concrete cap. The anchor rods can then be attached to the concrete cap. However, if three piles are used, each frame can support a tie rod through the center pile and act independently. The pile angled toward the wall will be in compression while the pile or piles angled away from the wall will be in tension. The resulting forces are easily determined from a force polygon as shown in the figure. This method of support can be used effectively only if the brace piles can be adequately seated in a underlying stratum of soil or, preferably, rock.

H-Pile Tension Ties - Battered H-pile tension ties connected directly to a sheet pile wall through wales may also be used as anchors. An illustration of this type of anchor system is shown in Figure 48. The reaction is developed through friction and/or adhesion between the pile and the soil behind the wall.
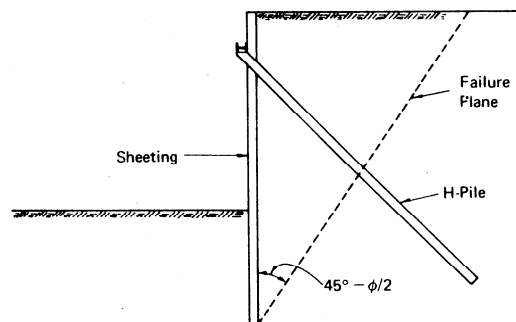
Fig. 48 - Battered H-Pile tension tie

Only the length of pile outside the active failure zone should be considered effective in mobilizing resistance. The actual capacity of the H-piles should be checked by pull out tests in the field. The tension ties should be prestressed to a percentage of the computed anchor pull by jacking against the wall before making the final connection. Particular attention should be given to the connection details at the wale since this may be subject to rotational stresses.

DESIGN OF COFFERDAMS FOR DEEP EXCAVATIONS

GENERAL

A cofferdam is a retaining structure, usually temporary in nature, which is used to support the sides of deep excavations. Such structures generally consist of vertical steel sheet piling braced by a system of (a) wales and struts, (b) circular wales, and (c) prestressed tiebacks. Cofferdams are used primarily for the excavation of multi-level basements and trenches in construction situations where adjacent ground must be supported against settlement or slides. Usually in urban areas the need to prevent settlement of the adjacent ground is a matter of prime importance, as such settlements can have disastrous effects on the structural integrity of adjacent buildings. Sheet pile cofferdams can also be used with economy in the construction of bridge piers and abutments in relatively shallow water.

In general, the method of construction incorporates the following basic steps: (a) steel sheet piles are driven into the ground to a predetermined depth; (b) during excavation the sheeting is braced by horizontal wales supported by a system of struts or prestressed tiebacks; (c) the support system for each wale system must be in place and tightened or prestressed against the sheeting before further excavation can proceed in order to prevent lateral deflection. Figure 49 is a diagram demonstrating the in-place position of the components of a temporary cofferdam.
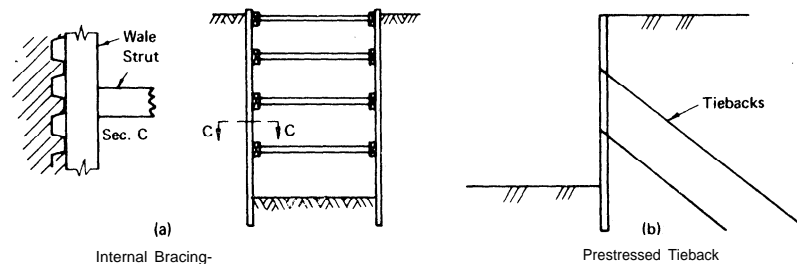
Fig. 49 - Steel sheet pile cofferdam (a) after Terzaghi & Peck[14]

The design of a temporary cofferdam follows an exploratory subsurface investigation conducted to provide general information about the site and the soil strata. With this information, the overall dimensions of the structure can be set. More detailed subsurface information (such as soil strength properties) is then obtained for design purposes. In this detailed subsurface study, several borings should extend to bedrock or to a depth below the design elevation of the bottom of the sheeting roughly equal to the width of the excavation. The subsurface investigation should also include a determination of the elevation range of the water table.

After the required soil parameters have been determined, the lateral earth pressures against the sheeting are computed. The various cofferdam components. can then be sized by selecting a wale spacing, sizing the sheeting (based on the maximum moment generated between supports), and sizing the struts (based on the maximum strut load) or determine the prestress tieback spacing. The spacing between wales may be reduced if the moments in the wall are too large. If the wale sizes are unreasonably large, the strut spacing may be reduced. However, the strut spacing should be kept as wide as possible to ease access through the bracing system during construction. Finally, the cofferdam should be analyzed for overall stability and for safety against piping.

Of significant importance are the benefits of driving the steel sheet piling to a greater depth than the design depth of excavation. In soft clays this usually results in resisting the heave of the bottom of the excavation. Greater wall depths may also be advantageous in excavations in granular soil below the water table thereby serving as a cutoff wall and reducing the danger of piping and the formation of boils. In addition, the continuity of sheet pile walls helps prevent excessive material loss from behind the wall.

A detailed explanation of the various stages of design of braced sheeted cofferdams is presented in the sections that follow.

LATERAL PRESSURE DISTRIBUTION

After the subsurface data has been obtained, the first step is to determine the loads acting on the cofferdam. The loads to which the cofferdam may be subjected include earth pressures, surcharge loads, hydrostatic pressures, wave pressures, and earthquake loads. With the exception of the earth pressures, the lateral forces on the cofferdam walls may be calculated in the manner presented in the first section of this manual. However, lateral earth pressures on braced cofferdams cannot be calculated by the classical theories (Rankine, Coulomb, etc.) because of differences in the behavior of the structure during construction.

At the time the first row of struts is placed (refer to Figure 50) the excavation is not deep enough to have appreciably altered the original state of stress in the soil. The lateral pressure at the level of the first row of struts is, therefore, higher than the active pressure since no significant yielding of the soil mass has occurred. As the excavation continues to the level of the second set of struts, the rigidity of the first set prevents horizontal yielding of the soil near the surface. However, the external lateral pressure tends to rotate the sheeting about the upper support level so that a certain inward displacement of the sheeting will occur at the level of the second set of struts by the time these struts are in place. As the excavation continues, greater deflections occur at the lower struts mobilizing soil strength and producing an arching effect which reduces lateral pressures. At thecompletion of the excavation, the sheeting will have deformed to a position indicated by line ab_1 in Figure 50. Thus, the resulting lateral pressure diagram will have the maximum values occurring in the upper portion of the wall which is in marked disagreement with the pressure distributions given by the Rankine or Coulomb Theories.
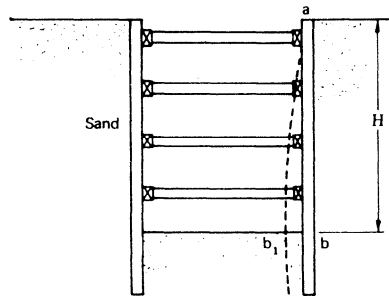
Fig. 56 - Deformation of sheet piling in a braced cofferdam (after Terzaghi & Peck[14])

For cofferdams in sand and soft to medium clays, a trapezoidal distribution similar to that proposed by Terzaghi and Peck[14] (1967) may be used for design. This distribution is shown in Figure 51 for granular soils. If ground water is present, its pressure is added to the trapezoidal soil pressure as shown in Figure 51 (c) and (d).
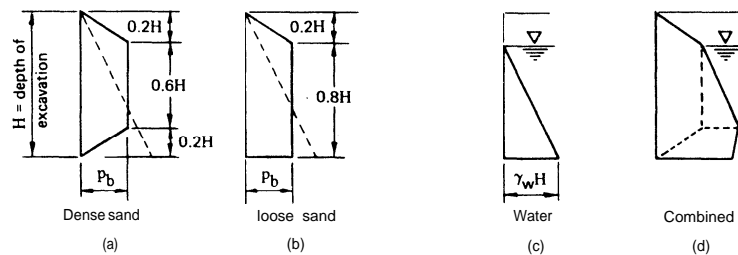
Fig. 51 - Earth pressure diagram for braced cuts in sand (after Teng[1])

$$p_b = 0.8K_a\gamma_e H \cos \delta$$

where
- K_a = active pressure coefficient determined from Figure 5a (page 10)
- γ_e = average effective unit weight
- H = depth of excavation
- δ = angle of wall friction estimated from Table 4 (page 13)

Problem No. 2, page 117, illustrates the design of a braced cofferdam in sand.

Experience indicates that this pressure distribution results in conservative designs for struts near the bottom of the excavation (the actual loads tend to be smaller than the values predicted). For soft to medium clays the trapezoidal pressure distribution is given in Figure 52 (a). An alternate method using the stability number concept is given in Figure 52 (b).
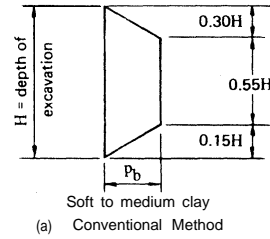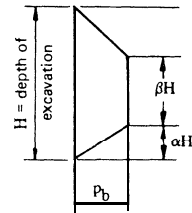

$$p_b = \gamma H - 2q_u$$

where

γ = wet unit weight

q_u = unconfined compressive strength

(a) Conventional Method

where

$$p_b = \frac{C}{150} (7N_o^2 + 10N_o)$$

C = Cohesion (psf)

$N_o = \gamma \dfrac{H}{C}$ (Stability No.) but not $>$

$\beta = 1.1(1 - \dfrac{N_o}{20})$ but not > 0.55

$\alpha = 0.3 (1 - \dfrac{N_o}{20})$ but not > 0.15

(b) Stability number method

Fig. 52 - Earth pressure diagram for braced cuts in plastic clay

The distribution of pressure in the stability number method acts between the heights of αH and $(\alpha+\beta)H$ above excavation level with linear reduction to zero at the top and bottom. If ground water is present in clay, it is added to the pressure distribution as shown for granular soil in Figure 51. This pressure distribution for clays also gives maximum pressure values which result in conservative designs for some struts. However, with the passage of time creep effects cause the lateral earth pressure to increase appreciably. This phenomenon was studied in model tests by Kirkdam[34] from which it was concluded that the design of more permanent cofferdams in clay should be based on earth pressures calculated according to the classical theories (Rankine, Coulomb or Log-Spiral) using a cohesion value of zero and a $-angle as determined by drained triaxial tests. Problem No. 1 (pages 114-116) is a design example illustrating the Stability Number Method.

For stratified soils, Peck[30] suggested the use of the pressure diagram given in Figure 52 (a), substituting $\overline{q}$ and $\overline{\gamma}$ for q_u and γ in any sand strata that are interbedded with clay. The values $\overline{q}$ and $\overline{\gamma}$ are determined as follows:

$$\overline{q} = \frac{1}{H} [\gamma_s K_s H_s^2 \tan\phi + (H - H_s)nq_u]$$

$$\overline{\gamma} = \frac{1}{H} [\gamma_s H_s + (H - H_s)\gamma_c]$$

where
γ_s = saturated unit weight of sand
K_s = hydrostatic pressure ratio for the sand layer, may be taken as 1.0 for design purposes
H_s = thickness of the sand layer
ϕ = angle of internal friction of the sand
H = total depth of excavation
q_u = unconfined compression strength of the clay
γ_c = saturated unit weight of the clay
n = coefficient of progressive failure, the value ranges usually from 0.5 to 1.0. This value varies with the creep characteristics of the clay, the length of time during which the excavation remains open, and the care exercised in construction. In Chicago clay, the value ranges between 0.75 and 1.0.

Problem No. 3 (pages 118-126) illustrates the design of a braced cofferdam in stratified soil.

Because of the seemingly conservative nature of the trapezoidal pressure distribution for design, current engineering practice permits the sheeting, wales, and struts in temporary bracing systems to be designed for a 65 per cent overstress, as shown in Teng[1], in instances of carefully controlled and inspected construction. Such construction conditions should include a detailed subsurface drilling program with careful determination of the soil parameters' by laboratory tests, installation of the cofferdam by a contractor with considerable experience in the construction of braced cofferdams, and the use of strain gages to periodically measure stresses in typical members.

SIZING OF COFFERDAM COMPONENTS

When the pressure diagram has been completed, a structural analysis can be performed on the sheeting, the wales, and the struts and from this analysis the components can be sized. A design example is given in Problem No. 3 (pages 118-126) illustrating a method of sizing cofferdam components.

Sheeting - The steel sheet piling may be designed either as a continuous beam supported at the strut levels or by assuming pins exist at each strut thereby making each span statically determinant. It is also customary to assume a support at the bottom of the excavation. The resulting moment distributions are illustrated in Figure 53.
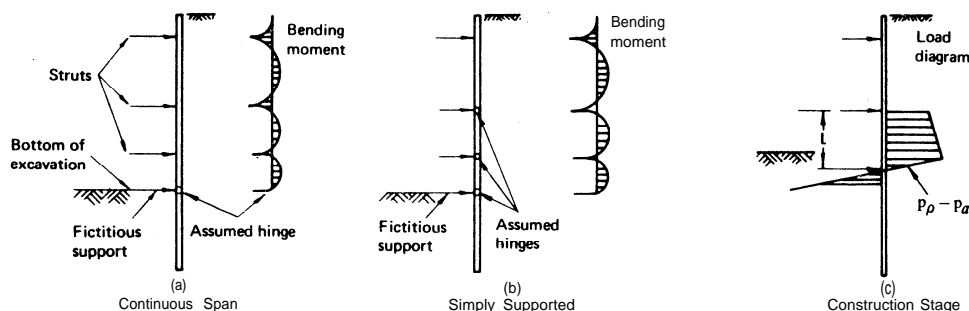
Fig. 53 - Assumptions used in the design of sheet piling (a and b after Teng[1])

The maximum moment per foot of width along the sheeting may then be computed from

$$M_{max} = (1/10) \, wL^2 \quad \text{(three continuous spans - simply supported, Figure 53(a), usually used on middle spans)}$$

or

$$M_{max} = (1/8) \, wL^2 \quad \text{(single span - simply supported, Figure 53(b), usually used on top span)}$$

where w = average lateral pressure on the wall over the longest span
  L = maximum distance between wales, often governed by construction stage as shown in Figure 53 (c)

If the base is unstable (see Stability of Cofferdams, page 63) the sheeting is driven deeper, as shown on Figure 54, and the unbalanced force, P_b', acts on the buried length. The steel sheeting is then designed as a cantilever below point X using

$$M_{max} = \frac{1}{3} \, wL^2$$

where L = vertical strut spacing
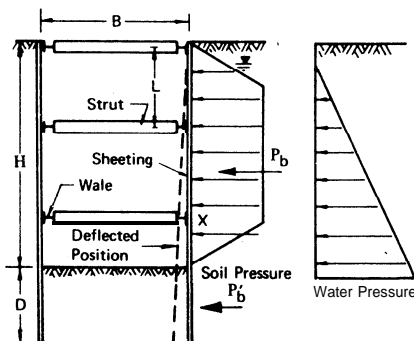
Fig. 54 - Deflected sheet pile wall with unbalanced force

These moment equations represent the range where the actual moment lies. The accuracy with which the maximum moment can be determined depends primarily on the accuracy of the pressure diagram. The required section modulus of the sheeting would then be given by

$$S = \frac{M_{max}}{\sigma_{all}}$$

where σ_{all} = allowable steel bending stress

Wales - The wales are designed to resist the horizontal reactions from the sheeting as previously described in the section on anchorage systems. However, in braced cofferdams, since the excavation is usually of closed geometry, the wales are also subject to an axial load due to the reaction from the perpendicular wales at the corners as shown in Figure 55. Thus, the wales should be designed as continuous beams subjected to both lateral and axial loads.
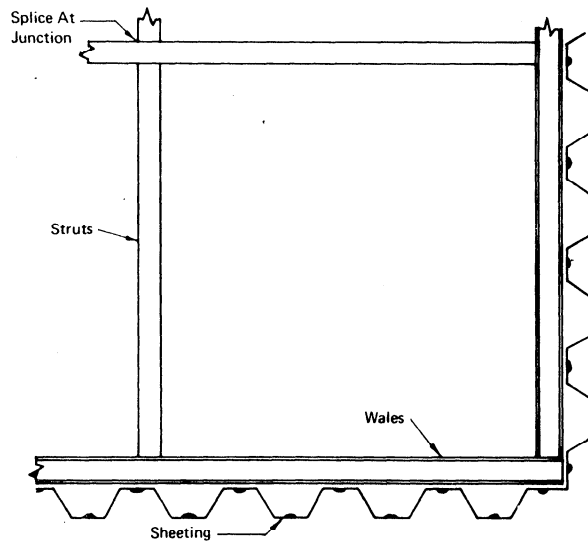
Fig. 55 - Plan at corner of braced cofferdam

Struts - Figure 56 illustrates a typical arrangement of struts in a braced excavation. The struts are designed as compression members, with buckling being the primary consideration. The spacing between struts in both directions must be designed in such a manner that the axial loads and the ℓ/r ratios are kept within acceptable limits. Frequent cross-strutting is recommended from. the design standpoint as it reduces the R/r ratios. However, from the construction standpoint the spacing between struts may be dictated by the required accessibility to the bottom of the excavation. An eight-foot strut spacing is usually considered the minimum acceptable for construction.
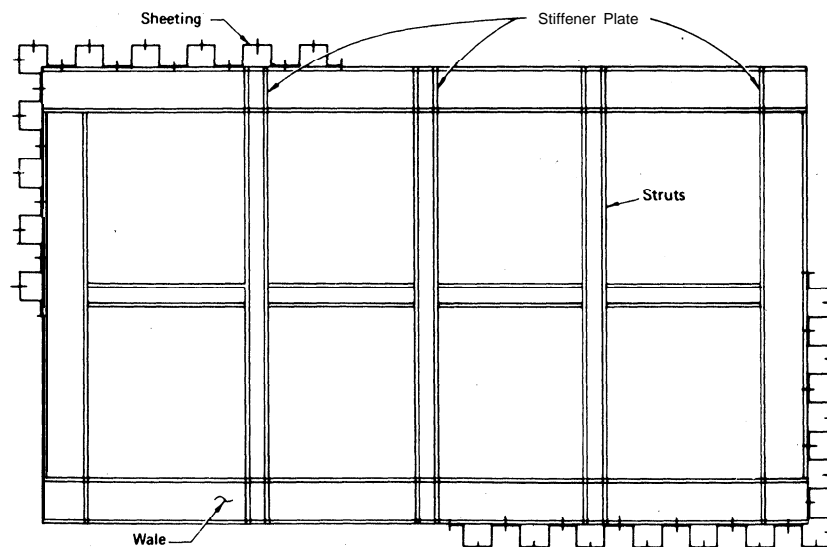
Fig. 56 - Typical strut arrangement for a braced excavation

The designer must also consider whether or not the tiers of struts should be located at the same elevation in both directions. If the tiers are located at the same elevation, the struts must be framed into each other at the points of intersection. This is commonly done by cutting interlocking notches in the struts at the junctions or by splicing the struts in one direction. An alternative is to pass the tier of struts in one direction directly above the tier of struts in the perpendicular direction. However, with such an arrangement the wales will be at slightly different elevations at the corners and the transfer of reaction will result in eccentric axial loads in the wales. If such eccentricity does occur, the wales must be designed for the combined stresses due to the axial load and the biaxial bending moment from the lateral pressure and the eccentric axial load.

Raking Braces - For large excavations it may not be practical to permit horizontal braces to extend completely across the excavation. In such cases the sheeting can be supported by raking braces as shown in Figure 57.
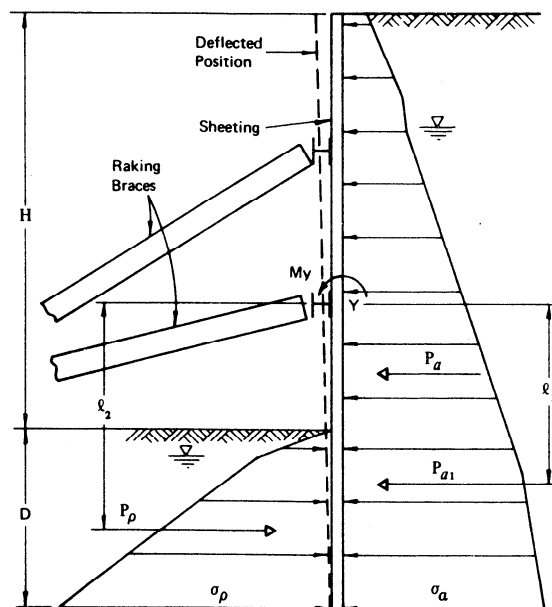
Fig. 57 - Diagram illustrating the use of raking braces in construction of a deep cut

In such cases the sequence of excavation and installation of braces is quite different from that normally assumed for a braced cofferdam with horizontal struts. Deflections of the wall during construction permit mobilization of active pressures according to the classical theories. Thus, the triangular lateral earth pressure diagram should be used as described previously for cantilevered and anchored bulkheads. The bending moments in the sheet piling must be determined for each stage of construction (just prior to installation of each brace and wale) and will depend on the method and sequence of construction. The maximum moment is usually assumed using simple span between the lowest brace then in place 'and the point of zero net pressure below excavation, as shown on Figure 53 (c). A safety factor of 1.5 is usually recommended for computation of passive pressure counted on for support. In addition, an increase of 15 per cent to the load on the upper wale and brace is also recommended.

Sheet piling penetration below final excavation bottom is controlled by stability considerations (next section). Penetration requirements are determined by equilibrium of the cantilever span below point y. By assuming a point of fixity at point y,

$$P_{a1} \ell_1 - \frac{P_\rho}{FS} \ell_2 - M_y = 0$$

where M_y = allowable moment in steel sheet piling at point y

P_{a1} = resultant active pressure below point y

Circular Bracing - A ring wale bracing system has been developed for a circular excavation.[36] This design is based upon experience in rock tunneling using the equation

$$f_s = \frac{T}{A} + \frac{M}{S}$$

where

f_s = stress in the circular ring wale, pounds per square inch

T = radius of excavation times the total load per foot between the ring wales, pounds

M = approximate moment at blocking point based upon experience in tunneling, inch-pounds

= 0.86 T x b

b = rise of arc at blocking points, inches

$$= R - \sqrt{R^2 - \left(\frac{C}{2}\right)^2}$$

A_s = area of steel cross section, square inches

R = radius of neutral axis of rib, inches

C = chord length between neutral axis blocking points, inches

S = section modulus, inches cubed

To ease construction, a six-inch gap is left between the ring wale and the sheet piling. This gap is then "taken up" at the projection of each sheet pile (the blocking point) using two wooden wedges, one driven from above and one from below the ring wale, as shown on Figure 58. The ring wales should be checked for buckling, possibly by using the following references: "Stability of an Elastic Ring in a Rigid Cavity"[46] by E. A. Zagustin and G. Herrmann; "Note on the Instability of Circular Rings Confined to a Rigid Boundry"[47] by P. T. Hsu, J. Elkon and T. H. H. Pian; "Designing Underground Reservoirs"[48] by D. F. Moran; and "A Buckling Problem of a Circular Ring"[49] by Lo, Hsu, Bogdanoff, Goldberg and Crawford.

Fig. 58 - Sketch of circular ring wale system
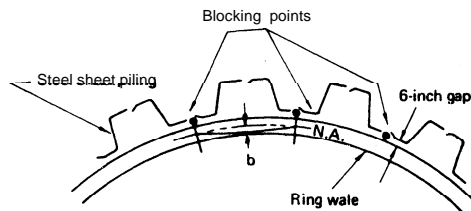
Prestressed Tiebacks - Prestressed tiebacks anchored in rock or granular soil, as shown on Figure 59, eliminate the need of interior bracing.
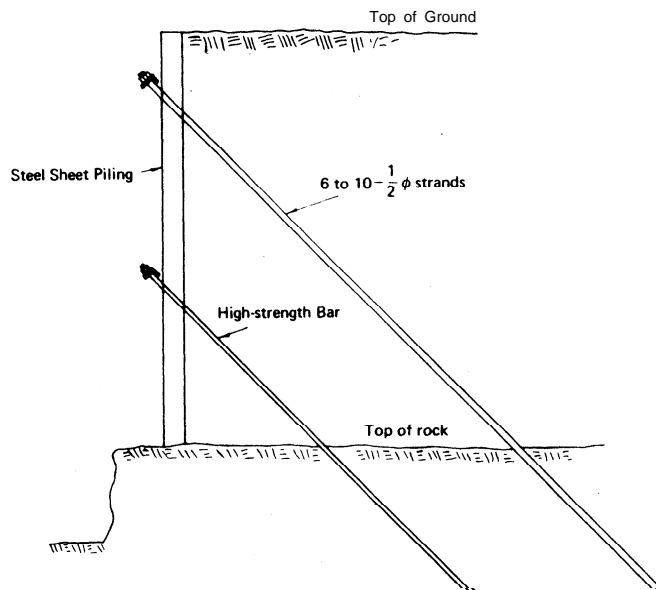
Fig. 59 - Typical cross section of tieback system

62

Thus it is possible to excavate using large power shovels instead of less efficient methods, such as using clamshells and hand excavation. This allows freer movement within the excavation. The higher initial installation costs of the tieback system are justified by the economies of an unobstructed excavation.

The lateral earth pressures exerted against the steel sheet piling may be calculated by any of the accepted conventional methods using the at-rest coefficient instead of the active coefficients.

Teng[1] suggests using

K_o = 0.35 to 0.60 for sand and gravel
= 0.45 to 0.75 for clay and silt
= 1.00 or more for overconsolidated clays

A typical tieback system uses high strength alloy steel bars, 1½ to 2½ inches in diameter, of 145,000 psi ultimate strength, or seven-wire strands of 250,000 or 270,000 psi nominal ultimate strength.

The tiebacks are installed by augering or driving 4 to 8 inch diameter pipe into the ground at the desired angle. A pneumatic drifter will drill a 3 to 6 inch diameter rock socket approximately 10 to 25 feet deep from the same rig that drove the pipe. The holes in rock are cleaned by an air or water jet prior to installing tendon tiebacks. Quick drying nonexpanding grout is installed by gravity flow. The tiebacks are then prestressed with hydraulic jacks to about 25 percent higher than their working stress. The working stress is equal to about 50 percent of ultimate strength.

The allowable design load on the prestressed tiebacks can be estimated using the bond strength between the rock or soil and the cement grout. Consideration must be made for the highest possible pore water pressure conditions. Also, the steel sheet piling must be driven to rock that is able to withstand the downward compressive stress exerted by the tieback system.

STABILITY OF COFFERDAMS

Heaving In Soft Clay - For construction in soft clay, heave at the bottom of the excavation may occur, resulting in settlement of the surrounding ground surface. The conventional method of analysis for investigating heave was developed by Terzaghi[13] and is illustrated in Figure 60.
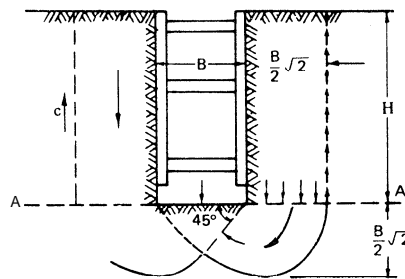

Fig. 60 - Diagram illustrating assumed mechanism for failure by heave of the bottom of a deep excavation

In this case, the vertical column of soil along the sheeting is assumed to exert a pressure on the horizontal plane A-A'. When the pressure exerted by this soil column exceeds the bearing capacity of the soil beneath the sheeting a bearing type failure will occur, resulting in heave of' the bottom of the excavation and settlement of the surrounding ground surface. Based on this failure model the depth of excavation at which heave will occur can be expressed by:

$$H_c = \frac{5.7c}{\gamma - \sqrt{2}\left(\frac{c}{B}\right)} \quad \text{(for H < B)}$$

where
H_c = critical height of excavation (feet)
B = width of excavation (feet)
γ = unit weight of soil (pcf)
c = unit cohesion of soil (pcf)

A factor of safety of 1.5 applied to the soil cohesive shear strength is normally recommended. This method of analysis gives reliable results for excavations in which the width of the cofferdam is larger than the depth of excavation and the cofferdam is very long. In cases where the cofferdam is square, rectangular, or circular in geometry and the depth of excavation exceeds the width, the proximity of the four walls aids in overall resistance to heave. In such cases a method of analysis developed by Bjerrum and Eide[31] can be used. Their method visualizes the cofferdam as a deep "negative footing." That is, the excavation produces shear stresses in the soil similar, but of opposite direction, to those caused by a deep foundation. Using this analogy the depth of excavation that would cause heave may be expressed by:

$$H_c = N_c \left(\frac{c}{\overline{\gamma}} \right) \qquad \text{(for } H > B\text{)}$$

or

$$S.F. = \frac{cN_c}{\overline{\gamma}H + q}$$

where

H_c = critical height of excavation

$\overline{\gamma}$ = average unit weight of soil within depth of excavation

c = unit cohesion of soil

N_c = bearing capacity factor - to be determined according to chart presented in Figure 61.

q = surface surcharge loading

N_c rectangular = (0.84 + 0.16 B/L) N_c square
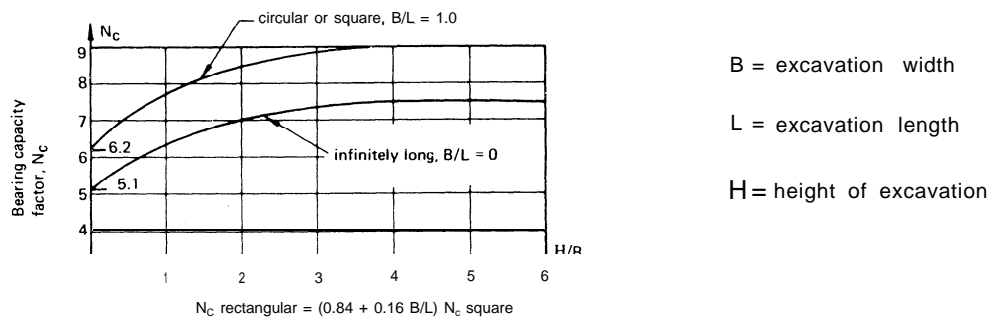
Fig. 61 - Diagram for the determination of bearing pressure coefficient, N^c (after Skempton)

Where the safety factor falls below a value of 1.5 the sheeting should be extended to a depth of one-half the excavation width below the excavation level. The additional pressures thereby incurred on the sheeting may be satisfactorily represented by inwardly directed horizontal forces acting at the mid-height of the embedded lengths and having the following magnitude:

$$P = 0.7 \left(\overline{\gamma}HB - 1.4cH - \pi cB \right)$$

Piping in Sand - For excavations in pervious materials the possibility of piping or "sand boiling" must be investigated. Piping occurs when an unbalanced hydrostatic head causes large upward seepage pressures in the soil at the bottom of the excavation. When piping takes place, the upward seepage pressure reduces the effective weight of the soil, thereby reducing the ability of the soil to offer lateral support to the sheeting. In extreme cases the sand "boils" in the bottom of the excavation. That is, a "quick" condition is produced.

Piping is controlled by dewatering (lowering the water table) outside the cofferdam or by driving the sheet piling deeper. The purpose of both corrective measures is to reduce the upward hydraulic gradient in the soil below the bottom of the excavation. Driving the sheeting deeper is particularly effective if the piling can be driven into an impervious layer that will stop or reduce flow around the bottom of the piling. The design of sheeting penetration to control piping for various subsurface conditions is presented in Figure 6.2 (a) and Figure 62 (b). Also, research by Marsland[32] incorporating a safety factor of 1.5 is published in chart form[1].
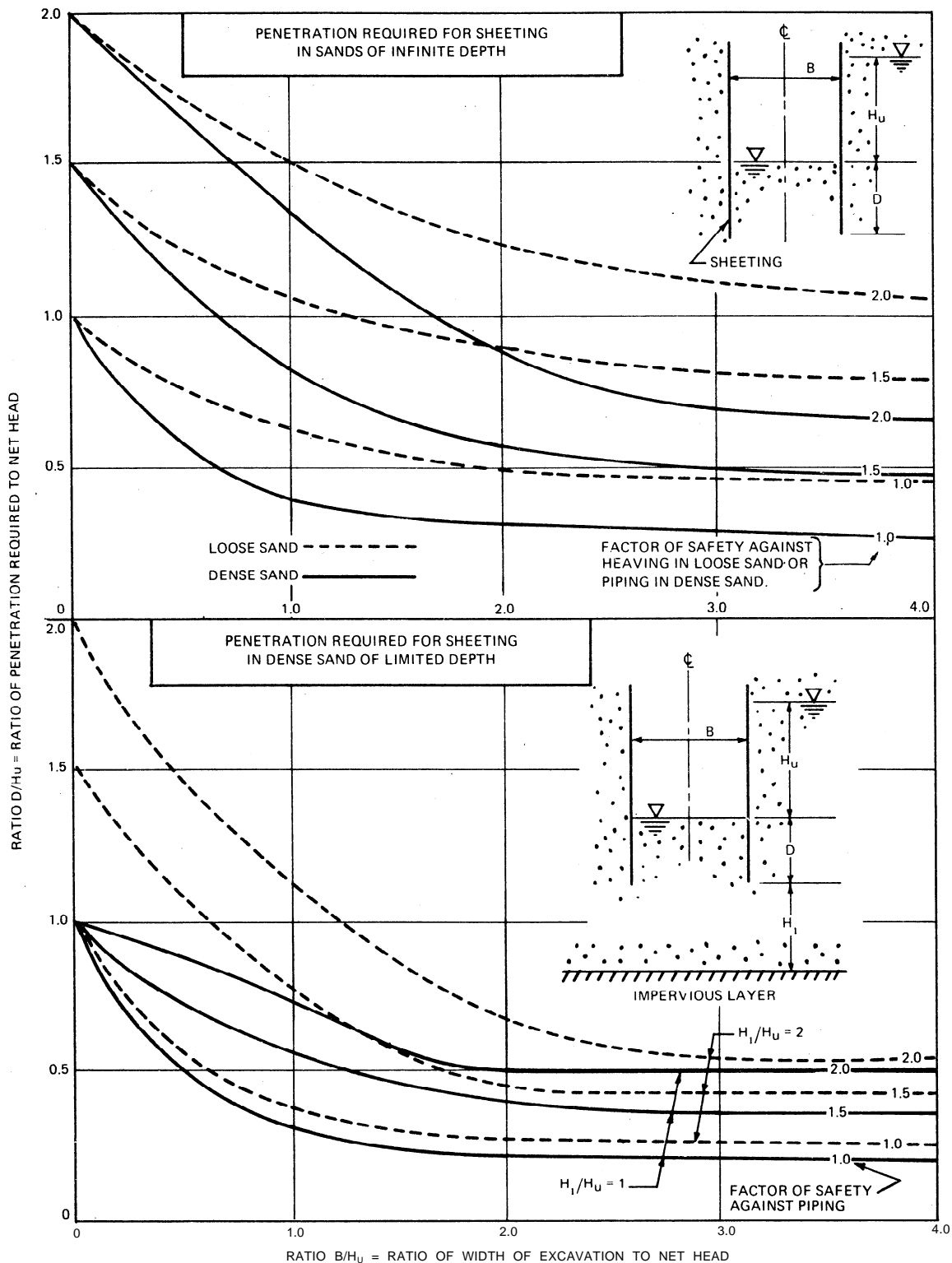
Fig. 62 (a) - Chart for obtaining the depth of sheet piling to prevent piping in a braced cofferdam (after Navdocks[11])

Coarse sand underlying fine sand

Presence of coarse layer makes flow in fine material more nearly vertical and generally increases seepage gradients in the fine layer compared to the homogeneous cross-section of Fig. 62 (a).

If top of coarse layer is at a depth below sheeting tips greater than width of excavation, safety factors of Fig. 62 (a) for infinite depth apply.

If top of coarse layer is at a depth below sheeting tips less than width of excavation, the uplift pressures are greater than for the homogeneous cross-section. If permeability of coarse layer is more than ten times that of fine layer, failure head (H_u) = thickness of fine layer (H_2).
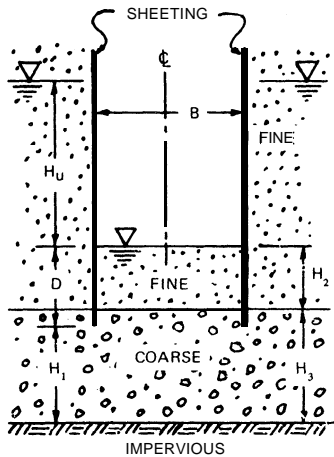
Fine sand underlying coarse sand

Presence of fine layer constricts flow beneath sheeting and generally decreases seepage gradients in the coarse layer.

If top of fine layer lies below sheeting tips, safety factors are intermediate between those for an impermeable boundary at top or bottom of the fine layer' in Fig. 62 (a).

If top of the fine layer lies above sheeting tips the safety factors of Fig. 62 (a) are somewhat conservative for penetration required.
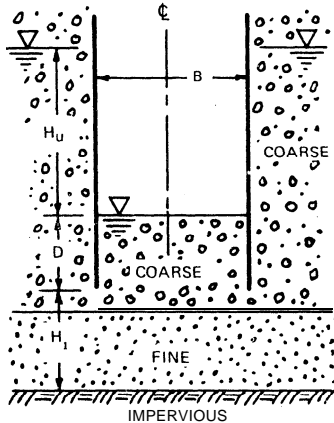
Fine layer in homogeneous sand stratum

If the top of fine layer is at a depth greater than width of excavation below sheeting tips, safety factors of Fig. 62 (a) apply, assuming impervious base at top of fine layer.

If top of fine layer is at a depth less than width of excavation below sheeting tips, pressure relief is required so that unbalanced head below fine layer does not exceed height of soil above base of layer.

If fine layer lies above subgrade of excavation, final condition is safer than homogeneous case, but dangerous condition may arise during excavation above the fine layer and pressure relief is required as in the preceding case.
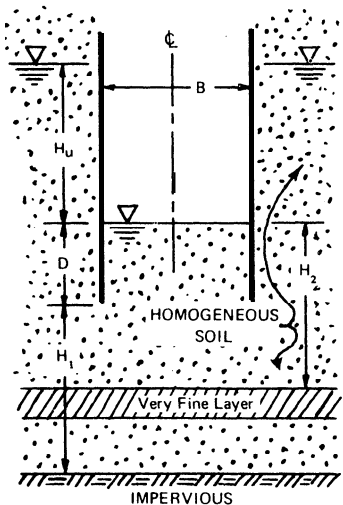
Fig. 62 (b) - Depth of sheet piling in stratified sand to prevent piping in a braced cofferdam (after Navdocks[11])

66

Another method to check base stability of a braced cofferdam in granular soil is as follows:

$$\text{S.F.} = 2N_{\gamma_2} \frac{(\overline{\gamma'_2})}{(\overline{\gamma'_1})} \times (K_a \ \tan\phi)$$

where $\overline{\gamma'_2}$ = average effective unit weight for soil within a depth below excavation level equal to excavation width.

$\overline{\gamma'_1}$ = average effective unit weight for soil above excavation level.

N_{γ_2} = bearing capacity factor for soil below excavation level, determined from Figure 62 (c).

Where an unbalanced water head exits across the sheeting the value of $\overline{\gamma'_2}$ must be determined by subtracting the upwards seepage from the weight of the soil.
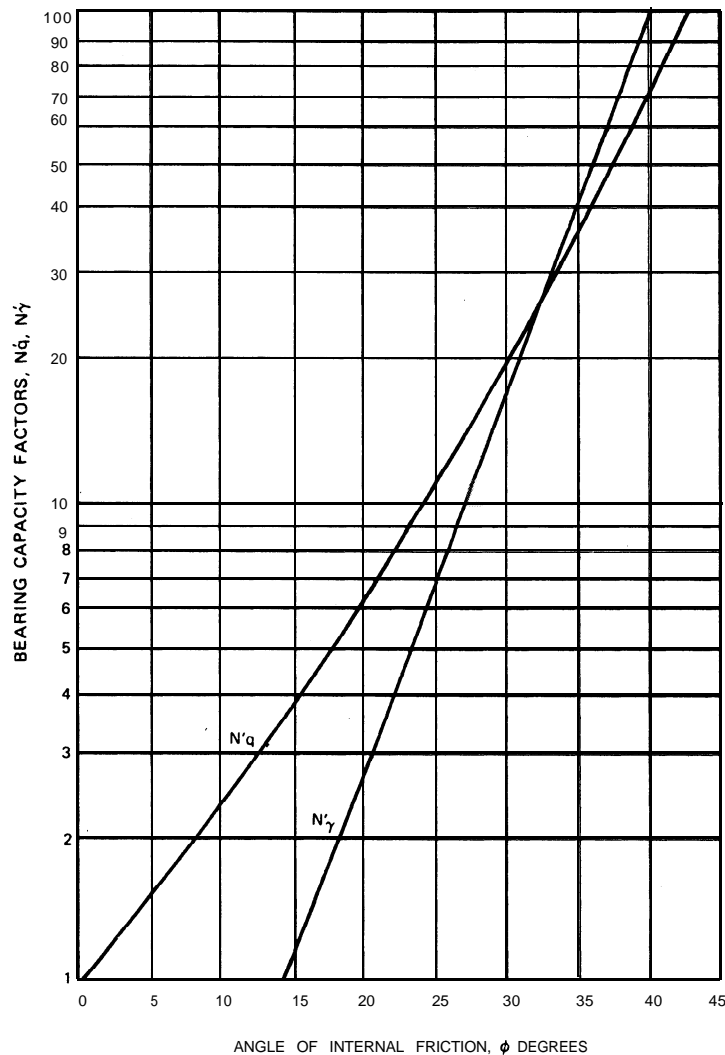
Fig. 62 (c) - Bearing capacity factors

CELLULAR COFFERDAMS

GENERAL

A cellular cofferdam is a gravity retaining structure formed from the series of interconnected straight web steel sheet pile cells filled with soil, usually sand,, or sand and gravel. The interconnection provides water-tightness and self-stability against the lateral pressures of water and earth.

Cellular cofferdams are usually classified according to the configuration and arrangements of the cells. Figure 63 shows three basic types of cellular cofferdams:
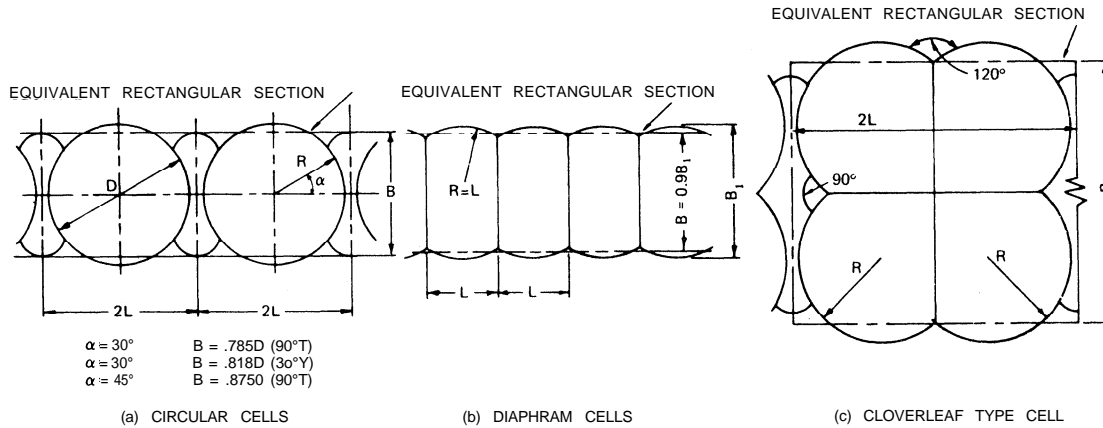
Fig. 63 - Cellular cofferdams

Circular Type - This type consists of individual large diameter circles connected together by arcs of smaller diameter. These arcs generally intercept the circles at a point making an angle of 30 or 45 degrees with the longitudinal axis of the cofferdam. The prime feature of the circular type cofferdam is that each cell is self-supporting and independent of the next. The circular type requires fewer piles per linear foot of cofferdam as compared with a diaphragm type of equal design, as shown in Figure 64.
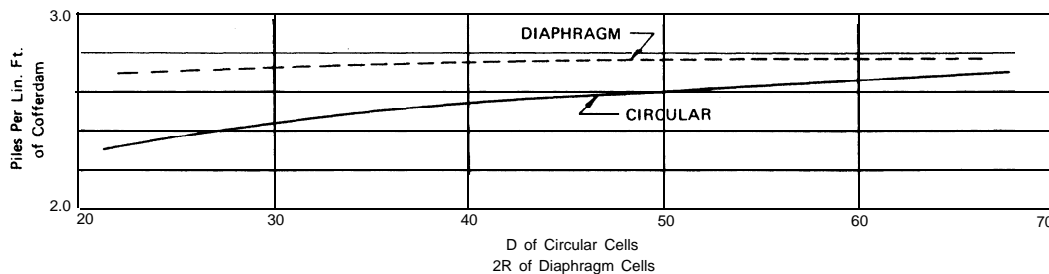
Fig. 64 - Piling required per linear foot of cofferdam (after TVA[36])

This chart is based on:

   a.   The diaphragm arc radius equal to the circular radius.

   b.   The average widths of both types are equal.

   c.   Eight piles in each connecting cell arc.

   d.   T's set 30° from the centerline.

Diaphragm Type - This type of cell consists of two series of circular arcs connected together by diaphragms perpendicular to the axis of the cofferdam. It is common practice to make the radii of the arcs equal to the distances between the diaphragms. At the intersection point the two arcs and the diaphragm make angles of 120 degrees with each other.

The diaphragm type cofferdam can easily be widened by increasing the length of the diaphragms. This increase will not raise the interlock stress, which is a function of the radius of the arc portion of the cell., At any given level, there is a uniform interlock stress throughout the section. The stress is smaller than that at the joint of a circular cell of an equal design.

Cloverleaf Type - This type of cell is a modification of the circular cell. It is generally employed for cases of large head where the large diameter required by stability would result in excessively high interlock stress if diaphragms were not added. Figure 65 shows the general trend in design heads for both circular and cloverleaf type cofferdams. Although the cloverleaf cell uses more steel than circular or diaphragm type cells, it is adaptable to greater heights.
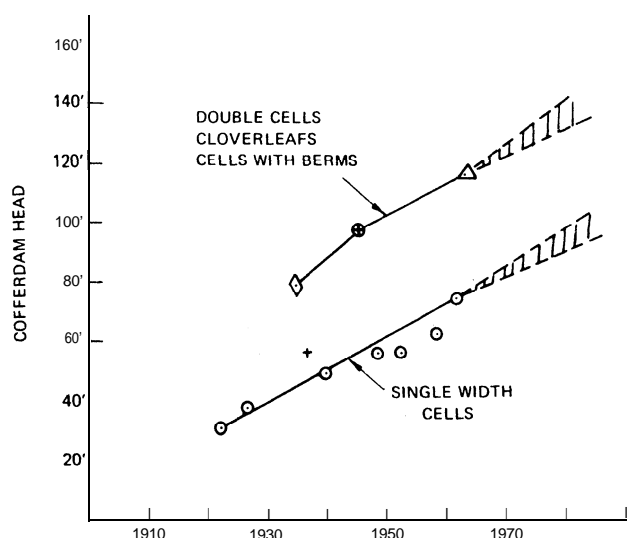

Fig. 65 - General trend in design of cellular cofferdams (after Swatek[41])

Modified Types - In a few cases where stability is not a problem, it may be possible to eliminate or change certain arcs in the circular or diaphragm arrangements, as shown in Figure 66. However, the remaining portions of the cells must be adequately anchored before this is practical.
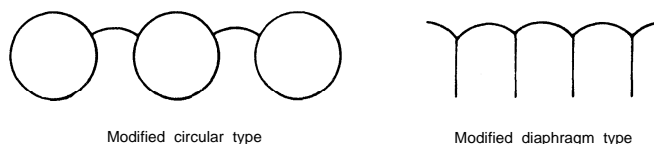

Modified circular type   Modified diaphragm type

Fig. 66 - Modified cellular cofferdams

Components of Cellular Cofferdams - The major components of cellular cofferdams are the steel sheet piling for the cells, the cell fill, and the earth berms that are often used to increase stability.

Straight sheet pile sections permit a maximum deflection angle of 10 degrees (refer to U. S. Steel Sheet Pile Catalog for limitations). When larger deflection angles are required

for small diameter cells, standard bent piles are available as shown in Figure 67. Junction points in cellular cofferdams required special prefabricated pieces, commonly 90 degree T's and 30 and 120 degree Y's. These standard connections are also shown in Figure 67.
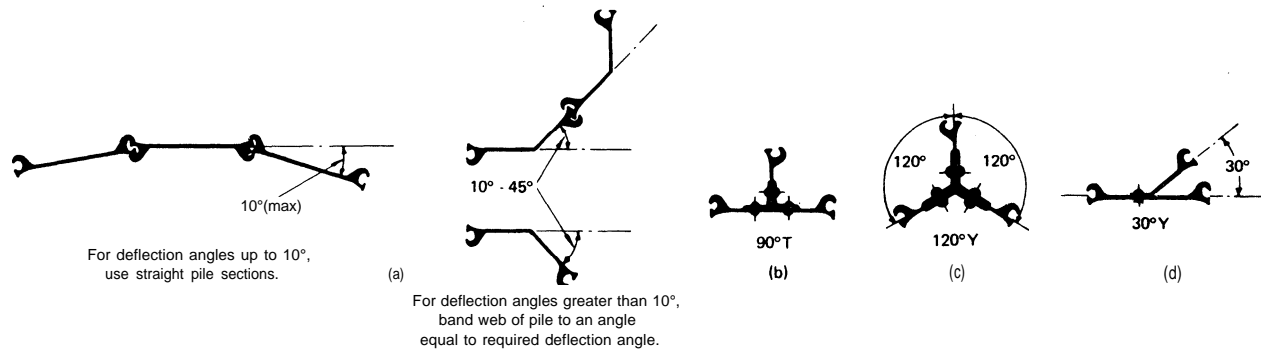

For deflection angles up to 10°, use straight pile sections. (a)

For deflection angles greater than 10°, band web of pile to an angle equal to required deflection angle.

10°(max)

10° - 45°

90°T (b)

120°Y (c)

30°Y (d)

Fig. 67 - Steel sheet piling for cellular cofferdams

Cellular cofferdams acquire a great deal of their stability from the shear resistance of the cell fill. Therefore, the selection of this material is vitally important for a successful design. The Tennessee Valley Authority has summarized the following properties as the most desirable for cell fill material.

1. Free-draining, granular soils with few fines.
2. High shear strength and high coefficient of friction.
3. High unit weight.
4. High resistance to scour and leakage; i.e., well graded soils.

General Design Concepts - Cellular cofferdams consist of two very different materials, steel and soil, resulting in a complex interaction that makes a rational design approach very difficult. Although various theories have been suggested to derive analytical solutions for the stresses in a cell, most designers in this field still rely heavily on past practice and experience. The theoretical considerations presented herein represent the most recent approaches to this problem and may be used with confidence. However, an attempt has also been made to supply the reader with past experience to enable him to develop designs consistant with proven sound engineering practices. It must be pointed out that good judgment should always prevail. Precise mathematical evaluations can result in misleading and dangerous conclusions in the hands of inexperienced designers. Under these circumstances, any cellular sheet pile structure of importance should have the benefit of the best obtainable professional engineering advice. This is particularly true for cases where difficult foundation conditions exist.

Generally, the design of a cellular cofferdam proceeds much the same as that of an anchored wall. Before a design can be initiated, the necessary controlling dimensions must be set and a site reconnaissance made. The height of the cofferdam must be established from flood records so that its top is at least at the level of the anticipated high water during the life of the cofferdam. For high cofferdams, a berm might also be considered to reduce the relative height above ground.

Site Conditions - The site reconnaissance should include information on the existing ground surface and the depth of scour, as well as a complete subsurface investigation. Exploratory borings extending to rock should be located so as to provide a complete picture of the soil strata and the general configuration of the rock surface. Laboratory tests give the engineer first-hand knowledge of the character and the properties of the materials in design. Care should be exercised, however, in the application of laboratory test results because of the complicated response of the structure to actual field conditions. These conditions are almost impossible to duplicate by ordinary testing procedures. It is advisable to extend several borings into the rock to determine its general character and competency. Also, the depth and extent of soft soils (soft clay, silt and

organic deposits, etc.) should be carefully ascertained, since these soils must be removed and replaced by granular soils.

Equivalent Width - After the height of the cofferdam is established and the pertinent physical properties of the underlying soils together with the cell fill are determined, a tentative equivalent width, B, is chosen. The equivalent width, B, of the cofferdam is defined as the width of an equivalent rectangular section having a section modulus equal to that of the actual cofferdam. For design purposes this definition may be simplified to equivalent areas, from which

$$\text{Equivalent Width, B} = \frac{\text{area of (main cell + one connecting cell)}}{\text{center to center distance of main cells}}$$

TVA engineers have found that the results by the two definitions differ by only about six per cent. For circular cells the area definition leads to the following relationship between diameter and equivalent width:

$$B = 0.785 \, D \text{ for } \alpha = 30 \text{ degrees } (90°T) \text{ [see Figure 63(a)]}$$
$$B = 0.818 \, D \text{ for } \alpha = 30 \text{ degrees } (3O°Y)$$
$$B = 0.875 \, D \text{ for } \alpha = 45 \text{ degrees } (90°T)$$

For diaphragm type cells

$$B = \frac{\text{area enclosed by cell}}{\text{distance between diaphragms}}$$

For design purposes this can be taken as 0.9 times the total dimension of the cell from front to back [see Figure 63 (b)].

Saturation Line - Before stability of the assumed cell configuration can be checked the degree of saturation within the cell fill must be considered, in particular, the location of the line of saturation must be located. The zone of saturation within the cell will be influenced by a number of factors including the condition of the pile interlocks, the permeability of the cell fill, whether a berm is used, and the number and position of weep holes on the inside row of piling. In general, the slope of the free water surface or saturation line may be assumed as shown in Figure 68 for the various types of cell fill. In cases where an earth berm is used, the saturation line slopes to the top of the berm. In the berm itself, two locations of saturation line should be considered, as shown in Figure 69 to make provision for the more critical location. A horizontal line, at an elevation so chosen as to represent the average expected condition of saturation should serve just as well, at the same time simplifying computations.
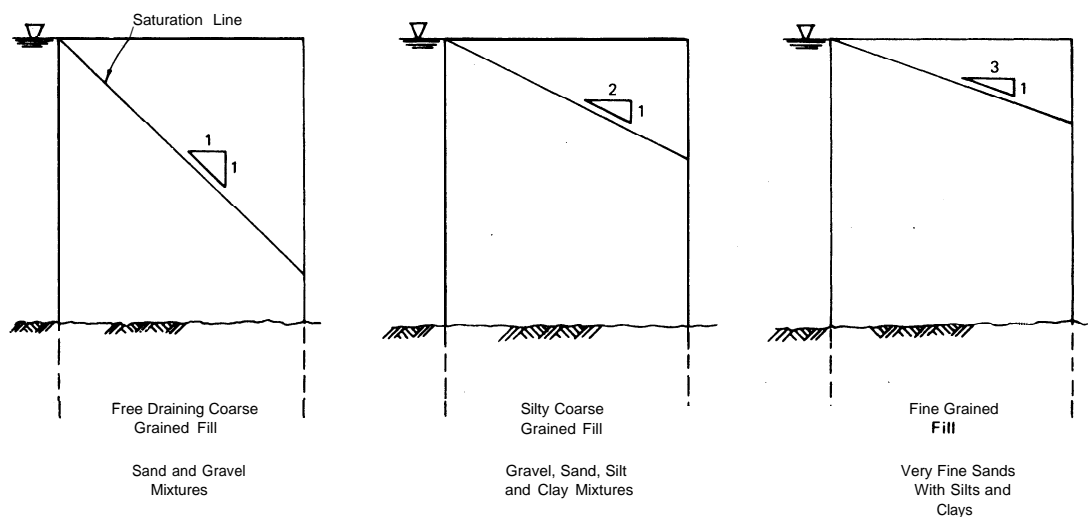

Fig. 68 - Recommended saturation lines for various soil types

STABILITY OF COFFERDAMS ON ROCK

For purposes of stability analysis cellular cofferdams are classified according to the type of foundation (i.e., cofferdams on rock and cofferdams on deep soil deposits). Cellular cofferdams founded on rock must be analyzed for several types of failure. Problem No. 1 (pages 127-132) illustrates the design of a circular cofferdam founded on rock.

Sliding on Foundation - The safety factor for horizontal sliding of the cofferdam is obtained by considering the driving forces and the potential resisting forces acting on a unit length. The cofferdam is subjected to the lateral driving pressures on the outboard face, the frictional resistance along the bottom of the cofferdam and berm (if one is used) and the passive resistance of the soil on the inboard face, as shown in Figure 69.
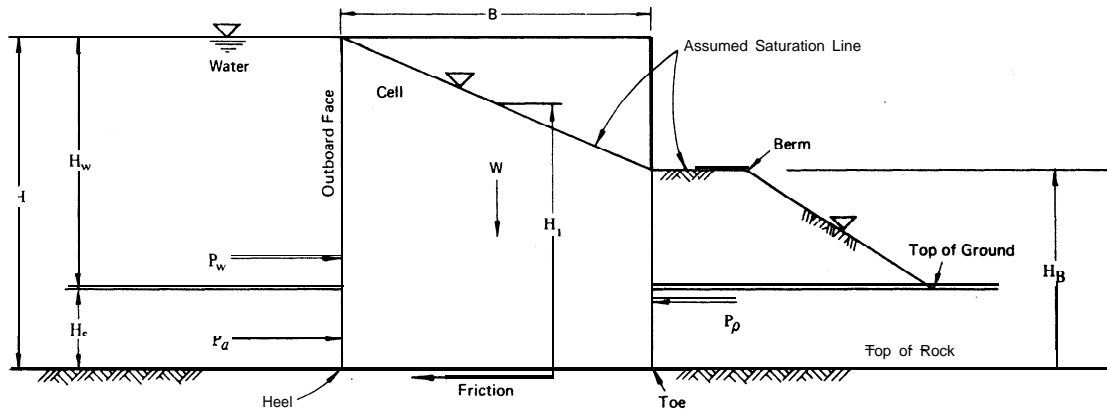
Fig. 69

Driving Forces:

Full water pressure, $P_w = \gamma_w H^2 /2$, per foot of wall

Active earth pressure, $P_a = \gamma' K_a H_s^2 /2$, per foot of wall

where
K_a = active earth pressure coefficient
γ' = submerged unit weight of soil on the outboard side of the cofferdam
γ_w = unit weight of water = 62.4 pounds per cubic foot
H and H_s = height of cofferdam and soil, respectively
H_B = height from toe of cofferdam to top of berm

Resisting Forces:

Friction force along bottom of the cell, $W \tan\delta'$;

$$W \tan\delta' = B[\gamma(H-H_1) + \gamma'H_1] \tan\delta'$$

where
W = effective weight of cell fill
B = equivalent width of cofferdam
γ = unit weight of cell fill above saturation line
H = total height of cofferdam
H_1 = average height of saturation line
γ' = submerged unit weight of cell fill
$\tan \delta'$ = coefficient of friction of cell fill on rock, for smooth rock = 0.5
δ' = @-angle of the soil for other types

Passive resistance of soil and berm on inboard face of cofferdams founded on rock, P_ρ should be determined by the sliding wedge theory or the Coulomb Theory modified to account for any intersection of the failure wedge with the back slope of the berm. These theories should be used because the presence of the rock will not permit a log-spiral failure to develop.

72

The resulting safety factor against sliding is:

$$F.S. = \frac{\text{Resisting Forces}}{\text{Driving Forces}}$$

$$= \frac{W \tan \delta' + P_\rho}{P_w, + P_a}$$

where $\quad P_\rho$ = effective passive resistance of the soil and berm on the inboard face, per foot of wall

The safety factor against sliding on the foundation should be at least 1.25 for temporary structures and 1.50 for permanent construction.

Slipping Between Sheeting and Cell Fill - When a cellular cofferdam is subject to large overturning forces, failure can occur by lifting the outboard piling and losing the cell fill as it runs out the heel of the cell. In such cases slippage occurs between the sheet piles on the outboard face and the cell fill. In order to compute the safety factor against such a failure, moments are summed about the inboard toe,. The resisting moment is due to the frictional forces on the inner and outer face of the outboard sheeting, plus the effective passive resistance of the soil and berm on the inboard face. The weight of the cell does not provide resisting moment, since it is assumed that the cell fill does not lift up with the piling. The resulting expression is:

$$F.S. = \frac{\text{Resisting Moment (Due to Friction on Outboard Piling)}}{\text{Driving Moment Due to Water and Soil Pressures}}$$

$$F.S. = \frac{B(P_w + P_a) \tan \delta + P_\rho \, H_B / 3}{1/3 \, (P_w H + P_a H_s)}$$

where $\quad \tan \delta$ = coefficient of friction between the steel sheet piling and the cell fill, see Table 4 (page 13)

Shear Failure on Centerline of Cell (Vertical Shear) - Figure 70 shows the customary assumed stress distribution on the base of a cofferdam due to a net overturning moment, M. The total shearing force on the neutral plane at the centerline of the cell is equal to the area of the triangle as shown. Then

$$Q = \left(\frac{1}{2}\right) \left(\frac{B}{2}\right) \left(\frac{6M}{B^2}\right) = \frac{3M}{2B}$$

where $\quad$ Q = total shearing force force per unit length of cofferdam

$\quad\quad\quad\quad$ M = net overturning moment, per unit length of cofferdam =

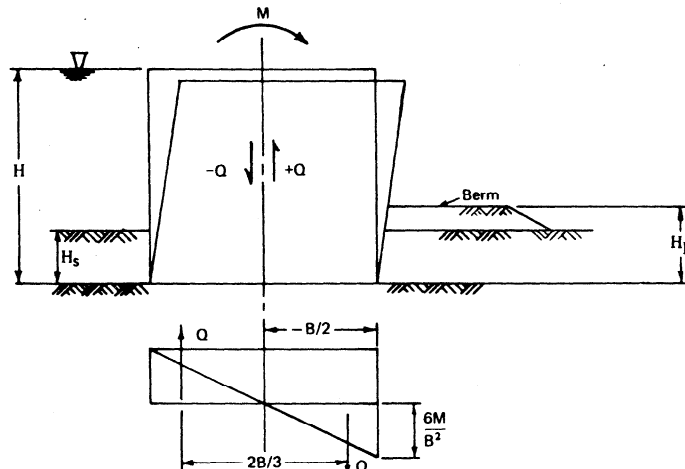$$\frac{1}{3} \, [P_w H + P_a H_s - P_\rho H_B]$$

Fig. 70 - Assumed stress distribution on base

The force Q is resisted by vertical shear within the cell fill and friction in the interlocks. The vertical resisting shear within the cell fill along the centerline of the cofferdam is equal to the horizontal pressure times $\tan\phi$. The horizontal pressure on the neutral plane at any depth, Z, is equal to the vertical pressure, γZ, times the coefficient of earth pressure, K. That is:

$$\sigma_h = K\gamma Z$$

The value of K is higher than K_a, the coefficient of active earth pressure. From Mohr's stress circle the value of K is given by:[42]

$$K = \frac{\cos^2\phi}{2-\cos^2\phi}$$

where ϕ = angle of internal friction of the cell fill

The horizontal pressure distribution on the centerline of the cofferdam is shown in Figure 71 (a). The resultant lateral force, per unit length of cofferdam, P_s, is then

$$P_s = \frac{1}{2}K\gamma(H-H_1)^2 + K\gamma(H-H_1)H_1 + \frac{1}{2}K\gamma'H_1{}^2$$

Therefore, the total centerline shear resistance per unit length of cofferdam is equal to
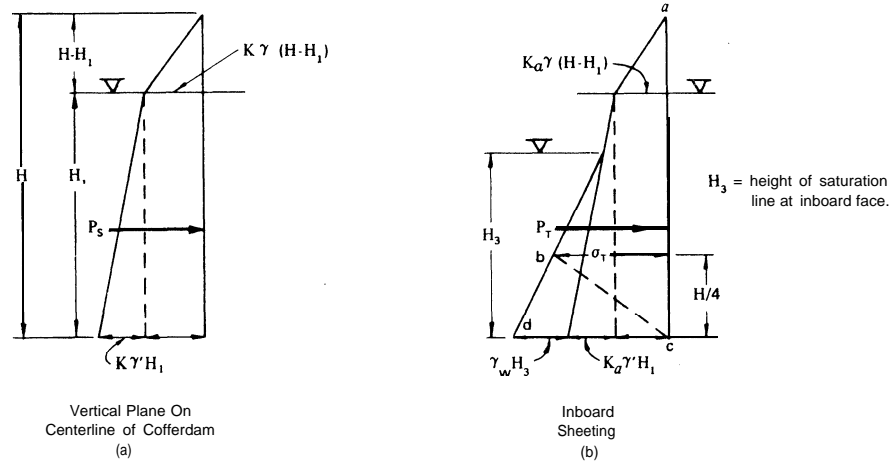
$$S = P_s\tan\phi$$

Fig. 71 - Horizontal pressure diagrams

The frictional resistance in the sheet pile interlock per unit length of cofferdam is equal to the interlock tension times the coefficient of friction, f, (for steel on steel at the interlock, f = 0.3). To calculate interlock tension, TVA engineers use the pressure resultant P_T shown in the triangle abc in Figure 71 (b). (See section on Interlock Tension.) The lateral pressure is assumed to reduce to zero at a point c because the lower end of the piling bites into the rock, reducing the ring tension. The total shearing resistance along the centerline of the cell is therefore

$$S_T = P_S\tan\phi + fP_T$$

where P_T = area abc on Figure 71 (b)

and the safety factor against failure is

$$F.S. = \frac{S_T}{Q} = \frac{(P_S\tan\phi + fP_T)\,2B}{3M} \geq \begin{array}{l} 1.25 \text{ (for temporary structures)} \\ 1.50 \text{ (for permanent structures)} \end{array}$$

74

Horizontal Shear (Cummings' Methods) - Cummings[3] has proposed a theory of cellular cofferdam failure known as the interior sliding theory, where the resistance of a cell to failure by tilting is gained largely through horizontal shear in the cell fill. Cummings concluded, based on model tests, that the shear resistance is developed only below plane A T (inclined at the angle of internal friction ϕ to the base) and that the cell fill above A T acts essentially as a surcharge as shown in Figure 72.
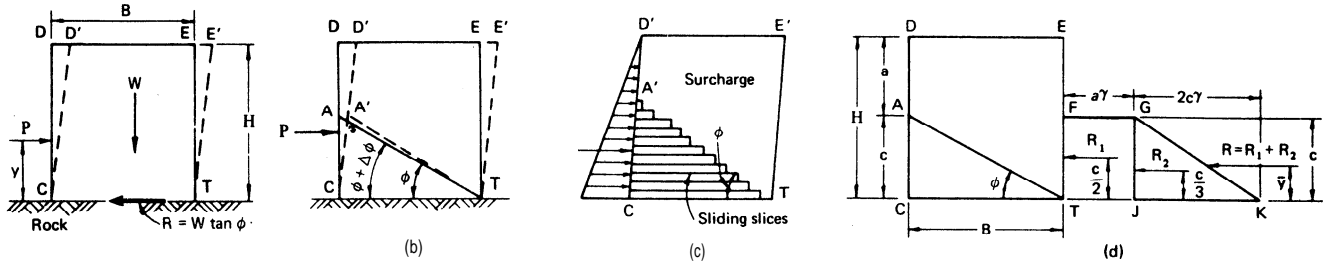

Fig. 72 - Cummings method

The soil below AT fails by sliding on horizontal planes as shown and thereby produces a resisting pressure on the outboard sheeting. The following equations derived by Cummings summarize his method of computing the resisting moment due to this pressure. The variables in the equations are as shown in Figure 72. The ultimate lateral shear resistance of the cell is given by:

$$R = W \tan\phi = \gamma BH \tan\phi$$

$$\text{substituting } H = a + c$$

$$\text{and } B = c/\tan\phi$$

$$R = ac\gamma + c^2$$

This equation is represented graphically by the diagram shown in Figure 72 (d), the area of which .is equal to the total resistance, R. This diagram is treated similar to a pressure diagram, from which the resisting moment about the base can be computed. The total moment of resistance per foot of wall about the base of the cofferdam is:

$$M_r = R_1 (c/2) + R_2 (c/3)$$

$$\text{where } R_1 = ac\gamma$$

$$\text{and } R_2 = c^2\gamma$$

$$\text{thus } M_r = \frac{ac^2\gamma}{2} + \frac{c^3\gamma}{3}$$

In addition, the interlock friction also provides shear resistance. It is computed as the tension caused by the pressure of the cell fill acting on a vertical one foot slice times the coefficient of interlock friction, f.

$$\text{Interlock friction force, } F_i = P_T \times L \times f$$

where P_T and L are as previously defined.

The friction force F_i is assumed to act equally on all interlocks; therefore, an individual pile will have equal but opposite friction forces at each end. The resisting moment, M_i, against tilting due to the interlock tension results from the summation of the individual couples caused by the opposite friction force on each pile. Therefore, resisting moment per foot width is:

$$M_i = \frac{F_i B}{L} = P_T f B$$

where   L is as shown in Figure 63.

If a berm is used, the resisting moment due to the effective passive pressure of the berm should be included. Thus, the safety factor against tilting is:

$$F.S. = \frac{\text{Resisting Moment}}{\text{Driving Moment}} = \frac{M_r + M_i + P_p H_B/3}{1/3\,(P_w H + P_a H_s)}$$

As an illustration, using the horizontal shear method, the factor of safety against tilting for various values of the ϕ-angle of the cell fill, varies as shown in Figure 73 due to the influence of water pressure only.
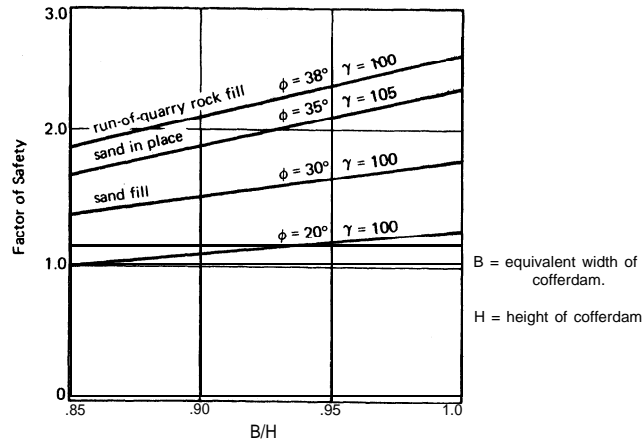

Fig. 73 - Factor of safety against tilting (after Cummings[37])

Interlock Tension - The interlock tension developed in a cellular cofferdam is a function of the variation of the internal cell pressure. TVA engineers generally assume that the maximum pressure occurs at a point one-fourth of the total cell height from the bottom. The pressure distribution shown in Figure 71 (b) on the inboard sheeting may be used.

$$\sigma_T = K_a \gamma (H - H_1) + K_a \gamma'(H_1 - H/4) + \gamma_w (H_3 - H/4)$$

where K_a = coefficient of active earth pressure (Figure 5). Terzaghi[38] suggests a minimum value of $K_a = 0.4$. "Navdock" uses $K_a = K = \dfrac{\cos^2 \phi}{2 - \cos^2 \phi}$. For hydraulic fill, TVA uses the Coulomb active coefficient together with full water pressure.

The maximum interlock tension in the main cell is given by

$$t = \frac{\sigma_T \times R}{12} \qquad \text{(pounds per linear inch)}$$

where σ_T = maximum inboard sheeting pressure (pounds per foot)

    R = radius (feet)

The interlock stress at the connections as shown in Figure 74 may be approximated by

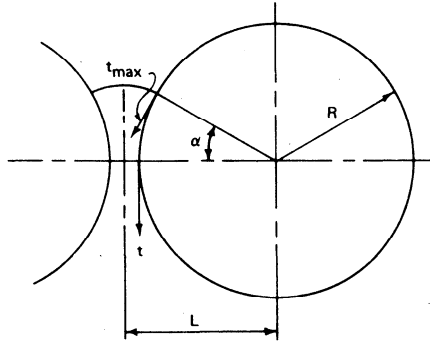$$t_{max} = \frac{\sigma_T \times L \text{ secant } \alpha}{12} \quad \text{(pounds per linear inch)}$$

Fig. 74 - Interlock stress at connection

This value of t_{max} is smaller than when computed by the "exact" analysis of combining the ring tension of the small and large cells into a force polygon.

The interlock stress for straight web piling in pounds per linear inch are given below:

	Guaranteed Value (pli)	Suggested Design Value (pli)	Factor of Safety
PSA 23 and PSA 28	12,000	3,000	4 *
PS 28 and PS 32	16,000	8,000	2
** PSX32	28,000	14,000	2

"Shallow arch sections subject to straightening   **Available only in USS EX-TEN 50 Steel
For other grades - inquire.

While no design values are given on interlock tension for connecting arcs, the maximum allowable tension is probably less than 4000 pounds per lineal inch, based on tests by Tschebotarioff[3] and others made on riveted "T's." A "bin effect" usually results in the fill within the connecting arcs that generally lessens the interlock tension. However, the junction between the main cells and connecting arcs should receive full attention. Often 30° Y's are used instead of 90° T's in large cells. The 30° Y's create less tension in the connecting arcs due to the smaller required radius.

COFFERDAMS ON DEEP SOIL FOUNDATIONS

General - Many of the items and requirements discussed above for cofferdams on rock are directly applicable to the design of cellular cofferdams founded on deep soil deposits. In addition several other requirements must be satisfied to insure stability. These requirements may be grouped into two areas: (1) stability with respect to bearing capacity failure of the underlying strata and (2) underseepage causing piping which results in boiling at the inboard toe.

In general, horizontal sliding of the cofferdam at its base will not be a problem on soil foundations. However, internal shear failures should be investigated as for cofferdams on rock foundations. The underlying soil may or may not cause sufficient restraint to reduce the horizontal pressure on the inboard face as shown in Figure 71 (b). Therefore, some designers prefer to use the full pressure diagram abdc to calculate P_T (shear failure on centerline of cell and interlock tension).

Stability - For cellular cofferdams on sand, the inboard sheet piles should be driven to a sufficient depth to counteract the vertical downward friction force F_1 caused by the interaction of the cell fill and the inner face. This friction force is given by

$$F_1 = P_T \tan\delta \quad \text{(force per unit length)}$$

where P_T is as shown in Figure 71 (b).
            $\tan \delta$ = coefficient of friction between steel sheet piling and cell fill

Generally a factor of safety of 1.5 applied to F_1 is sufficient.

Cellular cofferdams on sand or clay foundations involve a surcharge loading imposed upon the supporting stratum at the inboard toe. An estimate of the safety factor against a bearing capacity failure of the supporting stratum can be made by considering the entire cell to act as a unit. The resulting factor of safety will then be

$$F.S. = \frac{cN_c + \frac{1}{2}\,\overline{\gamma}'\,BN_\gamma}{\left(\dfrac{6M}{B^2}\right) + \gamma H} \geq \begin{array}{l} 2 \text{ (granular soils)} \\ 2.5\text{-}3.0 \text{ (fine grained soils)} \end{array}$$

where N_c and N_γ = Terzaghi bearing capacity factors (see Figure 75)

$\overline{\gamma}'$ = average effective unit weight of supporting stratum within a depth H

γ = average unit weight of cell fill

M = net overturning moment (see page 73)
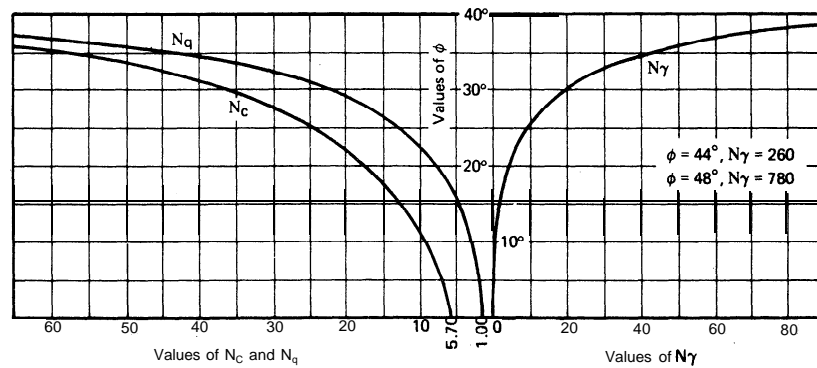
Fig. 75 - Relation between # and the bearing capacity factors
(after Terzaghi and Peck[14])

For clay foundations the ultimate bearing capacity can be used to determine the maximum height of cofferdam above ground and is:

$$H = 5.7\,\frac{c}{\gamma_e}$$

If a minimum safety factor of 1.5 is used, the maximum height of cofferdam founded on deep clay is given by

$$H = 3.8\,\frac{c}{\gamma_e}$$

where   H = maximum height of cofferdam above ground surface.

C = unit cohesion of the clay.

γ_e = effective unit weight of cell fill; i.e., use submerges weight below saturation line.

If the cofferdam rests on soft to medium clay or other compressible soils, a relatively small external moment will produce a very unequal distribution of pressure on the base of the fill in the cells causing the dam to tilt. The stability of the cofferdam is practically independent of the strength of the cell fill since the shearing resistance through vertical sections offered by the cell fill cannot be mobilized without overstressing the interlocks.

In this instance, stability can be realized if a heavy berm against the inner face of the cofferdam is provided or if some tieback system is utilized. In general, if an inside berm is used, bearing capacity should not be a problem. For cellular cofferdams on soft to medium, clay, the shearing resistance of the fill in the cells is neglected, and the factor of safety against a shear failure on the centerline of the cell is based on the moment resistance realized by interlock friction and is given by (Terzaghi[38]).

$$F.S. = \frac{\triangle P \; Rf \left(\frac{B}{L}\right) \left(\frac{L + 0.25B}{L + 0.5B}\right)}{M}$$

where $\triangle P$ = pressure difference on the inboard sheeting.
            = $P_T - P_\rho$
     M = net overturning moment (see page 73).
     R = radius
     f = coefficient of interlock friction (0.3)

The minimum factor of safety of 1.25 for temporary construction and 1.50 for permanent structures is usually adequate.

Underseepage - Figure 76 is a cross section through a cellular cofferdam founded on sand. The design of such a cofferdam must satisfy three conditions: (1) the sand along the outer face of the dam should be adequately protected against erosion, (2) the dam should be stable enough to withstand the lateral pressures imposed by soil and water; (3) the soil at the inboard toe must be able to support the pressure on the base of the dam despite the tendency of the seepage forces to reduce the buoyant weight and liquefy the sand at the toe.
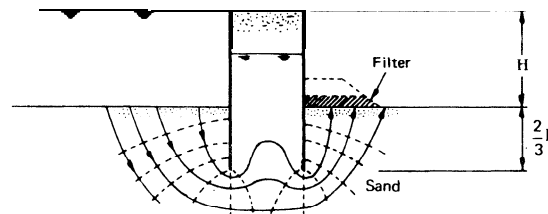

Fig. 76 - Seepage in cellular cofferdam in sand (after Terzaghi[22])

Condition (3) is known as boiling or a "quick condition," in which the shear strength of the sand is reduced to zero. Boiling thus eliminates the passive resistance of the sand against an inward movement of the buried part of the inner row of sheet piles, and the cofferdam may fail by toppling inward. The method of computing the upward seepage force due to the unbalanced hydrostatic head was presented previously on page 17.

The formation of boils can be prevented by two different methods: (1) by increasing the drainage path of the water by driving the sheet piling deeper, and (2) by covering the danger zone with a loaded, inverted filter as shown in Figure 76. Although the filter will have no influence on the shape of the flow net, the load that acts on the filter will counteract the upward seepage forces which tend to lift the sand in the danger zone. The problem of seepage forces and flow nets is discussed in detail in *Theoretical Soil Mechanics* by K. Terzaghi.[13]

The filter material must satisfy two independent conditions. It should be coarse enough to permit free discharge of the seepage water and its largest voids must be small enough to prevent clogging from the finer soil particles of the underlying soil. Many empirical criteria are in popular use today to satisfy these conditions. *Seepage, Drainage and Flow Nets* by Cedergren[44] contains a summary of these criteria.

In general, sheet piling in sand should be driven to a depth of about two-thirds the height of the cofferdam above the ground surface or until it bears on a hard stratum. If the water level is lowered to at least $H/6$ below the inboard ground surface, the penetration may be reduced about one-half the height.

Better drainage and, therefore, increased stability can often be realized by installation of wellpoints and deep wells underneath the cells near the inboard side. These serve to pick up the flow of water into the cofferdam area under the sheet pile perimeter.

Pull-Out of Outer Face Sheeting - The penetration of sheet piling in granular soils is controlled by the need to extend the length of the flow paths of the water percolating beneath the cell. However, the penetration must also be adequate to insure stability with respect to pull-out of the outboard sheeting due to tilting.

The average pile reaction due to the overturning moment on the outboard piling is given by:

$$Q_\rho = \frac{P_w H + P_a H_s - P_\rho H_B}{3B(1 + B/4L)}$$

where the variables are as defined previously.

The ultimate pile pull-out capacity per linear foot of wall, Q_u, depends on the material into which the pile is driven. For clay

$$Q_u = c_a \text{ x perimeter x embedded length}$$

where c_a can be determined from Table 5 (page 41) for various values of cohesion.

For granular soils

$$Q_u = \frac{1}{2} K_a \gamma_e D^2 \tan\delta \text{ x perimeter}$$

where
  K_a = active coefficient of lateral earth pressure
  D = embedded length
  $\tan\delta$ = coefficient of friction for steel against underlying soil
  γ_e = effective unit soil weight of underlying soil

A factor of safety of 1.5 is sufficient, therefore:

$$F.S. = \frac{Q_u}{Q_\rho} \geq 1.5$$

HANSEN'S THEORY

J. Brinch Hansen[43] has proposed an analysis of cofferdam stability by the extreme method based on a simple concave or convex surface of rupture. By this method a cofferdam founded on soil with a shallow depth of penetration will fail by rotation of the entire cofferdam about a point beneath itself, as shown in Figure 77 (a).
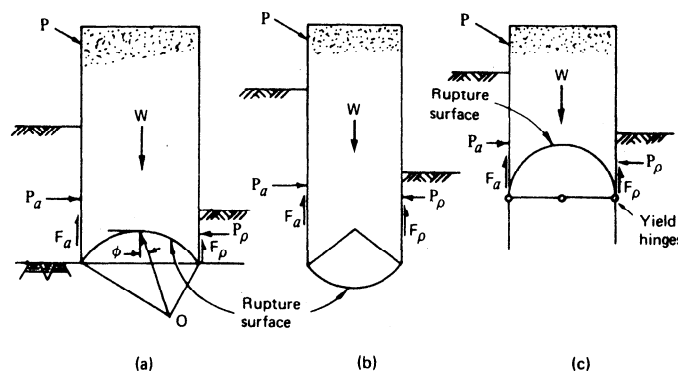

Fig. 77 - J. Brinch Hansen's extreme method

The earth below the rupture line remains at rest, whereas the whole earth mass above the line rotates as one rigid body about the center at 0. If the cofferdam penetration is deep, the surface of rupture may be either concave or convex, Figure 77 (a) or (b), and both possibilities are investigated, together with the possibility of plastic yield of the sheet piling as shown in Figure 77 (c). For a cofferdam founded on rock the surface of rupture is assumed to be convex, located within the cell fill.

Although the failure surface is generally considered to be a circular arc, it is convenient to assume a logarithmic spiral represented by the equation:

where r and θ = variables in the polar coordinate system

r_O = radius to the beginning of the spiral

ϕ = angle of internal friction

A trial position of the spiral is chosen and the weight above the spiral, W, and the external forces, P and F, are calculated using appropriate soil properties. The stability of the entire cofferdam is then investigated by taking moments about the pole 0. Since all the frictional forces acting on the spiral surface are directed towards the pole, they cause no moment. The forces W, P_p and F_p will contribute to the stabilizing moment while the forces P, P_a and F_a will contribute to the overturning moment. The reader is directed to *Earth Pressure Calculation* by J. Brinch Hansen[43] for a more detailed explanation of the extreme method together with numerous graphs and charts to aid in determining the minimum factor of safety.

BIBLIOGRAPHY

General

1. **Foundation Design,** Wayne C. Teng, Prentice-Hall, Inc., Englewood Cliffs, New Jersey, 1962.
2. **Substructure, Analysis and Design,** Paul Anderson, Ronald Press, New York, 1956.
3. **Soil Mechanics, Foundations and Earth Structures,** G. P. Tschebotarioff, McGraw-Hill, Inc., New York, 1951.
4. **Deep Foundations and Sheet Piling,** Donovan H. Lee, Concrete Publications Limited, London, 1961.
5. **Design and Construction of Ports and Marine Structures,** Alonzo DeF. Quinn, McGraw-Hill, Inc., New York, 1961.
6. **Pile Foundations, Robert Chellis,** McGraw-Hill, Inc., New York, 1961.
7. Steel Sheet Piling (Catalog), U. S. Steel Corporation (ADUSS-25-2369), U. S. Steel Corporation, 1968.
8. Protection of Piling in Marine Environments, U. S. Steel Corporation, (AUDCO-25003-58), U. S. Steel Corporation, 1958.
9. **Foundation Engineering, G. A. Leonards,** McGraw-Hill, Inc., New York, 1962.
10. **Foundations of Structures,** C. W. Dunham, McGraw-Hill, Inc., New York, 1962.
11. **Design Manual DM-7,** U. S. Navy Bureau of Yards and Docks, U. S. Government Printing Office, Washington, D. C., 1962.
12. **Design of Pile Structures and Foundations,** U. S. Army Engineers Manual, U. S. Government Printing Office, Washington, D. C., 1958.

Lateral Pressures and Soil Mechanics

13. **Theoretical Soil Mechanics,** Karl Terzaghi, John Wiley and Sons, Inc. New York, 1943.
14. **Soil Mechanics in Engineering Practice,** K. Terzaghi and R. Peck, John Wiley and Sons, Inc., New York, 1967.
15. **Engineering Geology and Geotechniques,** Krunine and Judd, McGraw-Hill, Inc., New York,
16. **Mechanics of Soils, Alfredo R. Jumikis,** D. Van Nostrand and Company, Inc., Princeton, New Jersey, 1964.
17. **Basic Soils Engineering,** B. K. Hough, Ronald Press, New York, 1957.
18. **Fundamentals of Soil Mechanics,** D. W. Taylor, John Wiley and Sons, Inc., New York, 1948.
19. "General Wedge Theory of Earth Pressure," K. Terzaghi, **Transactions; ASCE,** Vol. 106, 1941.
20. "Stability of Soil Subject to Seepage Forces Adjacent to Sheet Pile," H. Gray and K. Nair, **Geotechnique,** Vol. 17, No.2, 1967.
21. "Tables for the Calculation of Passive Pressure, Active Pressure, and Bearing Capacity of Foundations," A. Caquot and J. Kerisel, Gauthier-Villars, Paris, 1948.

Design of Sheet Pile Retaining Walls (Bulkheads)

22. "Anchored Bulkheads," K. Terzaghi, **Transactions, ASCE,** Vol. 119, 1954.
23. "Lateral Earth Pressures on Flexible Retaining Walls," G. P. Tschebotarioff and others, **Transactions, ASCE,** Vol. 114, 1949.
24. "Anchored Sheet Pile Walls," P. W. Rowe, **Proceedings, Institution of Civil Engineers,** Part I, Vol. I., London, England, 1952.
25. "A Theoretical and Experimental Analysis of Sheet Pile Walls," P. W. Rowe, **Proceedings, Institution of Civil Engineers,** Part I, Vol, I., London, England, 1955.
26. "Sheet Pile Walls Encastre at Anchorage," P. W. Rowe, **Proceedings, Institution of Civil Engineers,** Part I, Vol, I., London, England, 1955.
27. "Sheet Pile Walls in Clay," P. W. Rowe, **Proceedings, Institution of Civil Engineers,** Part I, Vol. I., London, England, 1957.

28. "The Design of Flexible Bulkheads," J. A. Ayers and R. C. Stokes, **Transactions, ASCE,** Vol. 119, 1954.

29. "Design and Construction of Flexible Retaining Structures," G. P. Tschebotarioff, Presented at the Chicago Soil Mechanics Lecture Series, Chicago, Illinois, 1964.

Braced Cofferdams and Deep Excavations

30. "Earth Pressure Measurements in Open Cuts, Chicago (Ill.) Subway," R. B. Peck, **Transactions, ASCE,** Vol. 108, 1943.

31. "Stability of Strutted Excavations in Clay," L. Bjerrum and O. Eide, **Geotechnique,** Vol. 6, No. 1, 1956.

32. "Model Experiments to Study the Influence of Seepage on the Stability of a Sheeted Excavation in Sand," A. Marsland, **Geotechnique,** Vol. 3, 1953.

33. "Design and Construction of Braced Cuts," E. D. White, presented at the Chicago Soil Mechanics Lecture Series, Illinois Section, ASCE, Chicago, 1964.

34. "Discussion," R. Kirkdam, **Proceedings, Brussels Conference 58 on Earth Pressure Problems,** Brussels, 1958.

35. **Rock Tunneling with Steel Supports,** R. V. Proctor, T. L. White, Youngstown Printing Company, Youngstown, Ohio, 1964.

Cellular Cofferdams

36. **Cofferdams on Rock,** Tennessee Valley Authority, Technical Monograph 75, Vol. 1, Nashville, Tennessee, 1958.

37. "Cellular Cofferdams and Docks," E. M. Cummings, **Transaction, ASCE,** Vol. 125, 1960.

38. "Stability and Stiffness of Cellular Cofferdams" K. Terzaghi, **Transactions, ASCE,** Vol. 110, 1945.

39. Cofferdams, White and Prentis, Columbia University Press, 1950.

40. "Field Study of a Cellular Bulkhead," A. White, J. Cheney and C. M. Duke, Journal of the Soil Mechanics and Foundations Division, **Proceedings, ASCE,** Vol. 87, No. SM4, 1961.

41. "Cellular Cofferdam Design and Practice," E. P. Swatek, Journal of the Waterways and Harbors Division, **Proceedings, ASCE,** Vol. 93, No. WW3, 1967.

42. Discussion on Stability and Stiffness of Cellular Cofferdams, D. P. Krynine, **Transactions, ASCE,** Vol. 110, 1945.

43. **Earth Pressure Calculation,** J. Brinch Hansen, The Danish Technical Press, The Institution of Danish Civil Engineers, Copenhagen, 1953.

44. **Seepage, Drainage, and Flow Nets, H. R. Cedergren,** John Wiley and Sons, Inc., New York, 1967.

Additional References

45. **Shore Protection, Planning and Design,** TR No. 4 Department of the Army, Corps of Engineers.

46. "Stability of an Elastic Ring in a Rigid Cavity," E. A. Zagustin, G. Herrmann, **Journal of Applied Mechanics,** June 1967.

47. "Note on the Instability of Circular Rings Confined to a Rigid Boundary," P. T. Hsu, J. Elkon, and T. H. H. Pian, **Journal of Applied Mechanics,** September 1964.

48. "Designing Underground Reservoirs," D. F. Moran, **Consulting Engineer,** January 1966.

49. "A Buckling Problem of a Circular Ring," **Proceedings of the Fourth U. S. National Congress of Applied Mechanics,** ASME, 1962.

50. "Anchor Slabs Calculation Methods and Model Tests," N. Krebs Ovesen, **The Danish Geotechnical Institute,** Bulletin No. 16, Copenhagen, 1964.

51. "Resistance of a Rectangular Anchor Slab," J. Brinch Hansen, **The Danish Geotechnical Institute,** Bulletin No. 21, Copenhagen, 1966.

52. "Strength of Deadman Anchors in Clay," Thomas R. Mackenzie, **Master's Thesis Princeton University,** Princeton, New Jersey, 1955.

Design Examples

DESIGN OF CANTILEVERED SHEET PILE WALL — GRANULAR SOIL

RESULTANT PRESSURE DISTRIBUTION

ORIGINAL GROUND

PASSIVE PRESSURE

H = 14'

LOW WATER LEVEL

DREDGE LINE

ACTIVE PRESSURE

PASSIVE

ACTIVE

O

PIVOT POINT

MEDIUM SAND

$\gamma = 115$ PCF

$\gamma' = 65$ PCF

$\phi = 35°$

$\delta/\phi = -0.5$

$K_a = 0.27$ ⎫ SEE
$K_p = 6.56$ ⎬ FIG. 5A

APPLY SAFETY FACTOR AT END

$K_p - K_a = 6.29$

γ_e = EFFECTIVE UNIT WEIGHT

CONVENTIONAL ASSUMED PRESSURE DIAGRAM

B

A   A₁

O₁

D

C

O

Z

E   F   A₂   J
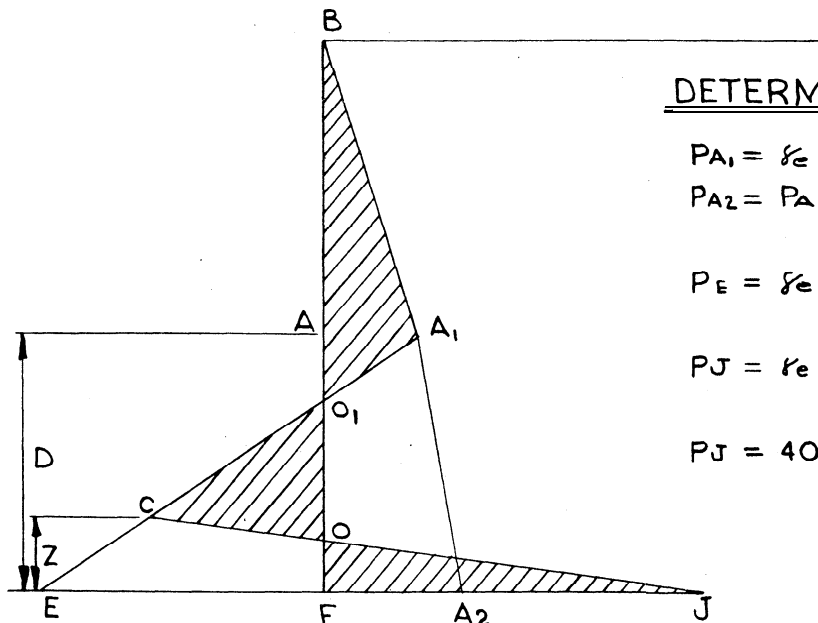
DETERMINE WALL PRESSURES

$P_{A_1} = \gamma_e H K_a = (115)(14.0)(0.27) = 435$ PSF

$P_{A_2} = P_{A_1} + \gamma_e D K_a = 435 + (65)(0.27)D$
$\qquad = 435 + 17.6\,D$

$P_E = \gamma_e D(K_p - K_a) - P_{A_1} = 65D(6.29) - 435$
$\qquad = 408.9\,D - 435$

$P_J = \gamma_e D(K_p - K_a) + \gamma_e H K_p = 65D(6.29)$
$\qquad\qquad + 115(14)(6.56)$

$P_J = 408.9\,D + 10,562$

From Statics, The Following Conditions Must Be Satisfied

(1) $\sum F_H = 0$ In Terms Of Areas:

Area (BAA_1) + Area (AA_1A_2F) + Area (ECJ) − Area (EA_1A_2) = 0

OR

$$\tfrac{1}{2}(H)\,P_{A_1} + (P_{A_1} + P_{A_2})\tfrac{D}{2} + (P_E + P_J)\tfrac{Z}{2} - (P_E + P_{A_2})\tfrac{D}{2} = 0$$

Solving For Z:

$$Z = \frac{(P_E - P_{A_1})D - H\,P_{A_1}}{P_E + P_J}$$

(2) $\sum M$ About Any Point Is Zero

$$\sum M_F = \tfrac{1}{2}(H)\,P_{A_1}\left(D+\tfrac{H}{3}\right) + (P_{A_1})\tfrac{D^2}{2} + (P_E + P_J)\tfrac{Z^2}{6} - (P_E + P_{A_2})\tfrac{D^2}{6}$$

Method of Solution:

$$+ (P_{A_2} - P_{A_1})\tfrac{D^2}{6} = 0$$

1. Assume A Depth Of Penetration, D
2. Calculate Z
3. Substitute Z Into $\sum M_F$ And Check If Zero. Adjust D And Recalculate If Necessary.

Try D = 10.5 Ft.

P_{A_1} = 435 PSF P_{A_2} = 620 PSF. P_J = 14,855 PSF. P_E = 3858 PSF.

$$Z = \frac{(3858-435)(10.5)-(14.)(435)}{14,855 + 3858} = \frac{29852}{18713} = 1.60 \text{ FT.}$$

$$\sum M_F = \tfrac{1}{2}(14.)(435)(10.5+4.67) + (435)\frac{(10.5)^2}{2} + (620-435)\frac{(10.5)^2}{6}$$

$$+ (3858 + 14,855)\frac{(1.60)^2}{6} - (3858+620)\frac{(10.5)^2}{6}$$
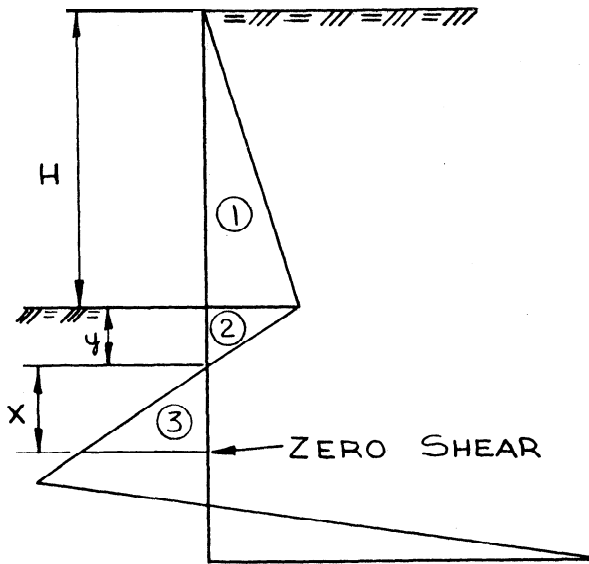
$$\sum M_F = 46,193 + 23,979 + 3399 + 7984 - 82,283$$

$$\sum M_F = -728 \text{ FT.-LB.}\quad \text{SAY O.K.}\quad \text{USE D=10.5 FT.}$$

To Assure A Margin Of Safety, D May Be Increased By 20 To 40 % Or, Alternately, A Reduced Passive Earth Pressure Coefficient Could Be Used.

USE D = 13.5 FT. (INCREASE = 28.5%)

~~MAXIMUM MOMENT AND SHEET PILE SIZE~~

LOCATE POINT OF ZERO SHEAR

$$y = \frac{P_{A_1}}{\gamma'(K_P - K_a)} = \frac{435}{65(6.29)} = 1.06 \text{ FT.}$$

$$\text{SAY } 1.0 \text{ FT.}$$

$$P_1 = \tfrac{1}{2} P_{A_1} H = \tfrac{1}{2}(435)(14) = 3040 \text{ LB}$$

$$P_2 = \tfrac{1}{2} P_{A_1} y = \tfrac{1}{2}(435)(1.0) = 218 \text{ LB.}$$

$$\tfrac{1}{2} \gamma'(K_P - K_a) X^2 = P_1 + P_2$$

$$X^2 = \frac{2(P_1 + P_2)}{\gamma'(K_P - K_a)}$$

$$X2 = \frac{2(3040+218)}{65(6.29)} = \frac{2(3258)}{407} = 16$$

$$X = 4.0 \text{ FEET}$$

MAXIMUM MOMENT

$$P_3 = \frac{1}{2} \gamma' (K_P - K_a) 4^2 = P_1 + P_2 = 3280 \text{ LB.}$$

$M_{MAX} = P_1 \ell_1 + P_2 \ell_2 - P_3 \ell_3$

$M_{MAX} = 3040 \left(\frac{14}{3} + 1.0 + 4.0 \right)$

$\qquad + 218 \left(\frac{2(1)}{3} + 4.0 \right)$

$\qquad - 3280 \left(\frac{4.0}{3} \right)$

$\ell_1 = \left(\frac{H}{3} + y + x \right)$

$\ell_2 = \left(\frac{2y}{3} + x \right)$

$\ell_3 = \frac{x}{3}$

$M_{MAX} = 29,300 + 1030 - 4360 = 26,000$ FT. LBS.

TRY REGULAR CARBON GRADE; $f_s = 25$ KSI

$\qquad$ REQUIRED SECTION MODULUS $= \frac{M}{f_s} = \frac{26000 \times 12}{25000} = 12.5$ IN^3

MUST USE PZ-27 - TRY EXTEN 45 STEEL; $f_s = 29$ KSI

$\qquad$ REQ'D. $S = \frac{26,000 \times 12}{29,000} = 10.76$ IN^3 USE PDA-27 $S = 10.7$ IN^3
$\qquad$ (ALTERNATE SECTION)

CHECK USING FIG. 18 (DESIGN CURVE)

$K_P/K_a = \frac{6.56}{0.27} = 24.2$ $\qquad\qquad \alpha = \frac{14.0}{14.0} = 1.0$

FROM CURVES $\frac{D}{H} = 0.8$ $\qquad\qquad \frac{M_{MAX}}{\gamma' K_a H^3} = 0.65$

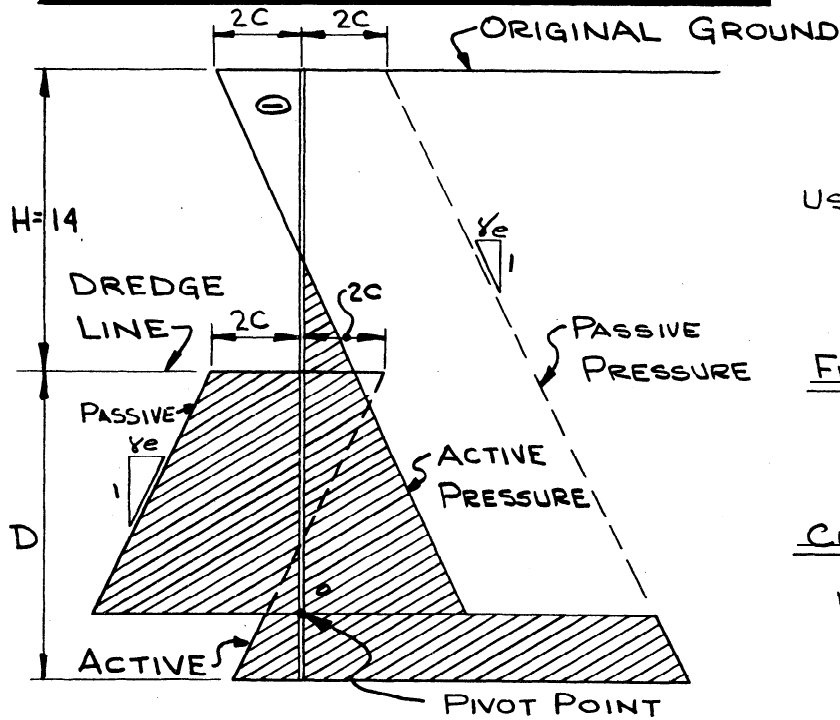$$D = 0.8H = (0.8)(14) = 11.2 \text{ FT. (COMPARED TO } 10.5 \text{ FT.)}$$

$$M_{MAX} = \gamma' K_a H^3 (0.65) = (65)(0.27)(14)^3 (0.65)$$

$$= 31,300 \text{ FT.LBS. (COMPARED TO } 26,000 \text{ FT. LBS.)}$$

THE DIFFERENCES BETWEEN FIG. 18 VALUES AND THE ACTUAL CALCULATED VALUES ARE DUE TO THE DIFFERENCES IN SOIL UNIT WEIGHT. THE DESIGN CURVES ARE BASED ON $\gamma/\gamma' = 2.0$, FOR THIS EXAMPLE PROBLEM $\gamma/\gamma' = 1.77$. THE CHARTS GIVE A REASONABLE ESTIMATE OF THE REQUIRED DEPTH OF PENETRATION, D, HOWEVER CAUTION SHOULD BE EXERCISED IN EXTRACTING THE MAXIMUM MOMENT WITHOUT CONSIDERING OTHER FACTORS.

DESIGN OF CANTILEVERED SHEET PILE WALL – COHESIVE SOIL

RESULTANT PRESSURE DISTRIBUTION

ORIGINAL GROUND

H=14

DREDGE LINE

2C | 2C

2C

2C

PASSIVE PRESSURE

γ_e / 1

PASSIVE γ_e / 1

ACTIVE PRESSURE

D

ACTIVE

PIVOT POINT

MEDIUM SOFT CLAY

$\gamma = 120$ PCF } γ_e = EFFECTIVE
$\gamma' = 60$ PCF }
$C = 750$ PSF
USE $C = 500$ PSF
$q_u = 2C = 1000$ PSF
$\phi = 0°$

FINAL STRENGTH (LONG TERM)

$C = 0$
$\phi = 27°$

CHECK CRITICAL HEIGHT

$$H_c = \frac{4c}{\gamma_e} = \frac{4(500)}{120} = 16.7 \text{ FT.} > H$$

CONVENTIONAL ASSUMED PRESSURE DIAGRAM

B'

Ho

O'

B A   A'

$\gamma_e H - 2C$

z

E F

C   O

J

4C - $\gamma_e H$

4C + $\gamma_e H$
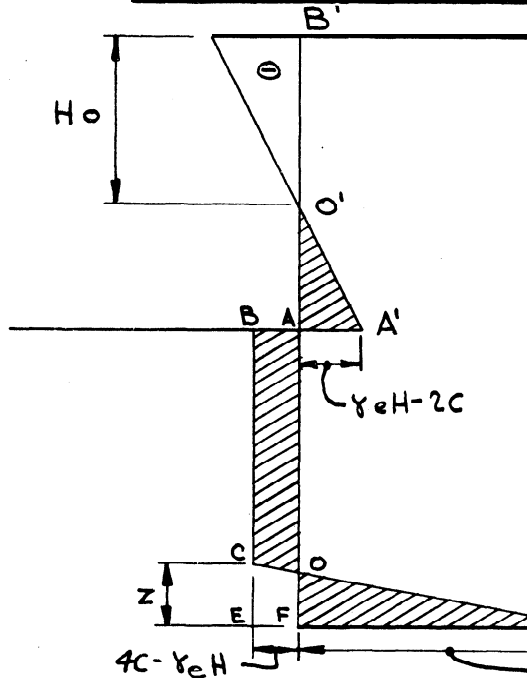
DETERMINE WALL PRESSURES

H_o= POINT OF ZERO PRESSURE
$$= \frac{2c}{\gamma} = \frac{1000 \text{ PSF}}{120 \text{ PCF}} = 8.3 \text{ FT.}$$

$H - H_o = 14.0 - 8.3 = 5.7$ FT.

$\gamma H - 2C = 120(14.0) - 1000 = 680$ PSF

$4C - \gamma H = 4(500) - 120(14.0) = 320$ PSF

$4C + \gamma H = 4(500) + 120(14.0) = 3680$ PSF

From Statics The Following Conditions Must Be Satisfied:

(1) $\Sigma F_H = 0$ In Terms Of Areas:

Area (O'A'A) + Area (CJE) − Area (BAFE) = 0

OR $\frac{1}{2}(\gamma H - 2C)H - H_0 + \frac{8C(Z)}{2} - (4C - \gamma H)D = 0$

Solving For Z:

$$Z = \frac{2D(4C - \gamma H) - (\gamma H - 2C)(H - H_0)}{8C}$$

(2) ΣM About Any Point Is Zero

$$\Sigma M_F = \frac{1}{2}(\gamma H - 2C)(H - H_0)\left(D + \frac{H - H_0}{3}\right) + \frac{8C Z^2}{6} - (4C - \gamma H)\frac{D^2}{2} = 0$$

Method Of Solution:

1. Assume A Depth Of Penetration, D

2. Calculate Z $(\Sigma F_H = 0)$

3. Substitute Z Into ΣM_F And Check If Zero. Adjust D And Recalculate If Necessary.

$$Z = \frac{2(320)D - 5.7(680)}{8(500)} = 0.16D - 0.97$$

$$\Sigma M_F = \frac{(680)(5.7)(D + 1.90)}{2} + \frac{8(500)Z^2}{6} = \frac{320 D^2}{2} = 0$$

$$1938(D + 1.9) + 666.7 Z^2 - 160 D^2 = 0$$

OR $$Z^2 = \frac{160 D^2 - 1938(D + 1.90)}{666.7}$$

TRY $D = 14.0$

$$Z = 0.16 (14.0) - 0.97 = 1.27 \text{ FT.}$$

CHECK $\Sigma M_F = 0$

$$Z^2 = \frac{160 (14.0)^2 - 1938 (14 + 1.90)}{666.7} = 0.82$$

$$Z = 0.9 \text{ FT.} < 1.27 \text{ FT.} \quad \text{No GOOD} \left(\text{INCREASE } D \right)$$

TRY $D = 14.5$ FT.

$$Z = 0.16 (14.5) - 0.97 = 1.35 \text{ FT.}$$

CHECK $\Sigma M_F = 0$

$$Z^2 = \frac{160 (14.5)^2 - 1938 (14.5 + 1.90)}{666.7} = 2.79$$

$$Z = 1.65 \text{ FT.} \quad \underline{\text{SAY O.K. } D = 14.5 \text{ FT.}}$$

NOTE: D CAN BE FOUND DIRECTLY BY SUBSTITUTING

EXPRESSION $[Z = 0.16 D - 0.97]$ INTO THE EQUATION

$[1938 (D + 1.9) + 666.7 \, Z^2 - 160 D^2 = 0]$. THIS REDUCES TO THE

QUADRATIC EQUATION $[142.9 \, D^2 - 1731.1 \, D - 4309.5 = 0]$

AND BY THIS METHOD $\underline{D = 14.23 \text{ FT.}}$ AND $\underline{Z = 1.31 \text{ FT}}$

Since A Factor of Safety of $^{750}/_{500} = 1.5$ Was Applied To The Cohesion, No Increase In Penetration Is Needed. Equilibrium Should Now Be Checked For The Long Term Case of $C=0$ And $\phi = 27°$ Following The Same Method As For The Design of A Cantilevered Sheet Pile Wall In Granular Soil (Example Problem (No.1))

ILLUSTRATION OF THE USE OF THE DESIGN CURVES

If It Is Assumed That This Cantilevered Sheet Pile Wall Which Is Driven Into The Cohesive Soil Has A Sand Backfill In Lieu Of The Medium Soft Clay, The Design Curves In Figure 21 May Be Used As Follows:

From The Original Assumption: $H = 14'$ And $C = 750$ PSF or $q_u = 1500$ PSF
Assume Medium Sand Backfill $\phi = 34°$
From Table 2 $\quad \gamma = 120$ PSF $\& \gamma' = 60$ PSF
From Table 4 $\quad \gamma = 17°$
From Fig. 32 $\quad K_a = 0.25$

Using Fig. 21: $\quad \dfrac{2 q_u - \gamma e H}{\gamma' K_a H} = \dfrac{2(2 \times 750) - 120(14)}{60(0.25)(14)} = 6.3$

$$X = \frac{14}{14} = 1.0$$

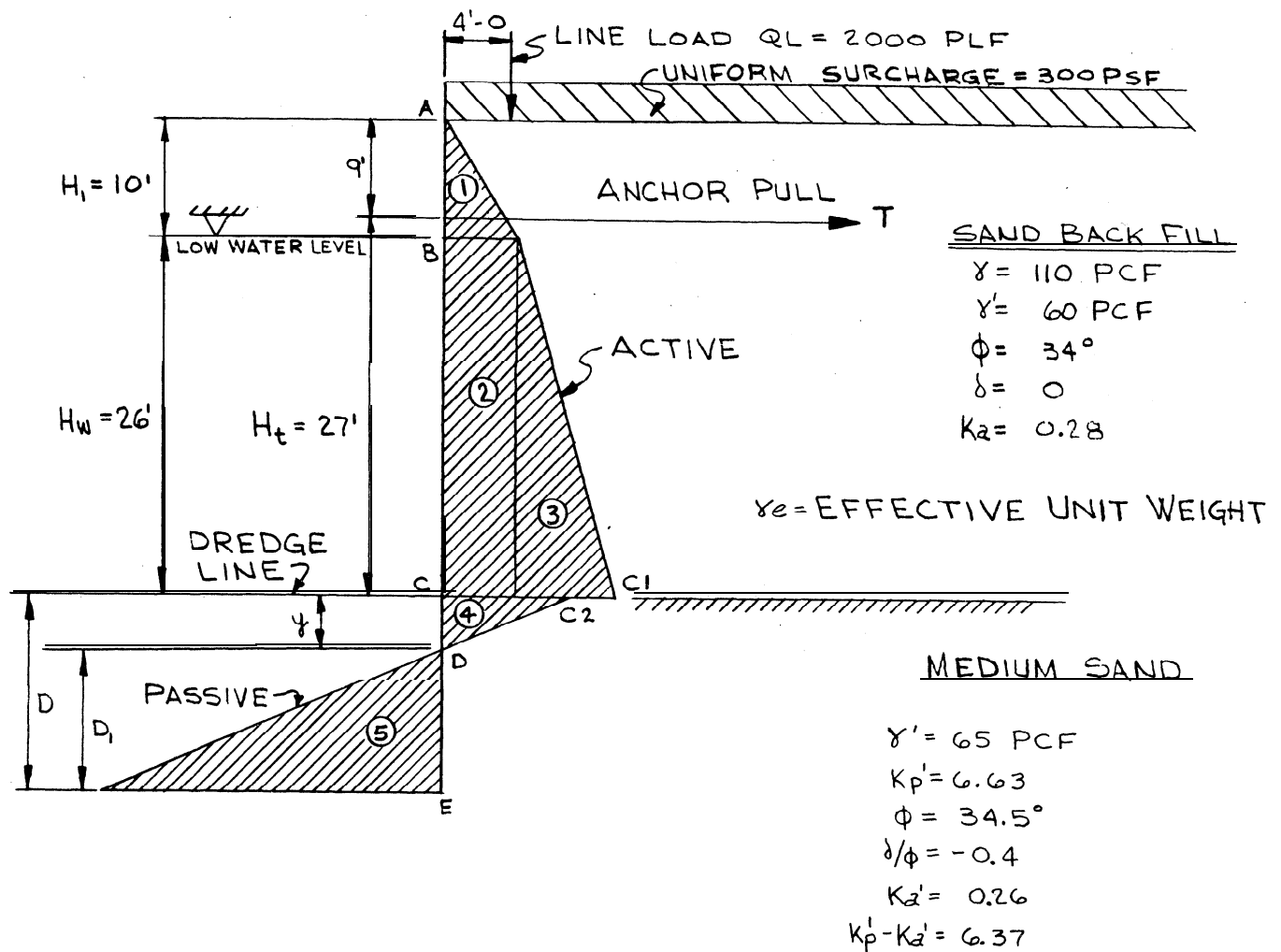From The Curves $\quad \dfrac{D}{H} = 0.62$ And $\quad \dfrac{M_{Max.}}{\gamma' K_a H_3} = 0.415$

$D = (0.62)(14) = 8.7$ Ft. $\qquad M_{Max} = (0.415)(60)(0.25)(14)^3$

Add 40%, $\quad \underline{D = 12.2 \text{ Ft.}} \qquad \underline{= 17.1 \text{ KIP·Ft.}}$

<u>DESIGN OF ANCHORED SHEET PILE WALL - GRANULAR SOIL</u>

FREE EARTH SUPPORT METHOD

4'-0 | LINE LOAD Q_L = 2000 PLF

UNIFORM SURCHARGE = 300 PSF

ANCHOR PULL → T

H_1 = 10'

LOW WATER LEVEL

ACTIVE

H_W = 26' H_t = 27'

DREDGE LINE

PASSIVE

D D_1

SAND BACK FILL
γ = 110 PCF
γ' = 60 PCF
ϕ = 34°
δ = 0
K_a = 0.28

γ_e = EFFECTIVE UNIT WEIGHT

MEDIUM SAND

γ' = 65 PCF
K_p' = 6.63
ϕ = 34.5°
δ/ϕ = -0.4
K_a' = 0.26
$K_p' - K_a'$ = 6.37

DETERMINE PRESSURES ON WALL

$$P_B = \gamma_e H_1 K_a = (110)(10)(0.28) = 308 \text{ PSF}$$

$$P_{C_1} = P_B + \gamma_e H_W K_a = 308 + 60(26)(0.28) = 308 + 437 = 745 \text{ PSF}$$

$$P_{C_2} = [\gamma_e H_1 + \gamma_e H_W] K_A' = [110(10) + 60(26)] \, 0.26 = 692 \text{ PSF}$$

$$P_E = \gamma_e (K_p' - K_A') D_1 = 65(6.37) D_1 = 414 D_1$$

DETERMINE PRESSURE ON WALL DUE TO SURCHARGE (NOT SHOWN ON DIAGRAM)

ABOVE C: $P_{SUR.} = 300\ K_a = 300\ (0.28) = 84\ PSF.$

BELOW C: $P_{SUR.} = 300\ K_a' = 300\ (0.26 = 78\ PSF.$

DETERMINE PRESSURE ON WALL DUE TO LINE LOAD (NOT SHOWN ON DIAGRAM)

$m = \dfrac{X}{H} = \dfrac{4.0}{36} = 0.111$

$P_H = 0.55\ Q< = 0.55\ (2000) = 1100\ LB.\ (RESULTANT)$

LOCATION OF RESULTANT (SEE FIG. 11) $= 0.60\ H = 0.60\ (36) = 21.6\ FT.$

FROM DREDGE LINE

LOCATE $\forall$

$$\forall = \frac{PC_2}{\gamma'(K_P - K_a')} = \frac{692}{65(6.37)} = 1.67\ FT.$$

RESULTANTS OF PRESSURES

$P_1 = \frac{1}{2} \times 10 \times 308 = 1540\ LB.$

$P_2 = 26 \times 308 = 8008\ LB.$

$P_3 = \frac{1}{2} \times 26 \times (745 - 308) = 5681\ LB.$

$P_4 = \frac{1}{2} \times 692 \times 1.67 = 578\ LB.$

$P_{SUR.}\ (+C) = 84 \times 36 = 3024\ LB.$

$P_{SUR.}\ (-C) = 78\ (D_1 + 1.67) = 78\ D_1 + 130$

$P_5 = \frac{1}{2} \times (414\ D_1)\ D_1 = 207\ D_1^2$

SOLVE FOR D USING $\Sigma M_{Ap} = 0$

	FORCE	ARM	MOMENT
①	1540	−2.33	−3588
②	8008	+14.0	+112,112
③	5681	+18.33	+104,133
④	578	+26.56	+15,930
SUR.(+C)	3024	+9.0	+27,216
SUR.(−C)	$78D_1 + 130$	$+\left(\dfrac{D_1 + 1.67 + 27.0}{2}\right)$	$39D_1^2 + 2236D_1 + 3619$
LINE LOAD	1100	+5.4	+5940
PASSIVE	$207D_1^2$	$-\left(27 + 1.67 + \dfrac{2D_1}{3}\right)$	$-(138D_1^3 + 5935D_1^2)$
⑤			

$$\Sigma(+M) = 39 D_1^2 + 2236 D_1 + 268,950$$

$$\Sigma(-M) = 138 D_1^3 + 5935 D_1^2 + 3588$$

$$\Sigma(+M) = \Sigma(-M) \quad 138D_1^3 + 5935 D_1^2 + 3588 = 39D_1^2 + 2236D_1 + 268950$$

OR $\quad 138 D_1^3 + 5896 D_1^2 - 2236 D_1 = 265,362$

SOLVE FOR D_1

$$D_1^3 + 42.72 D_1^2 - 16.20 D_1 = 1923$$

BY TRIAL & ERROR $D_1 \approx 6.5$
TOTAL PENETRATION = 6.5 + 1.67 = 8.17 FT.
TO PROVIDE A MARGIN OF SAFETY, INCREASE D BY A FACTOR
OF 20 TO 40%
USE D = 11.0 FT.

DETERMINE TIE ROD TENSION

T = ACTIVE - PASSIVE FORCES

$$= 1540 + 8008 + 5681 + 578 + 3024 + (78)6.5 + 130 + 1100 - 207(6.5)^2$$

$$= 11873 \text{ LB.}$$

FOR SIZING THE TIE ROD INCREASE BY APPROX. 33% : USE T=16000LB.

MAXIMUM MOMENT

LET POINT OF ZERO SHEAR BE AT x FEET BELOW LOW WATER LEVEL

$$11,873 = 1540 + 1100 + 308(x) + \frac{1}{2}(16.8)(x)^2$$

$$x^2 + 37x - 1100 = 0$$

$$x = 20 \text{ FT.}$$

MOMENTS

$$-(1540) \times (20 + 3.33) = -35,900$$

$$-\frac{(308) \times (20)^2}{2} = -61,600$$

$$-\frac{1}{2}(16.8)(20)^2 \frac{(20)}{3} = -22,400$$

$$+ 11873 \times (20 + 1.0) = +249,000$$

$$-(1100) \times (20 + 10 - 14.4) = -\underline{17,150}$$

MAXIMUM MOMENT = 112,000 FT-LB. = 112 FT-KIPS = 1340 IN-KIPS.

USE EX-TEN 50 GRADE STEEL   ALLOWABLE STRESS=32 KSI

REQ'D. SECTION MODULUS $= \frac{1340}{32.0} = 42 \text{ IN}^3/\text{FOOT OF WALL}$

Assuming No Moment Reduction Due To Flexibility of Sheet Piling:

Use PZ-38 Section (Ex-Ten 50) S = 46.8 in³ /Foot of Wall

Rowe's Theory of Moment Reduction

(1) Select The Appropriate Moment Reduction Curves (See Fig.27) Corresponding To The Relative Density of The Sand. For This Case, The Curve For Medium Compact And Compact Corse Grained Soil is Used.

(2) Calculate $P(H+D)^4/EI$ For The Sheet Pile Sections Being Considered. Obtain The Ratio of The M_{DESIGN}/M_{MAX} From The Curves (Fig.27). Calculate The Design Moment And Stress For The Sheet Pile Sections Being Investigated.

$$P = \frac{(H+D)^4}{EI} = \frac{[(36+11)\times12]^4}{30\times10^6 I} = \frac{3373}{I}$$

	PILE SECTIONS		
	PZ-38	PZ-32	PZ-27
S (Per Foot)	46.8 in.³		30.2 in.³
I (Per Foot)	280.8 in.⁴	220.4 I₁	184.2 in.⁴
P = 3373/I	12.0	15.3	18.3
Ratio (M_DESIGN /M_MAX.)	0.73	0.67	0.62
M_DESIGN = Ratio (M_MAX) = Ratio (1340)	980 in K		833 in K
Stress = $\frac{M_{DESIGN}}{S}$	$\frac{980}{46.8}=21.0 K$	$\frac{900}{38.3}=23.5 KSI$	$\frac{833}{30.2}=27.6 KSI$

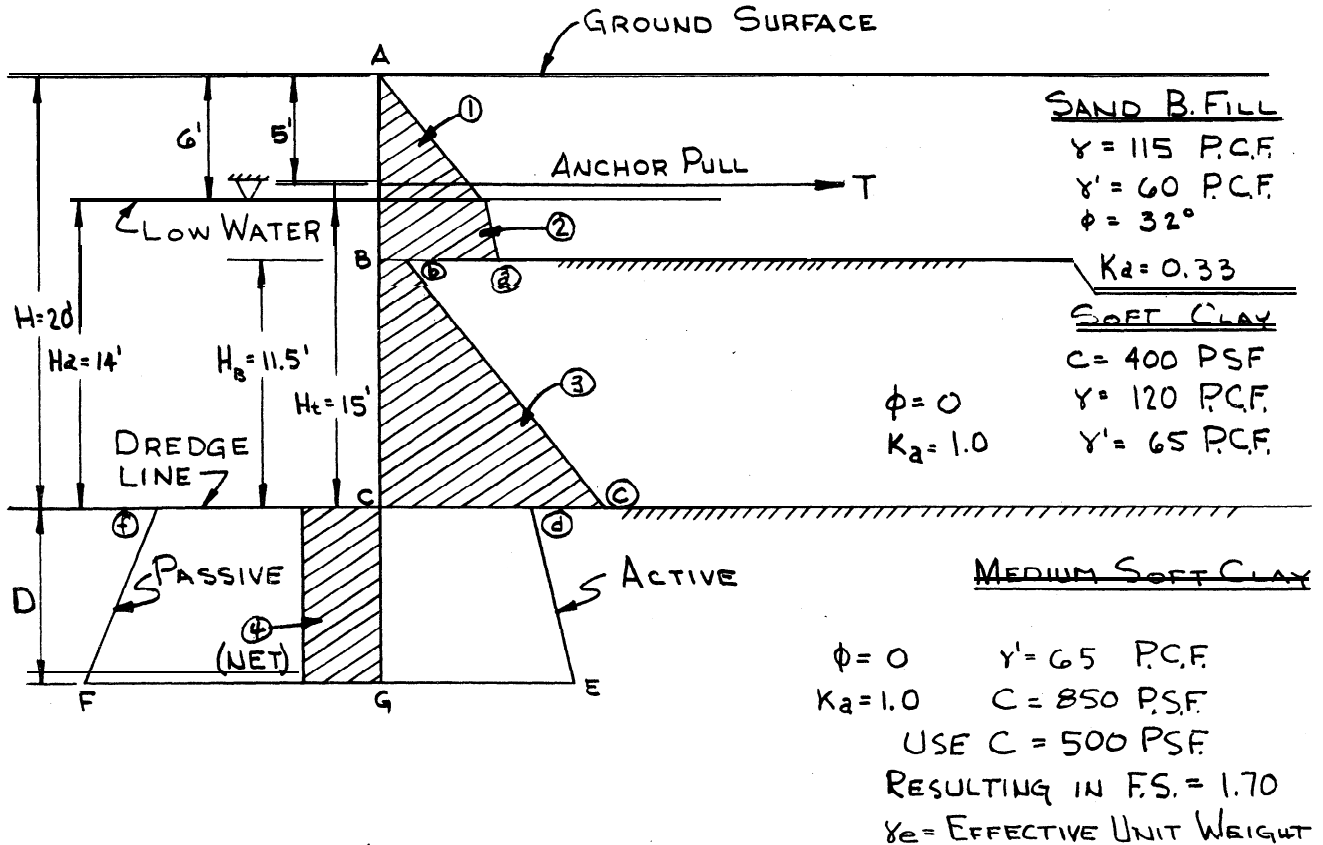BASED ON ROWE's THEORY OF MOMENT REDUCTION THE FOLLOWING SHEET PILE SECTIONS MAY BE USED

PZ - 38 - REGULAR CARBON GRADE STEEL $f_s = 21.0$ KSI < 25 KSI

PZ - 32 - REGULAR CARBON GRADE STEEL $f_s = 23.5$ KSI < 25 KSI

PZ - 27 - EX-TEN 45 STEEL $f_s = 27.6$ KSI < 29.0 KSI

DESIGN OF ANCHOR SHEET PILE WALL - COHESIVE SOIL WITH

SAND BACKFILL - FREE EARTH SUPPORT METHOD

RESULTANT PRESSURE DISTRIBUTION

GROUND SURFACE

A

6' 5'

ANCHOR PULL → T

LOW WATER

B

H=20'

H_2=14' H_B=11.5'

H_t=15'

DREDGE LINE

C

D

PASSIVE

(NET)

ACTIVE

F   G   E

SAND B. FILL
$\gamma = 115$ P.C.F.
$\gamma' = 60$ P.C.F.
$\phi = 32°$
$K_a = 0.33$

SOFT CLAY
$C = 400$ PSF
$\phi = 0$ $\gamma = 120$ P.C.F.
$K_a = 1.0$ $\gamma' = 65$ P.C.F.

MEDIUM SOFT CLAY
$\phi = 0$ $\gamma' = 65$ P.C.F.
$K_a = 1.0$ $C = 850$ P.S.F.
USE $C = 500$ PSF
RESULTING IN F.S. = 1.70
γ_e = EFFECTIVE UNIT WEIGHT

DETERMINE WALL PRESSURES

$P_{B_{ⓐ}} = \gamma_e (H - H_B) K_a = 115(6)(0.33) + 60(2.5)(0.33) = 228 + 50 = 278$ P.S.F.

$P_{B_{ⓑ}} = \gamma_e (H - H_B) - 2C = 115(6) + 60(2.5) - 2(400) = 40$ PSF.

$P_{C_{ⓒ}} = P_{B_{ⓑ}} + \gamma_e (H_B) = 40 + 65(11.5) = 788$ P.S.F.

$P_{C_{ⓓ}} = \gamma_e (H) - 2C = 115(6) + 60(2.5) + 65(11.5) - 2(500) = 588$ P.S.F.

$P_{C_{ⓕ}} = 2C = 2(500) = 1000$ PSF.

101

$$Pc_{net} = Pc_{(f)} - Pc_{(d)} = 1000 - 588 = 412 \text{ PSF}$$

<u>RESULTANT OF PRESSURE DISTRIBUTION</u> (SEE NUMBERED AREAS)

$$P_1 = \frac{115(6)^2(0.33)}{2} = 684 \text{ LB}$$

$$P_2 = \frac{(228 + 278)}{2} \times 2.5 = 633 \text{ LB.}$$

$$P_3 = \frac{(40 + 788)}{2} \times 11.5 = 4760 \text{ LB.} \quad c.g. @ 8.5 + 7.48 = 15.98 \text{ FT. FROM A}$$

$$P_4 = 412D$$

FROM STATICS, THE FOLLOWING CONDITIONS MUST BE SATISFIED:

(1) $\Sigma F_H = P_1 + P_2 + P_3 - P_4 - T = 0$

(2) ΣM ABOUT THE ANCHOR TIE ROD MUST BE ZERO

$$\Sigma M_{AP} = 684(1) - 633(1 + 1.29) - 4760(15.98 - 5.0) + 412D\left(\frac{D}{2} + 15\right) = 0$$

<u>OR</u> $\quad D^2 + 30D = 257.4$

SOLVING $\underline{D = 7.0'}$

TENSILE FORCE IN TIE ROD IS GIVEN BY

$$T = 6077 - 412(7) = 3193 \text{ LB.} \quad \text{SAY } 3200 \text{ LB./FOOT.}$$

ILLUSTRATION OF THE USE OF DESIGN CURVES

IF IT IS ASSUMED THAT THE ANCHORED SHEET PILE WALL IN DESIGN EXAMPLE No.2 HAS THE SAND BACKFILL INSTALLED TO THE DREDGE LINE, THE DESIGN CURVE IN FIGURE 26 MAY BE USED AS FOLLOWS:

$$\frac{(2 q_u - \gamma_e H)}{\gamma' K_a H} = \frac{2(1700) - (115 \times 6 + 60 \times 14)}{60 \times 0.33 \times 20} = \frac{1870}{396} = 4.72$$

$$\alpha = \frac{6}{20} = 0.30$$

FROM THE CURVES IN FIG. 26:

$$\frac{D}{H} = 0.1 \quad, \quad D = 0.1(20) = 2.0'$$

ADDING 40% AS A SAFETY FACTOR, $\underline{D \cong 3.0'}$

ALSO, MOMENT RATIO, $\dfrac{M_{max}}{\gamma' K_a H^3} = 0.07$

$$\therefore M_{max} = 0.07 (\gamma' K_a H^3) = 0.07(60)(0.33)(20)^3/_{1,000}$$

$$= \underline{11.1 \ KIP \cdot FT. \ / FT \ WIDTH}$$

ANCHOR PULL RATIO, $\dfrac{T}{\gamma' K_a H^2} = 0.38$

$$\therefore T = 0.38 (\gamma' K_a H^2) = 0.38 (60)(0.33)(20)^2/_{1,000}$$

$$= \underline{3.01 \ KIPS/FT. \ WIDTH}$$

NOTE THAT, IN COMPARING THIS SOLUTION WITH THE ORIGINAL EXAMPLE No.2, THE FRICTIONAL STRENGTH OF THE SAND BACKFILL, WHICH REDUCES ACTIVE PRESSURES, RESULTS IN LESS REQUIRED DEPTH OF PENETRATION, BUT DOES NOT SIGNIFICANTLY REDUCED THE ANCHOR PULL.

Equivalent Beam Method

Resultant Pressure Distribution

SURCHARGE = 400 PSF

A

6' 5'

LOW WATER LEVEL

B

ANCHOR PULL → T

$H = 26'$

SURCHARGE

DREDGE LINE

C   C₁

C₂

y

O

D

D'

F   g / C   E

Pt. of Vertical Tangent

SAND BACKFILL

$\phi = 34°$
$K_a = 0.28$
$\gamma = 110$ PCF
$\gamma' = 60$ PCF
$\delta = 0$

$\gamma_e =$ EFFECTIVE UNIT WEIGHT

MEDIUM SAND

$\phi = 36°$
$-\delta/\phi = 0.4$
$K'_a = 0.26$
$K'_p = 6.63$
$K'_p - K'_a = 6.37$
$\gamma' = 65$ PCF
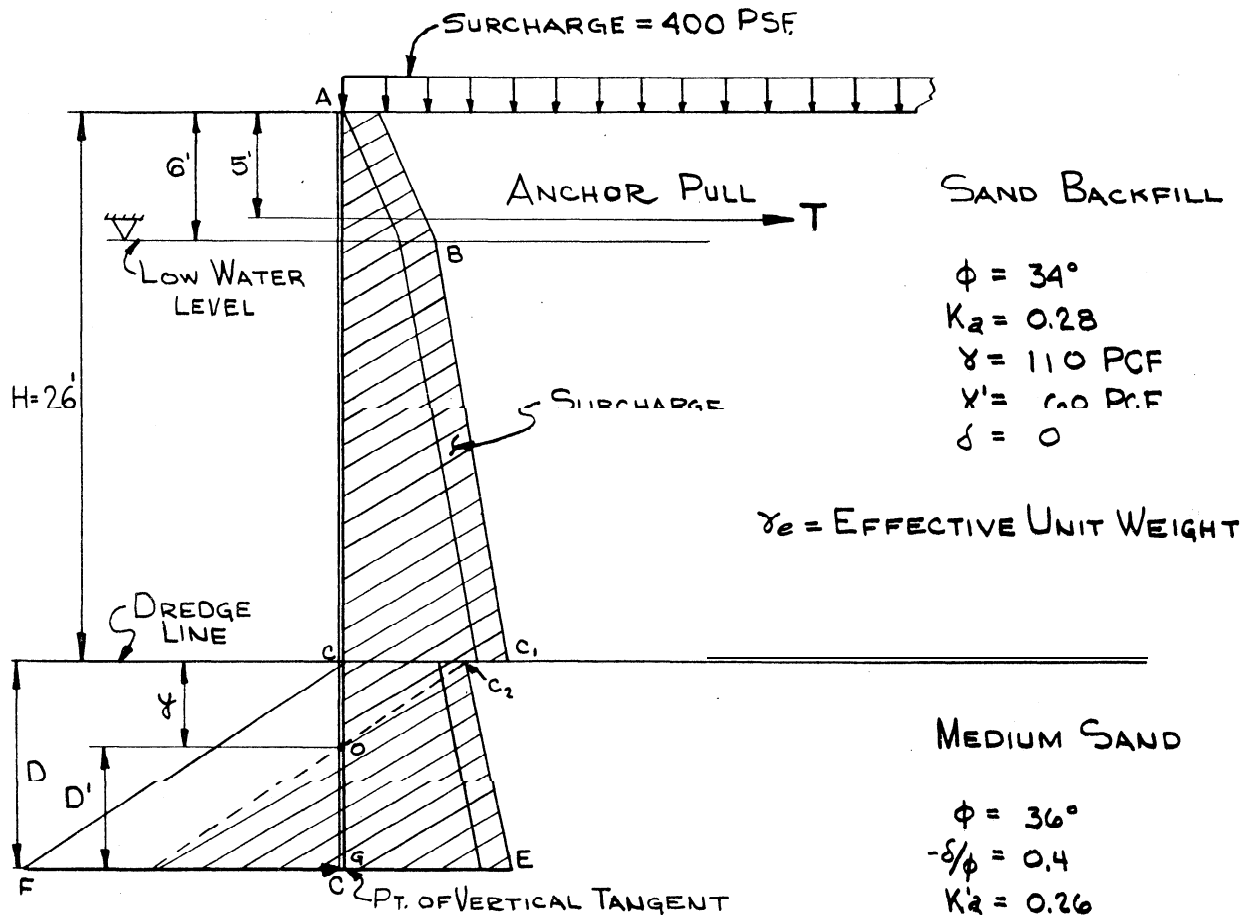
$P_B = \gamma_e Z K_a + q K_a = 110(6)(0.28) + 400(0.28) = 297$ PSF

$P_{C_1} = P_B + \gamma_e Z K_a = 297 + 60(20)(0.28) = 633$ PSF

$P_{C_2} = \gamma_e Z K'_a + q K'_a = [110(6) + 60(20)] 0.26 + 400(0.26) = 588$ PSF

$P_E = P_{C_2} + \gamma_e D K'_a = 588 + 65(0.26)D = 588 + 16.9 D$

$P_F = \gamma_e D K'_p = 65(6.63)D = 431 D$

POINT OF ZERO PRESSURE, O:

$$y = \frac{588}{(65)(6.37)} = 1.4 \; FT.$$

ASSUME POINT OF CONTRAFLEXURE IS AT POINT OF ZERO PRESSURE

EQUIVALENT BEAM
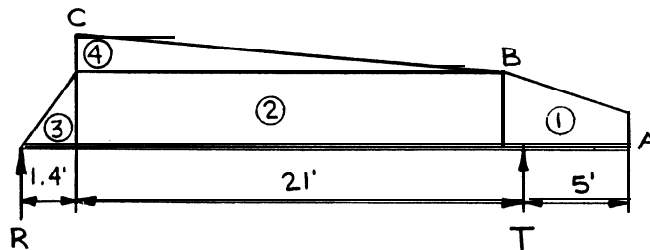
FORCES

$$P_1 = \frac{(112+297)(6)}{2} = 1227 \; LB./FT. \quad c.g. = \frac{112(6)(3)+0.5(6)(185)(6/3)}{\frac{1}{2}(112+297)6} = 2.25 \; FT \; FROM \; B$$

$$P_2 = 297(20) = 5940 \; LB./FT.$$

$$P_3 = \frac{588(1.4)}{2} = 412 \; LB./FT.$$

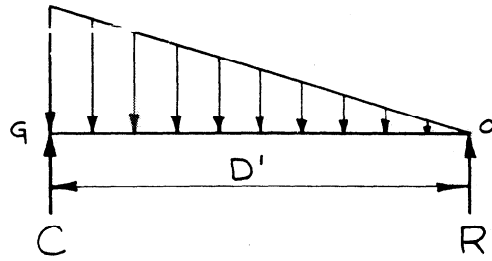$$P_4 = \frac{(633-297)(20)}{2} = 3360 \; LB./FT.$$

SOLVE FOR R BY $\Sigma M_T = 0$

$$\Sigma M_{AP} = R(22.4) + 1227(2.55-1) - 5940(11) - 412(21+0.47) - 3360(13.3+1)$$

$$R = \frac{120,331.8}{22.4} = 5372 \; LB/FT.$$

$$T = 1227 + 5940 + 412 + 3360 - 5372 = \underline{5567 \; LB./FT.}$$

105

FROM STATICS, $\Sigma M_G = 0$

$$\Sigma M_G = \frac{\gamma_e (K'_p - K'_A) D'^2}{2} \left(\frac{D'}{3}\right) - RD' = 0$$

OR $\quad D' = \sqrt{\dfrac{6R}{\gamma_e (K'_p - K'_A)}}$

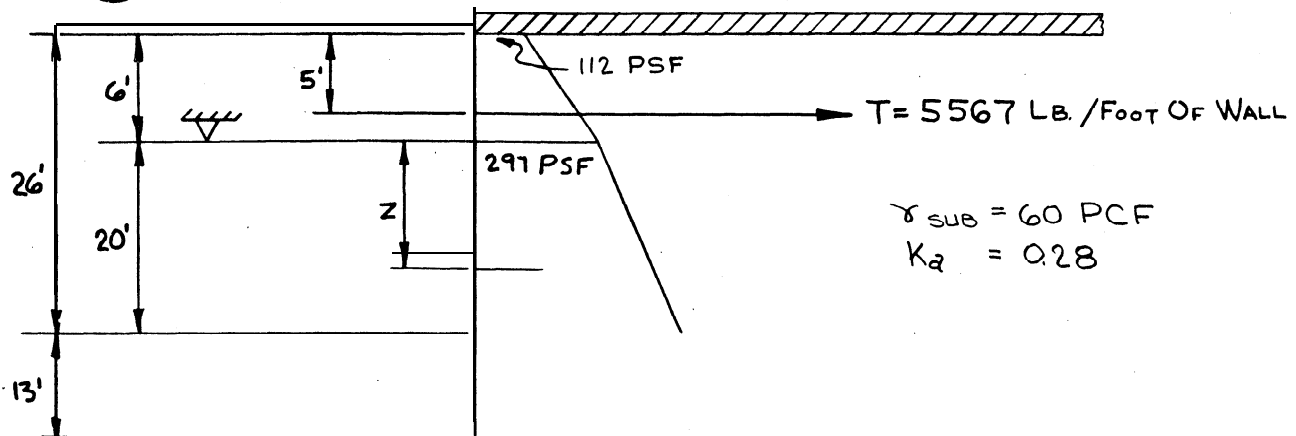$$D' = \sqrt{\frac{6(5372)}{65(6.37)}} = \sqrt{77.9} = 8.83 \text{ FT.}$$

$$D = y + D' = 1.4 + 8.83 = 10.2 \text{ FT.}$$

<u>USE $D = 13$ FT.</u> $(27.4\% \text{ INCREASE})$

DESIGN OF ANCHORAGE SYSTEM FOR THE WALL ANALYZED PREVIOUSLY

BY THE EQUIVALENT BEAM METHOD

(A) SHEET PILE ANCHOR WALL

SIZE PILING

LET POINT OF ZERO SHEAR BE AT A DISTANCE Z BELOW WATER LINE

$$P_1 = 1227 \text{ LB.}$$
$$T = 5567 \text{ LB.}$$

THEN $297(Z) + \frac{1}{2}\gamma_{sub}K_a(Z)^2 = 5567 - 1227 = 4340 \text{ LB.}$

$$297 Z + 8.4 Z^2 = 4340 \text{ LB.}$$

$$Z = 11.1 \text{ FEET}$$

MAXIMUM MOMENT @ Z = 11.1 FT. FROM WATER LINE

(A) $M_{MAX} = 1227 (2.55 + 11.1) + \dfrac{297(11.1)^2}{2} + \dfrac{60(0.28)(11.1)^3}{6}$

$- 5567 (11.1 + 1) = -67,361 + 38,875 = -28,486 \text{ FT. LB.}$

USE REGULAR CARBON GRADE STEEL $\sigma_{all.} = 25000\ PSI$.

REQ'D. SECTION MODULUS $= \dfrac{28,486 \times 12}{25,000} = 13.7\ IN.^3/FOOT\ OF\ WALL$

USE PZ-27 $S = 30.2\ IN.^3/FOOT$
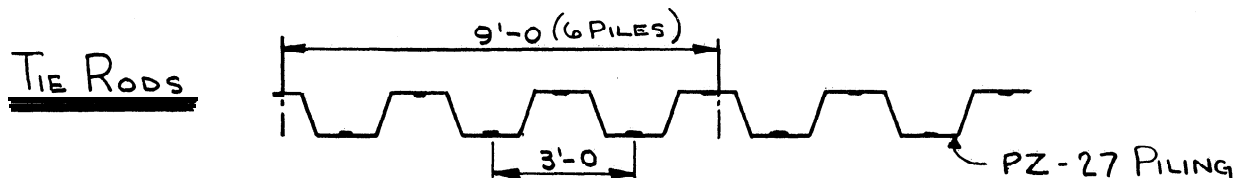
TIE RODS

USE SPACING OF 9'-0 FOR TIE RODS

ASSUME $\alpha = 0$ (LEVEL TIE ROD)

$A_P = \dfrac{T \times d}{\cos \alpha} = 5567 \times 9.0 = 50,103\ LB./TIE\ ROD$

INCREASE 30% FOR DESIGN, THEN $A_P = 65,134\ LB/TIE\ ROD$

USE A-36 STEEL; $\sigma_{all.} = 22,000\ PSI$

REQ'D. CROSS SECTIONAL AREA $= \dfrac{65,134}{22,000} = 2.96\ SQ.IN./ROD$

USE 2" ϕ UPSET TO 2½" ϕ ($A_S = 3.14\ SQ.IN.$)

WALES – ASSUME OUTSIDE WALES

FOR MAXIMUM MOMENT USE $M_{MAX} = \frac{1}{9} T d^2$ (AVERAGE BETWEEN SIMPLE AND CONTINUOUS SUPPORTS)

$M_{MAX} = \frac{1}{9}(5567)(9.0)^2 = 50,103\ FT.-LB.$

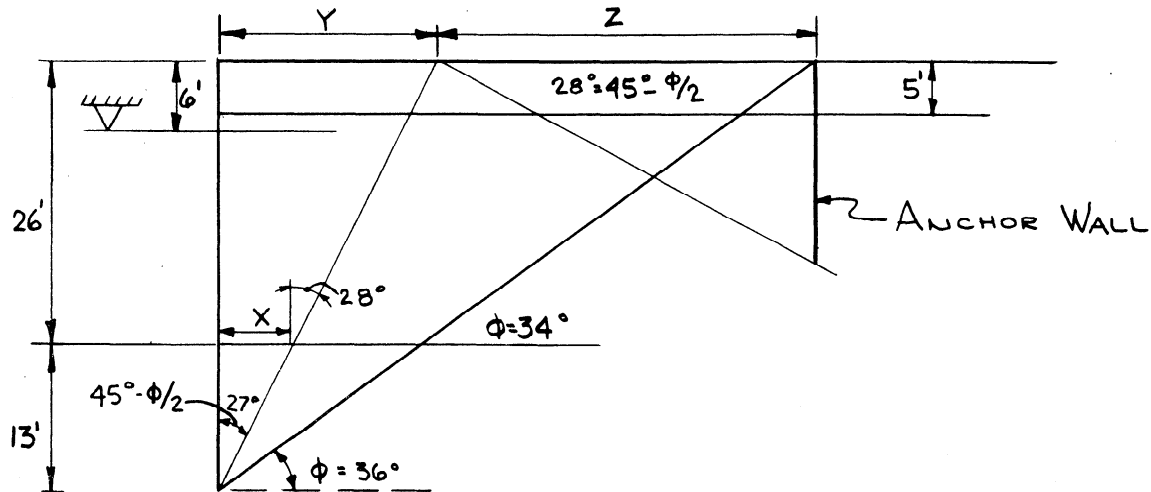USE A-36 STEEL, $\sigma_{all} = 22,000\ PSI$ (BENDING)

$S_{X-X} = \dfrac{M_{MAX}}{\sigma_{all.}} = \dfrac{50,103 \times 12}{22,000} = 27.32\ IN^3$

$S_{X-X} = 13.66\ IN^3/CHANNEL$

108

USE 2-C10×15.3 S_{xx} = 13.4 IN³/CHANNEL, CLOSE ENOUGH

USE 1" φ BOLTS +1½" φ PIPE SEPARATORS TO BOLT CHANNELS

TOGETHER BACK TO BACK. ASSUME CLEAR DISTANCE OF 3 INCHES.

ANCHOR WALL

X= 13 TAN 27° = 6.62 FT.

Y= X + 26 TAN. 28°= 6.62 + 13.84 = 20.46 FT.

Z = 13 COT 36° + 26 COT 34°- Y = 17.88 + 38.60 - 20.46

Z= 36.02 FT.

ASSUME G.W.L. AT 6 FT. DEPTH   φ = 34° δ/ϕ = -0.4 $\begin{cases} K_P = 5.72 \\ K_A = 0.28 \end{cases}$
                                       γ = 110 PCF
                                       γ´= 60 PCF

THE PRESSURE DISTRIBUTION ON THE ANCHOR WALL WOULD BE AS ILLUSTRATED IN THE SKETCH ON THE FOLLOWING PAGE.
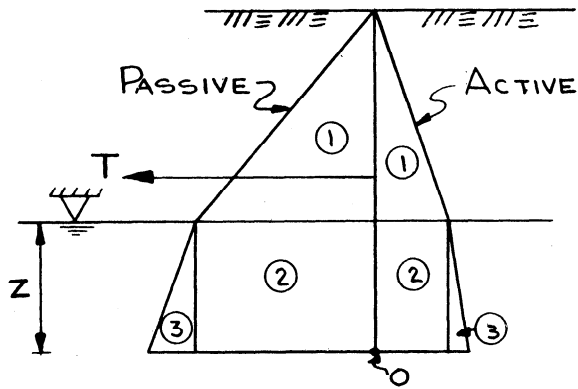
$$P_{P_1} - P_{A_1} = \frac{1}{2}(110)(5.72 - 0.28)(6)^2$$

$$= 10,771 \text{ LB.}$$

$$P_{P_2} - P_{A_2} = 6(110)(5.72 - 0.28)Z$$

$$= 3590 Z$$

$$P_{P_3} - P_{A_3} = \frac{1}{2}(60)(5.72 - 0.28)Z^2$$

$$= 163 Z^2$$

$$\Sigma F_H (o) = 0$$

$$\Sigma F_H (o) = (P_{P_1} - P_{A_1}) + (P_{P_2} - P_{A_2}) + (P_{P_3} - P_{A_3}) - T = 0$$

$$\Sigma M(o) = 0$$

$$\Sigma M(o) = (P_{P_1} - P_{A_1})(z + 2) + (P_{P_2} - P_{A_2})\frac{z}{2} + (P_{P_3} - P_{A_3})\frac{z}{3} - T(z+1) = 0$$

OR

① $10,771 + 3590 Z + 163 Z^2 = T$

② $10,771(z+2) + 3590Z\left(\frac{z}{2}\right) + 163 Z^2\left(\frac{z}{3}\right) - T(z+1) = 0$

COMBINING

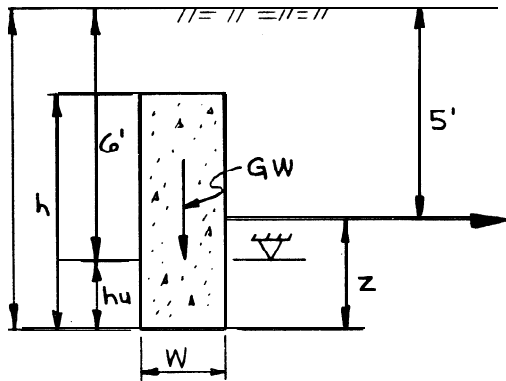$$109 Z^3 + 1958 Z^2 + 3590 Z = 10,771$$

$$Z = 1.55 \text{ FT.}$$

FROM ① $T = 10,771 + 3590(1.55) + 163(1.55)^2 = \underline{16,727 \text{ LB./FOOT}}$

FACTOR OF SAFETY $= \frac{16,727}{5567} = \underline{3.0}$ DRIVE TO DEPTH OF $\underline{8.0 \text{ FT.}}$

NOTE: WALE DESIGN SIMILAR TO MAIN WALL EXCEPT DESIGN AS INSIDE WALE.

B. Design A Concrete Anchor Slab Using Ovesen's Model

Test Criteria For A Factor of Safety = 2.0

Assumed: $\phi = 34°$ $\delta/\phi = -0.4$

$\gamma = 110 \text{ PCF}$ $\gamma' = 60 \text{ PCF}$

$T_{act} = 5567 \text{ #/}_1$ $K_a = 0.28$

Use $H = 7.5'$ & $W = 2.0'$

Then $h_u = 1.5'$ & $z = 2.5'$

$\delta = 0.4(34) = 13.6°$; $\tan\delta = 0.2419$

From Figure 46c $K_\gamma = 5.0$

$R_o = K_\gamma - K_a = 5.0 - 0.28 = 4.72$

$P_H = \frac{1}{2}\gamma H^2 - \frac{1}{2}(\gamma - \gamma')h_u^2 = \frac{1}{2}(110)(7.5)^2 - \frac{1}{2}(110-60)(1.5)^2 = 3038 \text{ }^{PSF}/_{FT.}$

Calculate Ultimate Resistance For The "Basic Case" ($h/H = \ell/L = 1.0$)

$T_o = P_H R_o = 3038(4.72) = 14,339 \text{ #/}_{FT.}$ Of Wall

$F.S. = \dfrac{14,339 \text{ #/}_{FT.}}{5567 \text{ #/}_{FT.}} = 2.57$ High.

For $H = 7.5'$ Try Continuous Anchor ($\ell/L = 1.0$) With $h = 5.5'$

$h/H = \dfrac{5.5}{7.5} = 0.733$ From Figure 46d $\dfrac{R}{R_o} = 1.01$

$R = 1.01 \times 4.72 = 4.76$

$g_m = \gamma(H - \frac{1}{2}h) = 110(7.5 - \frac{1}{2} \times 5.5) = 522.5 \text{ PSF}$

$T_{ult} = g_m h R(\frac{\ell}{L}) = 522.5(5.5)(4.76)(1.0) = 13,679 \text{ #/}_1$

$F.S. \dfrac{13,679}{5567} = 2.46$ High

THE TIE ROD ANCHOR FORCES ARE 9.0' o.c.   (L = 9.0')

TRY ANCHOR SLABS WITH $\frac{\ell}{L} = 0.5$ (ie $\ell = 9(0.5) = 4.5'$)

H = 7.5', h = 5.5'

FROM FIGURE 46d FOR $\frac{\ell}{L} = 0.5$, $\frac{\ell}{h} = \frac{4.5}{5.5} = .82$

$\frac{h}{H} = .733$, AND $R_0 = 4.72$

BY INTERPOLATION $\frac{R}{R_0} \doteq 1.7$ & $R = (1.7)(4.72) = 8.02$

$A_{ult} = \gamma m h \ell R = 522.5(5.5)(4.5)(8.02) = 103,710^{\#}$

$T_{ult} = \frac{A_{ult}}{L} = \frac{103,710}{9.0} = 11,520^{\#}/\text{FT.}$

F. S. $\frac{11,520}{5567} = 2.07$ O.K.

CHECK TIE ROD FORCE LOCATION, Z

$M_H = \frac{1}{6} \gamma H^3 - \frac{1}{6}(\gamma - \gamma') h_w^3 = \frac{1}{6}(110)(7.5)^3 - \frac{1}{6}(110 - 60)(1.5)^3$

$M_H = 7734 - 28 = 7706$ FT. LB/FT

$GW = [(150 \times 2 \times 5.5 + 110 \times 2 \times 2) \times 4.5 + 110 \times 2 \times 7.5 \times 4.5] \frac{1}{9.0}$

$GW = (2090 + 1650) 4.5/9.0 = 1870^{\#}/\text{FT.}$

$P_A = P_H K_a = 3038(.28) = 851$ PSF/FT.

$F_A = -P_A \tan \phi = -851(.6745) = -574$ PSF/FT.

FROM FIGURE 46f FOR $\tan \delta = 0.2419$ $\zeta = 0.365$

FIND Z_0 FOR BASIC CASE

$Z_0 = \frac{1}{T_0}(3 M_H K_\gamma \zeta + W(.5 GW - F_A) - M_H K_a)$

$$Z_o = \frac{1}{14,339} \left[3 \times 7706 \times 5.0 \times 0.365 + 2(.5 \times 1870 + 574) - 7706 \times .28 \right]$$

$$Z_o = \frac{1}{14,339} [42190 + 3018 - 2158] \frac{43,050}{14339} = 3.00 \text{ FT.}$$

$$\frac{Z}{H} = \frac{0.5h}{H} - \left(0.5 - \frac{Z_o}{H}\right)\left(\frac{h}{H}\right)^{\frac{1}{1 - \frac{2Z_o}{H}}}$$

$$\frac{Z}{H} = \frac{0.5 \times 5.5}{7.5} - \left(0.5 - \frac{3.00}{7.5}\right)\left(\frac{5.5}{7.5}\right)^{\frac{1}{1 - \frac{2(3.00)}{7.5}}} = 0.367 - (0.100)(.733)^{5.00}$$

$$\frac{Z}{H} = 0.367 - (0.100)(0.212) = 0.346$$

$$Z = 0.346 (7.5) = 2.60 \text{ FT.}$$

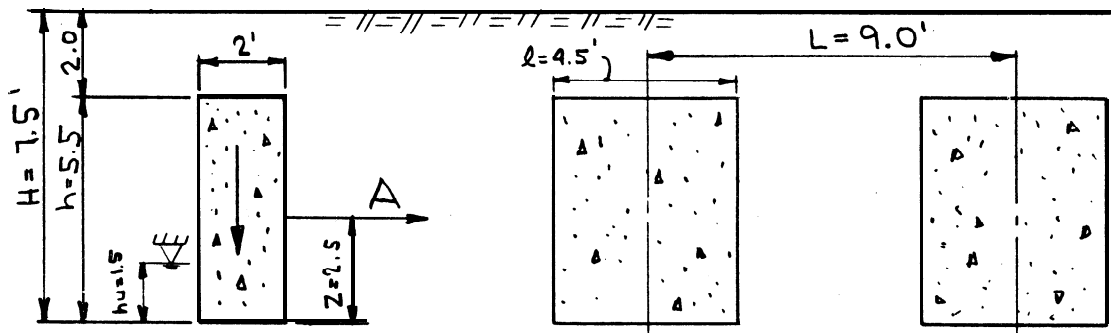$$\therefore \text{ACTUAL } Z = 2.50 \quad \text{O.K.}$$

ESTIMATE THE HORIZONTAL MOVEMENT, Δ, OF THE ANCHOR SLAB.

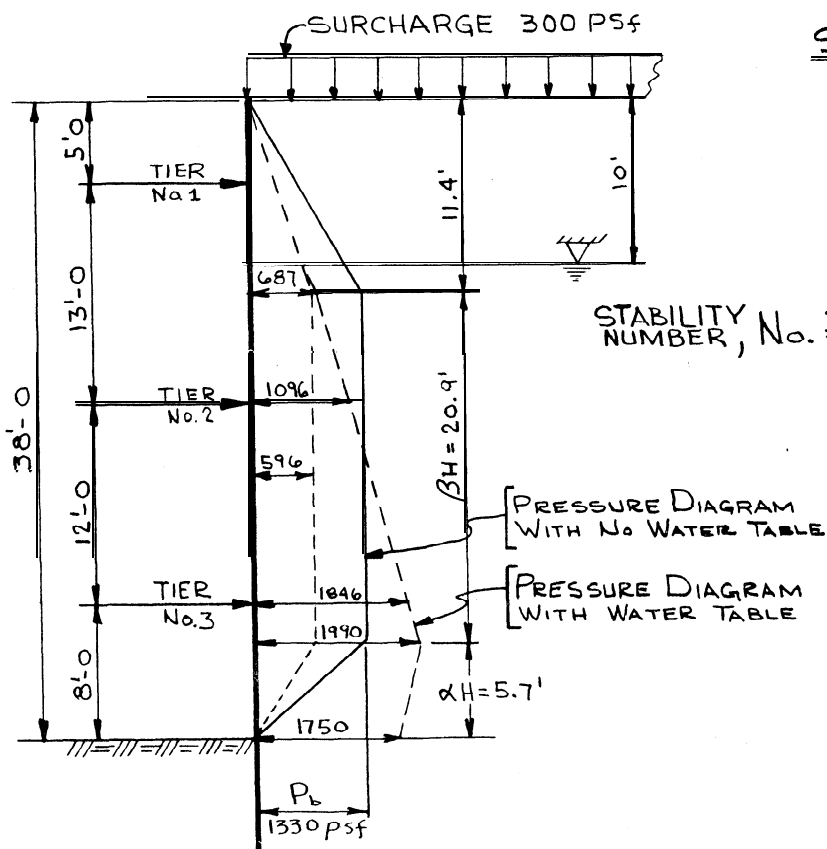$$\log_{10} \frac{\Delta}{H} = 2.5 \left(\frac{T_{act}}{T_{ult}}\right) - 2 \sin \phi - 2.6$$

$$\log_{10} \frac{\Delta}{H} = 2.5 \frac{5567}{11,520} - 2(.559) - 2.6 = -2.511$$

$$\left(\frac{\Delta}{H}\right) = \frac{1}{10^{2.511}} = \frac{1}{324.3}; \quad \Delta = \frac{7.5 \times 12}{324.3} = 0.277 \text{ INCHES}$$

IN SUMMARY THE FOLLOWING SET OF ANCHOR SLABS PROVIDES A FACTOR OF SAFETY OF ABOUT 2.0

DESIGN OF BRACED COFFERDAM IN COHESIVE SOIL
(STABILITY NUMBER METHOD–MEDIUM SOFT CLAY)

SURCHARGE 300 PSF

TIER No. 1

TIER No. 2

TIER No. 3

687

1096

596

1846

1990

1750

P_b
1330 PSF

5'-0
13'-0
12'-0
8'-0
38'-0

11.4'
10'

$\beta H = 20.9'$

$\alpha H = 5.7'$

PRESSURE DIAGRAM WITH No WATER TABLE

PRESSURE DIAGRAM WITH WATER TABLE

PRESSURE DIAGRAMS

SOIL PROPERTIES–MED. SOFT CLAY
$\gamma = 115$ PCF (SATURATED)
$\gamma' = 53$ PCF (SUBMERGED)
$c = 1000$ PSF.
$\phi = 0°$

STABILITY NUMBER, $N_o = \dfrac{\gamma H + SURCH.}{C}$

1) CONSIDER NO FREE WATER TABLE

$$N_o = \frac{\gamma H + SURCH.}{C} = \frac{115(38)+300}{1000} = 4.67$$

$$P_b = \frac{c}{150}\left(7N_o^2 + 10N_o\right)$$

$$= \frac{1000}{150}\left[7(4.67)^2 + 10(4.67)\right]$$

$$= 1330 \text{ PSF}$$

$$\alpha = 0.3\left(1-\frac{N_o}{20}\right) \text{ BUT NOT} > 0.15$$

$$\alpha = 0.23 > 0.15; \therefore \text{ LET } \alpha = 0.15$$

$$\beta = 1.1\left(1-\frac{N_o}{20}\right) \text{ BUT NOT} > 0.55$$

$$\beta = 0.85 > 0.55; \therefore \text{ LET } \beta = 0.55$$

$$\alpha H = 0.15(38) = 5.7'$$

$$\beta H = 0.55(38) = 20.9'$$

2) CONSIDER THE SATURATED AND SUBMERGED DENSITIES WITH A WATER TABLE

$$N_o = \frac{115(10)+53(28)+300}{1000} = 2.93$$

$$P_b = \frac{1000}{150}\left[7(2.93)^2 + 10(2.93)\right] = 596 \text{ PSF}$$

NOTE, $\alpha = 0.15$ AND $\beta = 0.55$. ADD HYDROSTATIC PRESSURE (SEE DIAGRAM)

SHEET PILE WALL

ASSUME MAXIMUM MOMENT OCCURS AT TIER No. 3 AND IS APPROX. EQUAL TO THE "NEGATIVE" MOMENT AT ANY INTERIOR SUPPORT OF A CONTINUOUS BEAM HAVING A UNIFORMLY DISTRIBUTED LOAD OF 2000 Plf (LOAD AT TIER No. 3 IS 1846 PSF PER FT WIDTH).

$$M_{MAX} = \tfrac{1}{10} w \ell^2 = \tfrac{1}{10} (2000)(12)^2 / 1000$$
$$= 28.8 \text{ KIP·FT./FT. WIDTH}$$

REQ'D. SECTION MODULUS, $S = \dfrac{M_{MAX}}{\sigma_{ALL.}} = \dfrac{28.8(12)}{25 \text{ KSI}} = 13.8 \text{ IN.}^3/\text{FT. WIDTH}$

↳ REGULAR CARBON STEEL

OR $S = \dfrac{28.8(12)}{32 \text{ KSI}} = 10.8 \text{ IN.}^3/\text{FT WIDTH}$

↳ U.S.S. Ex-TEN 50 STEEL

USE   PZ-22 IN REGULAR CARBON STEEL
OR PDA-27 IN Ex-TEN 50 STEEL ALTERNATE SECTION

STRUTS

TO COMPUTE THE AXIAL LOAD IN EACH STRUT ASSUME A PLASTIC HINGE AT EACH STRUT POINT (A CONSERVATIVE ASSUMPTION) AND SUM MOMENT ABOUT TIER No. 2 TO SOLVE FOR TIER No. 1, SUM MOMENTS ABOUT TIER No. 3 TO SOLVE FOR TIER No. 2 AND SUM MOMENT ABOUT THE BOTTOM OF THE EXCAVATION TO SOLVE FOR TIER No. 3.

THE SOLUTIONS ARE:

AXIAL LOAD IN TIER No. 1 = 4.12 KIPS /FT. WIDTH

" 2 = 13.0 "

" 3 = 27.4 "

TOTAL AXIAL LOAD PER FOOT WIDTH = 44.52 KIPS

CHECK TOTAL LATERAL PRESSURE LOAD:

$$1000 \, P \, (\text{KIPS}) = \left[\tfrac{1}{2}(11.5) + 20.9 + \tfrac{1}{2}(5.7)\right](596) + \tfrac{1}{2}(26.6)(1750)$$

$$P = 40.9 \text{ KIPS/FT. WIDTH} \quad O.K. \text{ (LESS THAN TIER LOADS)}$$

<u>Determine Safety Factor Against Heave At The Bottom of</u> The Excavation (Use Bjerrum Relationship-"Negative" Footing)

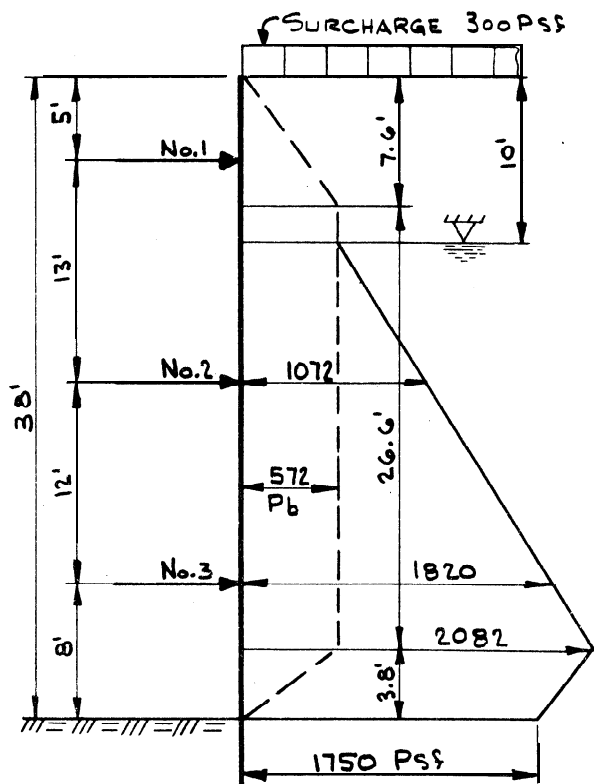Assume A Very Long Excavation And Width = 50 Ft. $\therefore \frac{H}{B} = \frac{38}{50} = 0.76$

$$N_c \cong 6.0 \ (\text{See Fig. 61})$$

$$\text{S.F.} = \frac{c N_c}{\gamma_c H + q} = \frac{1000(6)}{10(115) + 28(53) + 300}$$

$$= \underline{2.05} \ > 1.5$$

Base Is Stable Without Driving Sheeting Beyond Bottom of Excavation.

(No. 2) Design of Braced Cofferdam In Granular Soil

Surcharge 300 PSF

No.1

No.2 1072

572 / Pb

No.3

1820

2082

1750 PSF

Pressure Diagram

5'
13'
12'
8'
38'

7.6'
0'
26.6'
3.8'

Soil Properties - Med. Sand

$\gamma = 115$ PCF (Saturated)
$\gamma' = 53$ PCF (Submerged)
$\phi = 32°$ $C = 0$
$\cdots 17°$ $\cos \delta = 0.956$

Effective Density, $\bar{\gamma}_1' = \dfrac{300 + 115(10) + 53(28)}{38'}$

$$= 77.2 \text{ pcf}$$

$P_b = 0.7 K_a \bar{\gamma}' H \cos \delta$

(May be 0.7 or 0.8)

$$= 0.7(0.29)(77.2)(38)(0.956) = 572 \text{ psf}$$

Add Hydrostatic Pressure (See Diagram)

$0.2 H = 7.6'$ $0.1 H = 3.8'$

Determine Loads on Wales And

Struts As In Design Example No. 1 (Pages 114-116)

Check Base Stability

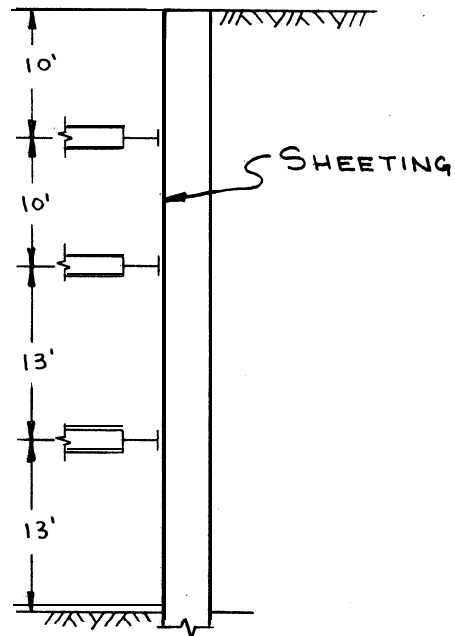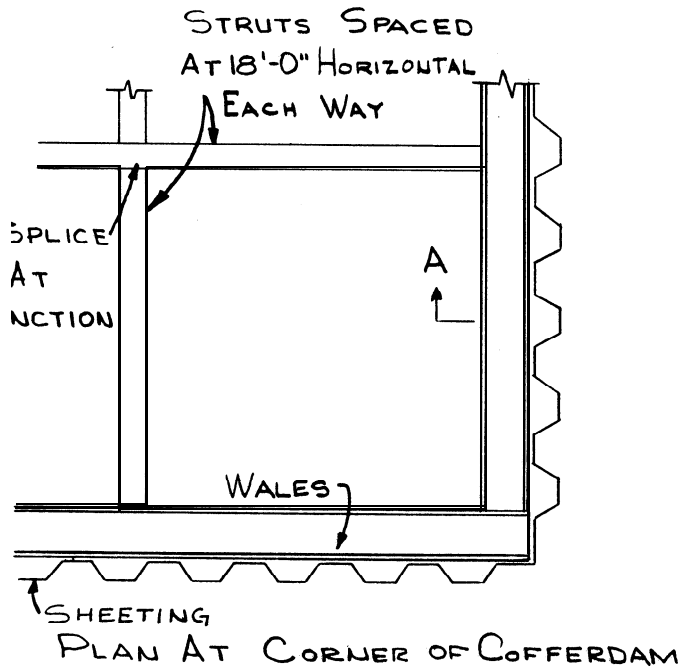$$\text{S.F.} = 2 N_{\gamma_2} \left(\frac{\bar{\gamma}_2'}{\bar{\gamma}_1'} \right) K_a \tan \phi$$

$\bar{\gamma}_2' = 53$ pcf; $\bar{\gamma}_1' = 77.2$ pcf; $N_{\gamma_2} = 23$ (From Fig. 62(c))

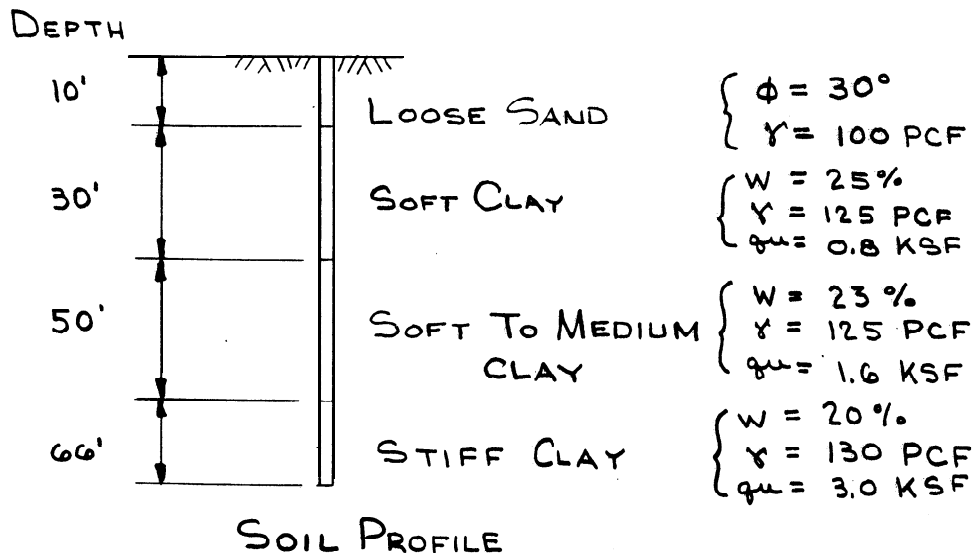$$\text{S.F.} = 2(23)\left(\frac{53}{77.2}\right)(0.29)(0.625) = 5.71 > 1.5 \quad \text{O.K.}$$

DESIGN OF BRACED COFFERDAM - STRATIFIED SOIL
(REFERENCE - FOUNDATION DESIGN BY TENG PP. 404-407)

I - SELECT SPACING OF WALES AND STRUTS BASED ON
DETAILS OF PERMANENT STRUCTURE AND
ACCESSIBILITY REQUIREMENTS.

STRUTS SPACED
AT 18'-0" HORIZONTAL
EACH WAY

SPLICE
AT
NCTION

A

WALES

SHEETING

PLAN AT CORNER OF COFFERDAM

10'

10'

13'

13'

SHEETING

SECTION A-A

DESIRED DEPTH OF EXCAVATION = 46 FT.

DEPTH

10'	LOOSE SAND	$\phi = 30°$ $\gamma = 100$ PCF
30'	SOFT CLAY	$w = 25\%$ $\gamma = 125$ PCF $q_u = 0.8$ KSF
50'	SOFT TO MEDIUM CLAY	$w = 23\%$ $\gamma = 125$ PCF $q_u = 1.6$ KSF
66'	STIFF CLAY	$w = 20\%$ $\gamma = 130$ PCF $q_u = 3.0$ KSF

SOIL PROFILE

118

$\text{II} - $ CALCULATE LATERAL EARTH PRESSURE
(FOR STRATIFIED SOILS, USE PECK'S PRESSURE DISTRIBUTION)

$$q_a = \frac{1}{H}[\gamma_s \, k_s \, H_s^2 \, \tan \phi_s + (H - H_s) \, n \, q_u]$$

$$\gamma_a = \frac{1}{H}[\gamma_s \, H_s + (H - H_s) \, \gamma_c]$$

$H = 46$ FT.
$\gamma_s = 100$ PCF $\gamma_c = 125$ PCF
$k_s = 1.0$
$H_s = 10$ FT.
$\phi_s = 30°$
$q_u = 800$ PSF AND 1600 PSF

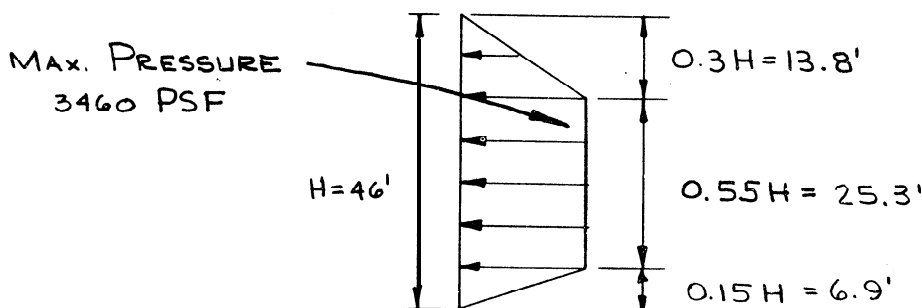$$q_a = \frac{1}{46}[(100)(1.0)(10)^2(0.577) + (20)(800) + (16)(1600)]$$

$$q_a = 1030 \text{ PSF}$$

$$\gamma_a = \frac{1}{46}[(100)(10) + (36)(125)]$$

$$\gamma_a = 120 \text{ PCF}$$

MAX. PRESSURE $= \gamma_a \, H - 2 \, q_a = (120)(46) - 2(1030)$

MAX. PRESSURE $= 3460$ PSF

LATERAL EARTH PRESSURE DIAGRAM

III - Size Cofferdam Components

(a) Sheet Pile Wall

$$\text{Max Mom} = \frac{1}{10} (3.46)(13)^2 = 58.5 \text{ Ft. Kips}/\text{Ft. Width}$$

$$S = \frac{(58.5)(12)}{*(1.65)(25)} = 17.0 \text{ In.}^3/\text{Ft. Width}$$

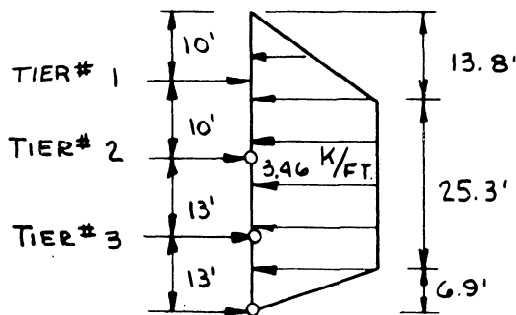<u>Use PZ22 Regular Carbon Grade Steel Sheet Piles S = 19.0 In³</u>

(b) Struts

Determine Axial Loads
(Assume Pinned Supports)

Take Moments About Tier 2

$$T_1(10) - 6.2(3.46)(3.1)$$
$$- (13.8)(\tfrac{1}{2})(3.46)(6.2 + \tfrac{13.8}{3}) = 0$$

$$T_1 = 32.43 \text{ }^K/\text{Ft.}$$

TIER # 1   10'

TIER # 2   10'   13.8'

3.46 K/FT.   25.3'

TIER # 3   13'

13'   6.9'

Take Moments About Tier 3

$$(32.43)(23) + T_2(13) - (19.2)(3.46)(9.6) - (13.8)(\tfrac{1}{2})(3.46)(19.2 + \tfrac{13.8}{3}) = 0$$

$$T_2 = 35.39 \text{ }^K/\text{Ft.}$$

Take Moments About Bottom of Excavation

$$(32.43)(36) + (35.39)(26) + T_3(13) - (25.3)(3.46)(6.9 + \tfrac{25.3}{2})$$
$$- (13.8)(\tfrac{1}{2})(3.46)(32.2 + \tfrac{13.8}{3}) - (6.9)(\tfrac{1}{2})(3.46)(\tfrac{2}{3})(6.9) = 0$$

$$T_3 = 42.86 \text{ }^K/\text{Ft.}$$

* See Note At End of Example Concerning Permissible Overstress

TIER #1   AXIAL LOAD = $32.43 \times 18 \times \left(\frac{1}{1.5}\right)^* = 390$ KIPS

TRY W14×90 $L/r = \frac{18 \times 12}{3.70} = 58$

Fa = 17.58   LOAD = $17.58 \times 26.5 = 466$ KIPS O.K.

($F_y = 36$ KSI)

<u>USE W14×90</u>

TIER #2   AXIAL LOAD = $35.39 \times 18 \times \left(\frac{1}{1.5}\right)^* = 424$ KIPS

TRY W14×90 $L/r = \frac{18 \times 12}{3.70} = 58$

Fa = 17.58   LOAD = $17.58 \times 26.5 = 46.6$ KIPS O.K.

($F_y = 36$ KSI)

<u>USE W14×90</u>

TIER #3   AXIAL LOAD = $42.86 \times 18 \times \left(\frac{1}{1.5}\right)^* = 514$ KIPS

TRY W14×99 $L/r = \frac{18 \times 12}{3.71} = 58$
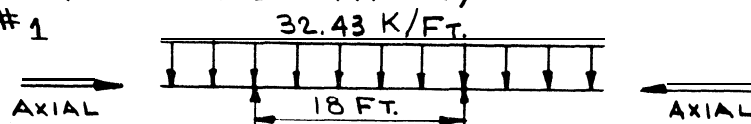
Fa = 17.59   LOAD $17.59 \times 29.10 = 512$ KIPS O.K.

($F_y = 36$ KSI)

<u>USE W14×99</u>

(c) WALES
(ASSUME ALL WALES AND STRUTS IN EACH TIER ARE
AT SAME ELEVATION)

TIER #1

32.43 K/FT.

AXIAL   18 FT.   AXIAL

INTERIOR SPANS   AXIAL = $32.43 \times 9 \times \left(\frac{1}{1.65}\right)^* = 177$ KIPS

MAX. MOM. = $\frac{1}{10}(32.43)(18^2)\left(\frac{1}{1.65}\right)^* = 636.8$ FT. KIPS

* SEE NOTE AT END OF EXAMPLE CONCERNING PERMISSIBLE OVERSTRESS

Tier #1

TRY W33×141 USING AISC FORMULAE:

PROPERTIES OF

$A = 41.6 \text{ IN}^2$ $r_x = 13.4$ IN. $F_y = 36$ KSI

$S_x = 448$ IN^3 $r_y = 2.43$ IN. $K_x = K_y = 1.0$

AXIAL STRESS

$f_a = \dfrac{P}{A} = \dfrac{177}{41.6} = 4.25$ KSI

$\dfrac{K_y \ell_y}{r_y} = \dfrac{18 \times 12}{2.43} = 89$ $\dfrac{K_x \ell_x}{r_x} = \dfrac{18 \times 12}{13.4} = 16.1$

MINOR AXIS GOVERNS USE $\ell/r = 89$ AND SELECT THE PERMITTED
STRESS, F_a, FROM THE AISC COLUMN DESIGN TABLES FOR
$F_y = 36.0$ KSI $F_a = 14.32$ KSI.

THE MAJOR AXIS BENDING STRESS IS, $f_{bx} = \dfrac{M}{S_x} = \dfrac{636.8 \times 12}{448} = 17.06$ KSI

DETERMINATION OF COMPACT SECTION:

THE AISC SPECIFICATION INDICATES THAT THE W33×141 DOES MEET
THE FLANGE WIDTH TO THICKNESS RATIO AND THE WEB DEPTH TO
THICKNESS RATIO REQUIREMENTS FOR COMPACT SECTIONS — ASSUME
THE SHEET PILE PROVIDES ADEQUATE LATERAL SUPPORT TO MEET
BRACING REQUIREMENTS FOR COMPRESSION FLANGE.
THEREFORE, THE W33×141 IS A COMPACT MEMBER, AND
$F_{bx} = 0.66 \, F_y = 24$ KSI

$F'_{ex} = \dfrac{12\pi^2 E}{23(K_x \ell_x/r)^2} = \dfrac{12\pi^2 (29000)}{23(16.1)^2} = 576.1$ KSI

$\dfrac{f_a}{F_a} = \dfrac{4.25}{14.32} = .297 > .15 \therefore$ USE FORMULA 1.6-1a AND 1.6-1b.

ASSUME $C_m = 0.85$

$(1.6-1a)$ $\dfrac{4.26}{14.32} + \dfrac{0.85 \, (17.06)}{(1 - \frac{4.25}{576.1}) \, 24.0} = 0.305 + 0.609 = 0.914 \; < 1.0$

$(1.6-1b)$ $\dfrac{4.25}{.6(36.)} + \dfrac{17.06}{24.0} = 0.197 + 0.711 = 0.908 \; < 1.0$

USE W33×141

Tier #2

TRY W33×152 USING AISC. FORMULAE:

Properties of

$A = 44.7$ IN^2 $r_x = 13.50$ IN. $F_y = 36$ KSI

$S_x = 487.0$ IN^3 $r_y = 2.47$ IN. $K_x = K_y = 1.0$

Axial Stress

$f_a = \dfrac{P}{A} = \dfrac{193}{44.7} = 4.32$ KSI $\left[P = (35.35)(9)\left(\dfrac{1}{1.65}\right)^* = 193 \text{ KIPS} \right]$

$\dfrac{K_y \ell_y}{r_y} = \dfrac{18 \times 12}{2.47} = 87.4$ $\dfrac{K_x \ell_x}{r_x} = \dfrac{18 \times 12}{13.50} = 16$

MINOR AXIS GOVERNS USE $\ell/r = 87.4$ AND SELECT THE PERMITTED
STRESS, F_a, FROM THE AISC COLUMN DESIGN TABLES $F_y = 36.0$ KSI

$F_a = 14.50$ KSI $M = \dfrac{1}{10}(35.39)(18)^2 \left(\dfrac{1}{1.65}\right)^* = 694.9$ FT. KIF

THE MAJOR AXIS BENDING STRESS IS, $f_{bx} = \dfrac{M}{S_x} = \dfrac{694.9 \times 12}{486.7} = 17.13$ KSI

Determination Of Compact Section

THE AISC SPECIFICATION INDICATES THAT THE · W33×152 DOES MEET THE
FLANGE WIDTH TO THICKNESS RATIO AND THE WEB DEPTH TO THICKNESS
RATIO REQUIREMENTS FOR COMPACT SECTIONS - ASSUME THE SHEET
PILE PROVIDES ADEQUATE LATERAL SUPPORT TO MEET BRACING REQUIREMENTS
FOR COMPRESSION FLANGE. THEREFORE, THE W33×152 IS A COMPACT
MEMBER, AND $F_{bx} = 0.66$ $F_y = 24$ KSI

$F'_{ex} = \dfrac{12 \pi^2 E}{23(K_x \ell_x/r_x)^2} = \dfrac{12 \pi^2 (29000)}{23(16)^2} = 583$ KSI

$\dfrac{f_a}{F_a} = \dfrac{4.32}{14.50} = .298 > .15 \therefore$ USE FORMULA 1.6-1a AND 1.6-1b

ASSUME $C_m = 0.85$

$(1.6-1a)$ $\dfrac{4.32}{14.50} + \dfrac{0.85(17.13)}{\left(1 - \dfrac{4.32}{583}\right)24.0} = 0.298 + 0.611 = 0.909 < 1.0$

$(1.6-1b)$ $\dfrac{4.32}{.6(36)} + \dfrac{17.13}{24.0} = 0.200 + 0.714 = 0.914 < 1.0$

USE W33 × 152

* SEE NOTE AT END OF EXAMPLE CONCERNING PERMISSIBLE OVERSTRESS

$\underline{\text{TIER } \#3} \quad A_{XIAL} = 42.86 \times 9 \times \left(\frac{1}{1.65}\right)^* = 234 \text{ KIPS}$

$M_{AX. MOM.} = \frac{1}{10} (42.86)(18^2)\frac{1}{1.65}^* = 841.6 \text{ FT. KIPS}$

TRY W30 × 173   USING AISC FORMULAE

<u>PROPERTIES OF</u>
$A = 50.8 \text{ IN}^2 \qquad\qquad r_x = 12.7 \text{ IN.} \qquad F_Y = 36 \text{ KSI}$
$S_x = 539.0 \text{ IN}^3 \qquad\qquad r_Y = 3.43 \text{ IN.} \qquad K_x = K_Y = 1.0$

<u>AXIAL STRESS</u>
$\qquad f_a = \frac{P}{A} = \frac{234}{50.8} = 4.61 \text{ KSI}$

$\qquad \frac{K_Y \ell_Y}{r_Y} = \frac{18 \times 12}{3.43} = 63.0 \; ; \quad \frac{K_x \ell_x}{r_x} = \frac{18 \times 12}{12.7} = 17.0$

MINOR AXIS GOVERNS USE $\ell/r = 63.0$ AND SELECT THE PERMITTED STRESS, Fa, FROM THE AISC COLUMN DESIGN TABLES FOR $F_Y = 36.0$ KSI Fa = 17.14 KSI

THE MAJOR AXIS BENDING STRESS IS, $f_{bx} = \frac{M}{S_x} = \frac{841.6 \times 12}{539} = 18.74$ KSI

DETERMINATION OF COMPACT SECTION

THE AISC SPECIFICATION INDICATES THAT THE W30×173 DOES MEET THE FLANGE WIDTH TO THICKNESS RATIO AND THE WEB DEPTH TO THICKNESS RATIO REQUIREMENTS FOR COMPACT SECTIONS–ASSUME THE SHEET PILE PROVIDES ADEQUATE LATERAL SUPPORT TO MEET BRACING REQUIREMENTS FOR COMPRESSION FLANGE. THEREFORE, THE W30×172 IS A COMPACT MEMBER, AND $F_{bx} = 0.66 F_Y = 24$ KSI

$F'_{ex} = \frac{12 \pi^2 E}{23(K_x \ell_x / r_x)} = \frac{12 \pi^2 (29000)}{23(17.0)} = 508 \text{ KSI}$

$\frac{f_a}{F_a} = \frac{4.61}{17.14} = 0.269 > .15 \; \therefore$ USE FORMULA 1.6–1a AND 1.6–1b

ASSUME $C_m = 0.85$

$1.6\text{–}1a) = \frac{4.61}{17.14} + \frac{0.85(18.74)}{\left(1 - \frac{4.62}{508}\right)24.0} = 0.267 + 0.670 = 0.937 < 1.0$

$1.6\text{–}1b) \frac{4.61}{.6(36)} + \frac{18.74}{24.0} = 0.213 + 0.781 = 0.994 > 1.0$ O.K.

$\qquad\qquad\qquad$ USE W30 × 173

* SEE NOTE AT END OF EXAMPLE CONCERNING PERMISSIBLE OVERSTRESS

IV- INVESTIGATE STABILITY AT BOTTOM OF EXCAVATION

DETERMINE CRITICAL DEPTH OF EXCAVATION FOR STABILITY AGAINST HEAVE CONSIDERING SHEETING DOES NOT EXTEND INTO STIFF CLAY USING TERZAGHI RELATIONSHIP

ASSUME EXCAVATION LENGTH = WIDTH = 54 FT.

$$H_c = \frac{5.7c}{\gamma - \frac{c}{B}\sqrt{2}}$$

$C = \frac{800}{1.5}$ PCF = 535 PCF (1.5 SAFETY FACTOR)

$B = 54$ FT

$\gamma = 125$ PCF (ASSUME AVERAGE OVERBURDEN DENSITY)

$$H_c = \frac{5.7(535)}{125 - \frac{535}{54}\sqrt{2}} = 27 \text{ FT. (UNSATISFACTORY)}$$

EXTEND SHEETING 5 FT. INTO STIFF CLAY

$$C = \frac{1500}{1.5} \text{ PCF} = 1000 \text{ PCF}$$

$$H_c = \frac{5.7(1000)}{125 - \frac{1000}{54}\sqrt{2}} = 58 \text{ FT (O.K.)}$$

CHECK USING BJERRUM RELATIONSHIP

$$H_c = N_c \frac{c}{\gamma} \qquad N_c = 7.5$$

$$H_c = \frac{7.5(1000)}{125} = 60 \text{ FT (O.K.)}$$

NOTES AND GENERAL COMMENTS

(1.) OVERSTRESSES ARE PERMITTED IN CAREFULLY CONTROLLED AND INSPECTED CONSTRUCTION SITUATIONS FOR THE DESIGN OF SHEETING STRUTS, AND WALES IN TEMPORARY BRACING SYSTEMS. SEE TEXT FOR DETAILS. THE AMOUNT OF THE OVERSTRESS IN THIS EXAMPLE IS CONSISTENT WITH RECOMMENDATIONS GIVEN IN "FOUNDATION DESIGN" BY TENG.

(2.) THE SIZE OF THE WALES MAY BE REDUCED BY WELDING THE WALES TO THE SHEETING WHICH WILL INCREASE THE ALLOWABLE AXIAL STRESS IN THE WALES.

(3.) IF THE DESIGN RESULTS IN COMPONENT SIZES WHICH ARE TOO LARGE FOR PRACTICAL USE, CONSIDERATION SHOULD BE GIVEN TO CHANGING THE SPACING BETWEEN STRUTS AND/OR WALES.
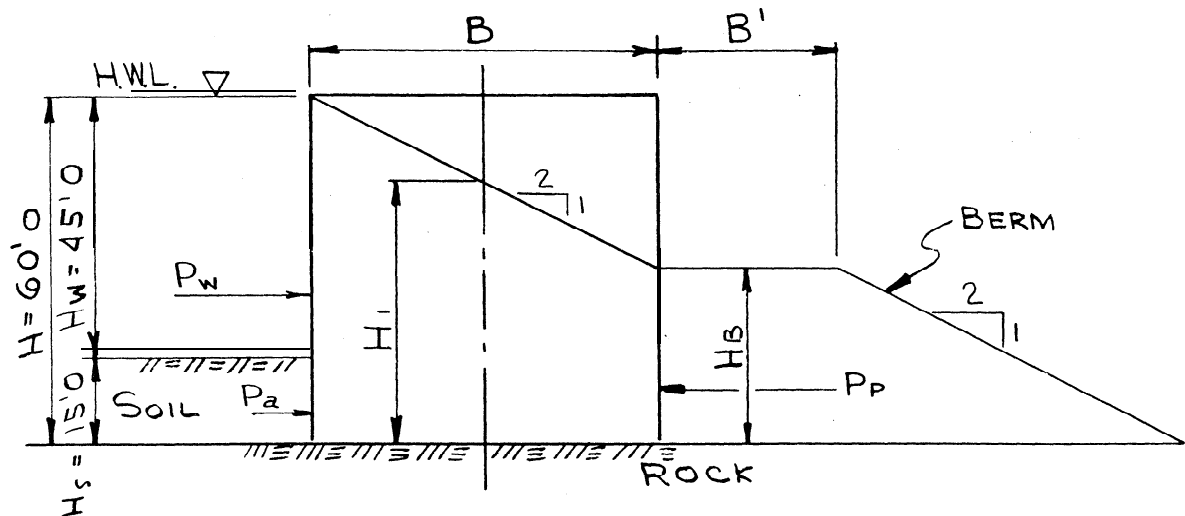
Given

γ (WEIGHT OF SOIL MOIST) $= 0.110 \ ^K/_{FT^3}$

γ' (WEIGHT OF SOIL SUB.) $= 0.065 \ ^K/_{FT^3}$

COEFF. OF FRICTION - SOIL ON ROCK $= 0.5$

COEFF. OF FRICTION - SOIL ON STEEL $= 0.4 = TAN. \delta$

ANGLE OF INTERNAL FRICTION, $\phi = 28° 50'$; TAN $\phi = 0.55$
     (FOR DRY OR SATURATED MATERIAL)

COEFF. OF FRICTION - STEEL ON STEEL (INTERLOCKS) $= 0.3 = f$

Assumption

CELL FILL IS A SANDY, FREE DRAINING MATERIAL.

TEMPORARY CONSTRUCTION - MINIMUM FACTOR OF SAFETY $= 1.25$

THE CELL IS FILLED WITH DRY MATERIAL

Allowable Piling Stress:

WEB TENSION $- f_Y = 38.5 \ ^K/_{IN^2}$ $f_a = 25.0 \ ^K/_{IN^2}$

INTERLOCK TENSION - GUARANTEED STRENGTH $= 16.0 \ ^K/_{IN}$
                  DESIGN STRENGTH $= 8.0 \ ^K/_{IN}$

Demension of Cell -

Assume Effective Width of Cofferdam, B Equals 0.9 Of The Height, H

$$B = 0.9 H = 0.9 (60) = 54.0'$$

The Actual Diameter Of The Circular Cofferdam Will Depend on The Angle $\propto$ To The Connecting Arcs.

Lateral Pressure on Cell

<u>Water</u> = $P_w = \frac{1}{2} (0.0625)(60.0)^2 = 112.5 \, ^K/_{FT.}$

<u>Soil</u> = Use Coulomb's Theory of Active Pressure (Assume Level Surface)

$$K_a = \frac{Cos^2 \phi}{Cos \, \delta \left[1 + \sqrt{\frac{Sin(\phi + \delta) \, Sin \, \phi}{Cos \, \delta}} \right]^2}$$

$Tan \, \delta = 0.4 \therefore \delta \cong 21° \, 50' \quad Cos \, \delta = 0.928$

$$K_a = \frac{(0.876)^2}{(.928) \left[1 + \sqrt{\frac{(0.766)(0.482)}{0.925}} \right]^2} = 0.311$$

$$P_a = \frac{1}{2} K_a \, \gamma ' H^2 = \frac{1}{2} (0.311)(0.065)(15.0)^2 = 2.27 \, ^K/_{FT}$$

Total Lateral Force on Outside of Cell

$$P_w + P_a = 112.5 + 2.27 = \underline{\underline{114.77 \, ^K/_{FT.}}}$$

Weight of Cell Fill

$$W_T = B\gamma'(H-H_1) + B\gamma'H_1$$
$$= 54\,(0.110)(13.5) + 54\,(0.065)(46.5)$$
$$= 243.4^K$$

Check Sliding (Without Berm)

$$F.S. = \frac{\text{Resisting Force}}{\text{Driving Force}}$$

$$= \frac{243.4\,(0.5)}{114.77} = 1.06 < 1.25 \quad \text{Berm Req'd.}$$

Properties of Berm

Try $B' = 30.0'$

$$H_B = 60. - 27. = 33.0'$$

γ' Soil - Berm (Assume Berm To Be Fully Saturated)
$$= 0.065\ ^K/_{FT}{}^3$$

Weight of Berm $= \left.\begin{array}{l}(30 \times 33)(0.065) = 64.4 \\ \tfrac{1}{2}(33)(2)(33)(0.065) = 70.7\end{array}\right\}\ 135.1\ K$

Calculate Passive Pressure Using Coulomb's Theory And Culmann Curve.

(1.) Draw Berm To Scale
(2) Layout Line OA From Pt. O @ $\phi\,(28°\,50')$ Below Horizontal
(3) Layout Line OB From Pt. O @ $90° + \delta\,(111°\,50')$ Below OA
(4) Assume Failure Planes Thru The Berm Originating @ Pt. O
    And Compute The Weight of Earth Above Each.
(5) Layout Weight Computed In (4) Along OA.
(6) Draw A Line Parallel To OB For Each Assumed Failure
    Wedge From Its Weight Plotted on OA To Its Failure Plane.
(7) Connect The Intersecting Points Resulting From (6)
    With A Smooth Curve - This Is The Culmann Curve

PROPERITES OF BERM (CONT'D)

(8) THE POINT ON THE CULMANN CURVE CLOSEST TO LINE OA MEASURED PARALLEL TO OB, IS THE PASSIVE PRESSURE THE BERM CAN ATTAIN.
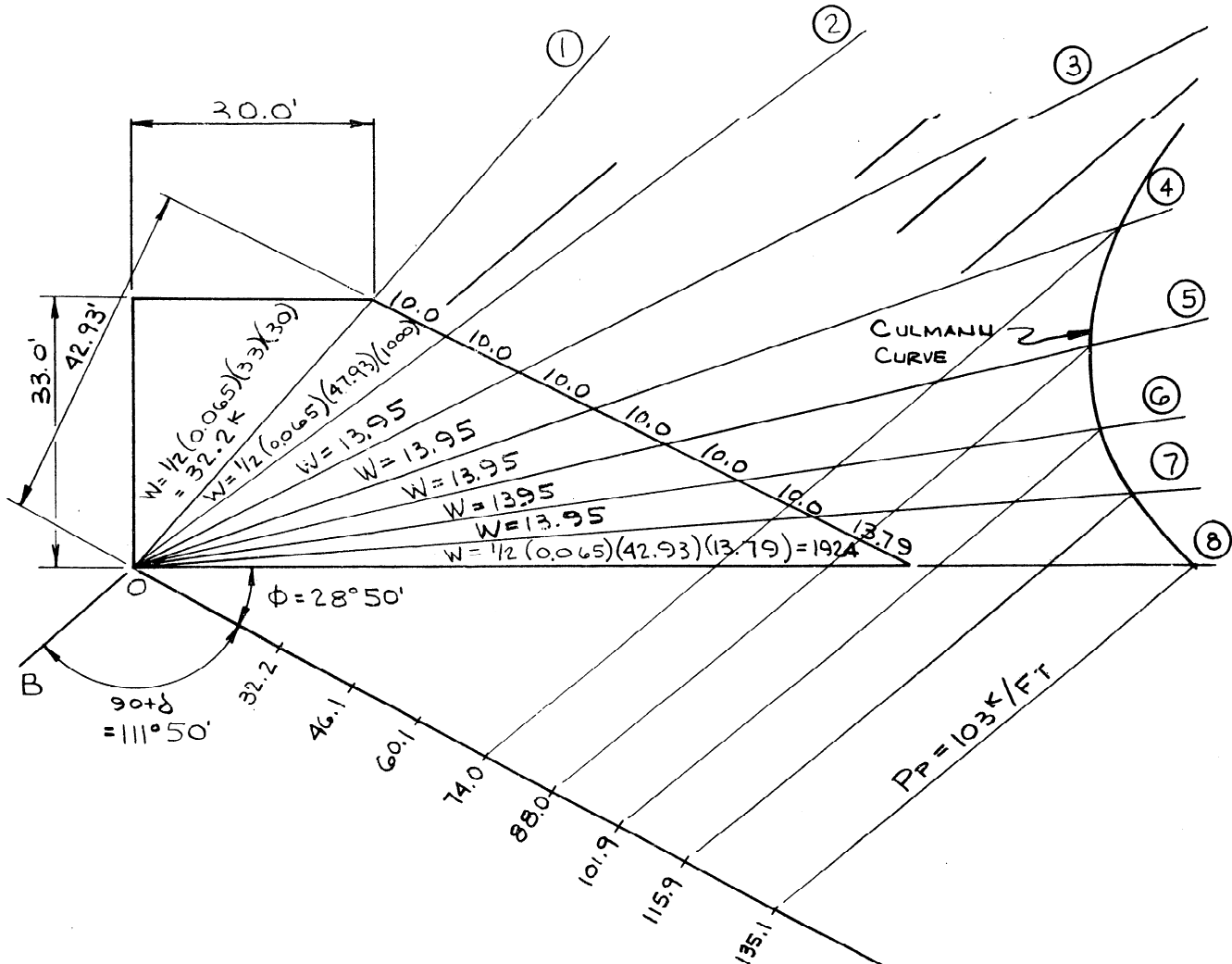
HORIZONTAL COMPONENT OF PASSIVE PRESSURE =
$P_P = 103 \cos \delta = 103 (\cos 21°50') = 103(0.928) = 95.6^K/FT$

SLIDING OF BERM ON ROCK = $(135.1)(0.5) = 67.5^K/FT < 95.6^K/FT$.
THUS, THE ENTIRE BERM WOULD SLIDE ON THE ROCK BEFORE A PASSIVE FAILURE COULD OCCUR.

CHECK SLIDING (WITH BERM)

$$F.S. = \frac{(243.4)(0.5) + (135.1)(0.5)}{114.6} = \frac{121.7 + 67.5}{114.6} = 1.65 > 1.25 \text{ OK}$$

SLIPPING BETWEEN PILING AND CELL FILL

$$F.S. = \frac{RESISTING\ MOMENT}{DRIVING\ MOMENT}$$

$$= \frac{(P_W + P_A)\ TAN\ \delta\ B + H_R P_p/3}{\frac{1}{3}(P_W H + P_a H_S)}$$

$$F.S. = \frac{(114.77)(0.4)(54) + (67.5)(33)/3}{\frac{1}{3}[112.5 \times 60 + 2.27 \times 15]} = \frac{3223}{2261} = 1.43 > 1.25\ O.K.$$

SHEAR FAILURE @ ₵ CELL (VERTICAL SHEAR)

$$DRIVING\ SHEAR\ Q = \frac{3M}{2B} = \frac{(3)\frac{1}{3}[112.5(60) + 2.27(15) - 67.5(33)]}{2(54)}$$

$$= 42.2\ ^K/_{FT.}$$

$$K = \frac{\cos^2\phi}{2 - \cos^2\phi} = \frac{(0.876)^2}{2 - (0.876)^2} = 0.622\ EARTH\ PRESSURE\ AT\ REST$$

$$P_S = \frac{1}{2}K\gamma(H - H_1)^2 + K\gamma(H - H_1)H_1 + \frac{1}{2}K\gamma'(H_1)^2$$
$$= \frac{1}{2}(0.622)(0.110)(13.5)^2 + (0.622)(0.110)(13.5)(46.5) + \frac{1}{2}(0.622)(0.065)(46.5)^2$$

$$P_S = 92.9\ ^K/_{FT.}$$

$$P_t = \frac{1}{2}K_a\gamma(H - H_1)^2 + K_a\gamma(H - H_1)H_1 + \frac{1}{2}K_a\gamma'(H_1)^2 + \frac{1}{2}\gamma_w H_s^2$$
$$- \frac{1}{2}(\frac{1}{4}H)[\gamma_w H_s + K_a\gamma H_1 + K_a(H - H_1)]$$
$$= \frac{1}{2}(0.311)(0.110)(13.5)^2 + (0.311)(0.110)(13.5)(46.5) + \frac{1}{2}(0.311)(0.065)(46.5)^2 + \frac{1}{2}(0.0625)(33.0)^2$$
$$- \frac{1}{8}(60)[0.0625(33.0) + 0.311(0.065)(46.5) + 0.311(0.110)(13.5)]$$

$$P_t = 53.1\ ^K/_{FT.}$$

SHEAR RESISTANCE = Ps + ... + Pt

$$F.S.\ \frac{SHEAR\ RESISTANCE}{DRIVING\ SHEAR} = \frac{92.9(0.55) + 0.3(53.1)}{42.2} \qquad \underline{F.S. = 1.59 > 1.25}$$

$$O.K.$$

HORIZONTAL SHEAR (CUMMINGS' METHOD)

$$C = B \tan \phi = 54.0 (0.55) = 29.7$$
$$a = H - C = 60 - 29.7 = 30.3$$

AS A CONSERVATIVE ASSUMPTION - TAKE UNIT WEIGHT OF SOIL IN CELL AS γ' THROUGHOUT

$$M_r = \frac{\gamma' a c^2}{2} + \frac{\gamma' c^3}{3} = \frac{1}{2}(0.065)(30.3)(29.7)^2 + \frac{1}{3}(0.065)(30.3)^3 = 1,430 \, ^K/_{FT}$$

$$M_i = P_T \, f \, B$$

$$M_i = (53.1)(0.3)(54) = 860$$

$$F.S. \quad \frac{\text{RESISTING MOMENT}}{\text{DRIVING MOMENT}} = \frac{M_r + M_i + P_o H_B/3}{\frac{1}{3}(P_w H + P_a H_s)} = \frac{1430 + 860 + (67.5)(33)/3}{2261}$$

$$= \frac{3032 \, K\text{-}FT}{2261 \, K\text{-}FT} = 1.34 > 1.25 \quad O.K.$$

INTERLOCK TENSION

THE METHOD OF FILLING AND THE FILL MATERIAL USED HAVE A PRONOUNCED EFFECT ON THE INTERLOCK TENSION. IN THIS SAMPLE PROBLEM, THE CELL WAS ASSUMED TO BE FILLED WITH DRY MATERIAL, AND THE (IN USE) CASE OF SATURATION ON THE INBOARD FACE IS THE WORST CASE. IF THE CELL WERE FILLED HYDRAULICALLY, THE INTERLOCK FORCES WOULD BE MUCH HIGHER.

COMPUTE INTERLOCK TENSION ON THE BASIS OF σ_T FROM FIGURE 71b
ASSUME $\alpha = 45°$ (CONNECTING TEE ANGLE)
$$\sigma_T = K_a \gamma (H - H_1) + K_a \gamma' (H - \tfrac{H}{4}) + V_w (H_B - \tfrac{H}{4})$$
$$\sigma_T = (0.311)(0.11)(13.5) + 0.311(0.065)(31.5) + 0.0625(18.0) \quad \underline{\sigma_T = 2.22 \, ^K/_{FT.^2}}$$

$$t = \sigma_T \times R = (2.22 \, ^K/_{FT.^2})(31 \, FT.)/12 \, ^{IN}/_{FT.} = 5.73 < 8.0 \, ^K/_{IN} \quad O.K.$$
$$t_{MAX} = \frac{\sigma_T \sec \alpha}{12} = \frac{1}{2}(2.22)(32.7)\sqrt{2} = 8.55 \, ^K/_{IN}$$

8.55 > 8.0 BUT STILL PERMISSABLE

$$S.F. = \frac{16.0}{8.55} = 1.87 \quad O.K$$

Allowable Bending Moments for Steel Sheet Piling Sections

Y-axis: Bending Moment — Inch Kips/Foot of Wall (100 to 1800)

X-axis: Design Stress - psi (thousands) (20 to 36)

Curves (top to bottom):
- PZ38 S = 46.8 in.³/ft. W = 38.0 lbs./sq. ft.
- PZ32 S = 38.3 in.³/ft. W = 32.0 lbs./sq. ft.
- PZ27 S = 30.2 in.³/ft. W = 27.0 lbs./sq. ft.
- PZ22 S = 19.0 in.³/ft. W = 22.0 lbs./sq. ft.
- PDA27 S = 10.7 in.³/ft. W = 27.0 lbs./sq. ft.
- PMA22 S = 5.4 in.³/ft. W = 22.0 lbs./sq. ft.

Grade bands: Regular Carbon Grade → * | EX-TEN 45 → * | USS MARINER and EX-TEN 50 → * | EX-TEN 55 → *
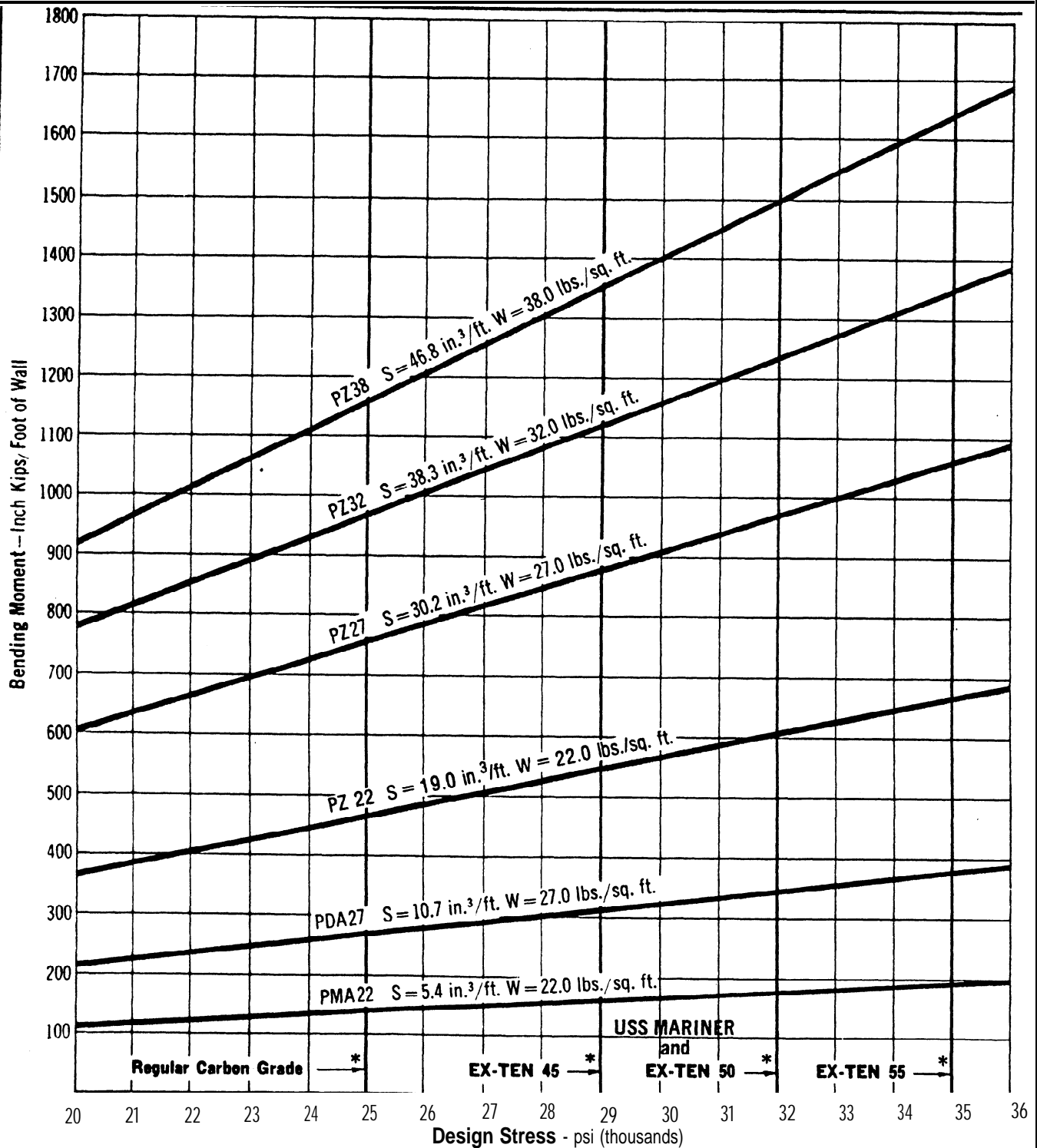
*Permanent stresses based on generally accepted design practice

Rankine Earth Pressure Coefficients for Level Back Fill

ϕ	10°	12.5°	15°	17.5°	20°	22.5°	25°	27.5°	30°	32.5°	37.5°	37.5°	40°
K_a	0.70	0.64	0.59	0.54	0.49	0.45	0.41	0.37	0.33	0.30	0.27	0.24	0.22
K_p	1.42	1.55	1.70	1.86	2.04	2.24	2.46	2.72	3.00	3.32	3.69	4.11	4.60